



Letter Report
TLR-RES/DE/CIB-2020-15

***SURVEY OF MODELING AND SIMULATION TECHNIQUES FOR
ADVANCED MANUFACTURING TECHNOLOGIES
VOLUME II – PREDICTING MATERIAL PERFORMANCE FROM
MATERIAL MICROSTRUCTURE***

Date:

December 2020

Prepared in response to Task 1C in NRC Advanced Manufacturing Technologies Action Plan, Revision 1 (ADAMS Accession No. ML19333B980), by:

Andrea Nicolas

Argonne National Laboratory

Noah Paulson

Argonne National Laboratory

Mark C. Messner

Argonne National Laboratory

NRC Project Manager:

Shah Malik

Senior Materials Engineer

Component Integrity Branch

**Division of Engineering
Office of Nuclear Regulatory Research
U.S. Nuclear Regulatory Commission
Washington, DC 20555-0001**

DISCLAIMER

This report was prepared as an account of work sponsored by an agency of the U.S. Government. Neither the U.S. Government nor any agency thereof, nor any employee, makes any warranty, expressed or implied, or assumes any legal liability or responsibility for any third party's use, or the results of such use, of any information, apparatus, product, or process disclosed in this publication, or represents that its use by such third party complies with applicable law.

This report does not contain or imply legally binding requirements. Nor does this report establish or modify any regulatory guidance or positions of the U.S. Nuclear Regulatory Commission and is not binding on the Commission.

Survey of Modeling and Simulation Techniques for Advanced Manufacturing Technologies Volume II – Predicting Material Performance from Material Microstructure

Applied Materials Division

About Argonne National Laboratory

Argonne is a U.S. Department of Energy laboratory managed by UChicago Argonne, LLC under contract DE-AC02-06CH11357. The Laboratory's main facility is outside Chicago, at 9700 South Cass Avenue, Argonne, Illinois 60439. For information about Argonne and its pioneering science and technology programs, see www.anl.gov.

DOCUMENT AVAILABILITY

Online Access: U.S. Department of Energy (DOE) reports produced after 1991 and a growing number of pre-1991 documents are available free via DOE's SciTech Connect (<http://www.osti.gov/scitech/>)

Reports not in digital format may be purchased by the public from the National Technical Information Service (NTIS):

U.S. Department of Commerce
National Technical Information
Service 5301 Shawnee Rd
Alexandria, VA 22312
www.ntis.gov
Phone: (800) 553-NTIS (6847) or (703) 605-6000
Fax: (703) 605-6900
Email: orders@ntis.gov

Reports not in digital format are available to DOE and DOE contractors from the Office of Scientific and Technical Information (OSTI):

U.S. Department of Energy
Office of Scientific and Technical Information
P.O. Box 62
Oak Ridge, TN 37831-0062
www.osti.gov
Phone: (865) 576-8401
Fax: (865) 576-5728
Email: reports@osti.gov

Disclaimer

This report was prepared as an account of work sponsored by an agency of the United States Government. Neither the United States Government nor any agency thereof, nor UChicago Argonne, LLC, nor any of their employees or officers, makes any warranty, express or implied, or assumes any legal liability or responsibility for the accuracy, completeness, or usefulness of any information, apparatus, product, or process disclosed, or represents that its use would not infringe privately owned rights. Reference herein to any specific commercial product, process, or service by trade name, trademark, manufacturer, or otherwise, does not necessarily constitute or imply its endorsement, recommendation, or favoring by the United States Government or any agency thereof. The views and opinions of document authors expressed herein do not necessarily state or reflect those of the United States Government or any agency thereof, Argonne National Laboratory, or UChicago Argonne, LLC.

Survey of Modeling and Simulation Techniques for Advanced Manufacturing Technologies Volume II – Predicting Material Performance from Material Microstructure

Applied Materials Division
Argonne National Laboratory

August 2020

Prepared for the
U.S. Nuclear Regulatory Commission
under interagency agreement 31310019F0057
with the U. S. Department of Energy

Prepared by

Andrea Nicolas
Noah Paulson
Mark C. Messner

ABSTRACT

This report describes the current state of modeling and simulation techniques for predicting the properties of materials fabricated with advanced manufacturing techniques, given the initial microstructure of the material. The report includes a literature survey and a gap analysis outlining and prioritizing key issues in applying these modeling and simulation techniques to nuclear reactor structural materials. The discussion covers both physics-based and data-driven modeling techniques and includes a broad range of manufacturing techniques and materials that may have future nuclear applications. This report is the second in a two-part series, with the first report covering modeling and simulation methods for predicting the initial, as-manufactured structure of advanced manufacturing materials, given a description of the process. Both reports focus on a set of manufacturing technologies likely to be applied to reactor structural components. Taken together, the two reports provide a complete summary of the current state of processing-structure-properties models for advanced manufacturing as well as a survey of applications to reactor structural materials.

EXECUTIVE SUMMARY

This report surveys the current state of modeling and simulation methods for predicting key material properties of advanced manufacturing processed materials given a description of the initial material microstructure when the component goes into service. This report is part two of a two-part series. The first report covers modeling and simulation techniques for predicting the initial microstructure of a component, given the critical parameters describing the manufacturing process. Taken together, these two reports summarize the current state of process-structure-properties models for advanced manufacturing materials, focusing on a set of technologies with likely future applications to nuclear reactor structural materials

The focus of this report is on identifying key gaps and recommendations on applying microstructure-properties models to nuclear reactor structural materials and components. The approach taken here is to summarize the current state of the field, via a broad literature survey, to identify current gaps that might impact applying the techniques to nuclear components, and from this survey develop a key set of recommendations. The report concentrates on technologies and materials likely to apply to nuclear components in the future, though it includes materials from other industries, especially aerospace, in order to draw on the extensive body of work developed in this field.

The initial section of the report briefly summarizes key microstructure-property relations in advanced manufacturing technologies (AMTs) to set the stage for the description of the modeling and simulation methods. Two chapters survey physics-based and data-driven methods for predicting material properties, including a gap analysis of particular methods and the field in general. Critical gaps include the lack of automated methods for bridging length and time scales, difficulties in *ab initio* modeling of new materials, and a general lack of application of AMTs and materials for nuclear applications. Nuclear reactor structural materials have not been a strong research focus, partly because existing modeling and simulation techniques are better suited to short time scales, which are not directly relevant to most material properties used in reactor component design, and partly because other industries have been driving the development of AMTs, leading to a focus on alloys of interest to those industries.

The report includes a high-level overview of widely available software tools for structure-property modeling. Compared to the first report on structure prediction, many of the research studies surveyed here use proprietary or in-house software, meaning there are few commercial or open source simulation tools dedicated to physics-based property modeling. However, the survey includes a more detailed description of a few commonly-used tools.

Based on the literature survey and gap analysis, the report formulates a collection of critical gaps and recommendations:

- Regulators are unlikely to see applications of the full multiscale method to develop or qualify new AMT materials in the near future
- Regulators are likely to see applications of microstructurally-based models complementing experimental data on new AMTs and to help qualify new materials and processes
- The community will need to develop new validation approaches to realize the potential of microstructural modeling and AMT materials

- Data-driven models will play an increasing role in qualification methods, both by themselves and in conjunction with physically-based models
- The development, by the wider research community, of improved, more automatic scale-bridging methods would greatly simplify the implementation of multiscale modeling, particularly in spanning between discrete and continuum models
- The time-scale of direct atomistic and defect modeling approaches prevents their direct application to AMTs for nuclear reactor applications
- There are comparatively few studies applying microstructural modeling to predict structural material properties for AMTs; there are almost no studies applying these techniques to likely nuclear structural materials
- Most current models focus on predicting short-term properties, particularly stress-strain flow curves under different conditions. Predicting long-term properties like creep, thermal aging, irradiation damage, and creep-fatigue will be more difficult
- There are few integrated modeling approaches for predicting material degradation due to environmental effects like corrosion or radiation damage

ACRONYMS AND ABBREVIATIONS

The following is a list of acronyms and abbreviations used throughout the document:

<i>Acronym</i>	<i>Expression</i>
AMT	Advanced Manufacturing Technology
BCC	Body Centered Cubic
CP	Crystal Plasticity
CPFEM	Crystal Plasticity Finite Element Method
CPFFT	Crystal Plasticity Fast Fourier Transform
CT	Computed Tomography
DD	Discrete Dislocation
DED	Directed Energy Deposition
DFT	Density Functional Theory
dpa	displacements per atom
EAM	Embedded Atom Model
EBM	Electron Beam Melting
EVP-CPFFT	Elasto-viscoplastic Crystal Plasticity Fast Fourier Transform
FCC	Face Centered Cubic
FEA	Finite Element Analysis
FE2	Finite Element Squared
HIP	Hot Isostatic Pressing
ICME	Integrated Computational Materials Engineering
KMC	Kinematic Monte Carlo
LMP	Larson Miller Parameter
L-PBF	Laser-Powder Bed Fusion
LWR	Light Water Reactor
MD	Molecular Dynamics
MEAM	Modified Embedded Atom Model
ML	Machine Learning
PBF	Powder Bed Fusion
PDE	Partial Differential Equation
PM-HIP	Powder Metallurgy - Hot Isostatic Pressing
RVE	Representative Volume Element
SEM	Scanning Electron Microscope
SLM	Selective Laser Melting
SOM	Self Organizing Map
SS	Stainless steel
SVE	Statistical Volume Element
Ti-6Al-4V	Titanium 6% Aluminum 4% Vanadium alloy

TABLE OF CONTENTS

Abstract.....	i
Executive Summary.....	iii
Acronyms and abbreviations.....	v
Table of Contents.....	vii
Table of Figures.....	ix
List of Tables.....	xi
1 Introduction.....	1
1.1 Overview: why use microstructural models?.....	1
1.2 The purpose of this report.....	3
1.3 Relation to the companion report.....	3
1.4 Organization.....	4
2 Material Properties and Microstructural Connections.....	5
2.1 Monotonic Loading Properties.....	5
2.1.1 Tensile.....	5
2.1.2 Fracture.....	7
2.2 Cyclic loading properties and fatigue.....	8
2.2.1 Fatigue strength and degradation.....	8
2.3 Time-dependent.....	10
2.3.1 Creep.....	10
2.3.2 Creep-fatigue.....	11
2.4 Environmental Degradation.....	13
2.4.1 Thermal aging.....	13
2.4.2 Corrosion.....	14
2.4.3 Radiation.....	17
3 Current State of the Art: Physics-based Modelling and Simulation.....	21
3.1 A hierarchical description of metallic materials.....	21
3.2 Brief summary and description of modeling techniques.....	26
3.2.1 Discrete approaches.....	28
3.2.1.1 Ab initio methods: Density Functional Theory and other electronic structure methods.....	28
3.2.1.2 Atomistics: Molecular Dynamics and Kinematic Monte Carlo.....	29
3.2.1.3 Defects: Discrete Dislocation dynamics.....	30
3.2.2 Mesoscale continuum approaches.....	31
3.2.2.1 Field Dislocation theories.....	31
3.2.2.2 Crystal Plasticity.....	31
3.2.2.3 Damage modeling on the microscale.....	34
3.2.3 Macroscale modeling: Homogenization and the multiscale method.....	35
3.2.3.1 Formal homogenization techniques.....	35
3.2.3.2 Multiscale frameworks.....	36
3.3 Applications to AMTs.....	37
3.3.1 Comprehensive models.....	37
3.3.2 Models targeting flow curve predictions.....	38
3.3.3 Models predicting fatigue initiation.....	40

3.3.4	Models including grain residual stresses	40
3.3.5	Summary	41
3.4	Gap analysis: Limitations of current models	43
4	Current State of the Art: Data-driven microstructure-property relationships	45
4.1	Introduction.....	45
4.2	Literature survey	45
4.3	Outlook and summary.....	48
5	Software Tools for Predicting Material Performance	51
5.1	Summary and overview	51
5.2	Overview of particular software tools	52
5.2.1	MUI.....	52
5.2.2	LAMMPS.....	53
5.2.3	EVP-CPFFT.....	54
5.2.4	DREAM.3D	55
5.2.5	ParaDiS	55
6	Gap Analysis and Recommendations	57
6.1	Overview of this chapter.....	57
6.2	Survey of verification and validation approaches.....	57
6.3	Key recommendations	59
7	Conclusions.....	67
	Acknowledgements.....	69
	References.....	71

TABLE OF FIGURES

Figure 1.1. Schematic of a processing-structure-properties model.....	1
Figure 2.1. Coarsening in a deposition layer at mid- and fill-raster of a laser beam during fabrication. The laser raster direction is to the right and the strip at the bottom of the figure is the previously deposited line. Reproduced from [9].....	6
Figure 2.2. SEM images of an SLM aluminum alloy fracture surface (a) before heat treatments and (b) after annealing heat treatment. Taken from [21].....	8
Figure 2.3. SEM image of fatigue crack origin in SLM Ti-6Al-4V. Taken From [24].	9
Figure 2.4. Schematic of functionally fabricated SLM Inconel 718 using variable processing parameters.	12
Figure 2.5. Optical post-mortem micrographs of a creep-fatigue A617 GTA specimen (at weld section) that was tested at 950°C, 1.0% total strain, and a 9,000 sec hold time at peak tensile strain. The specimen showed 103 cycles to failure. Taken from [45].	13
Figure 2.6. High magnification SEM (a) and EDS (b) image of corrosion damage nucleation at secondary phases (inclusions) in AMT SS 316L. The secondary phase may generate localized corrosion due to a different electrochemistry relative to the microstructure. Taken from [55].....	16
Figure 2.7. Schematic diagram of the effects of sub-grain boundaries and inclusions to radiation defects and He bubbles.....	18
Figure 3.1. Typical multiscale material hierarchy for a metal alloy.	22
Figure 3.2. Idealized representation of a pure edge and screw dislocation. Actual dislocations are typically a mixture of these two idealized types.	23
Figure 3.3. A lattice view of a 2D grain boundary.....	24
Figure 3.4. A coherent twin boundary. Note the coincidence of the lattice positions on the boundary plane.	25
Figure 3.5. A typical crystal plasticity finite element simulation. (a) The initial mesh, showing the orientation of each grain using an inverse pole figure map. (b) The deformed geometry after 50% rolling strain. (c) The von Mises stress in the deformed configuration. (Figure reproduced from [113]).....	33
Figure 4.1. Method adopted by Gan et. al to relate processing parameters to the material Vickers hardness. (Image reproduced from [171]).....	48
Figure 5.1. Typical raw MD simulation result: the position of atoms. Here the simulation is of debonding from a Si inclusion in a Cu matrix. Colors show the magnitude of the atomic displacement from the initial lattice position. Figure reproduced from [178].....	53
Figure 5.2. Comparison between CPFEM (a) and CPFEM (b) stress fields for a cracked polycrystal.	54
Figure 5.3. Left: reconstructed microstructure using EBSD images for a Ni-based superalloy. Right: synthetic constructed microstructure with statistics matching the original sample. Image reproduced from [181].....	55
Figure 6.1. Example of some of the datasets provided by AFRL for their modeling challenges. The reconstruction of this type of data requires a team of experts in XRD scanning and reconstruction. Reproduced from [183].	57
Figure 6.2. Comparison between predicted (top) and experimental (bottom) residual strains in a PBF bridge structure, modeled using SIMULIA. Reproduced from [189].....	59

LIST OF TABLES

Table 3.1. Summary of property-prediction modeling techniques.	42
Table 5.1. Survey of physics solvers/multiscale frameworks.	51
Table 6.1. Summary of key gaps and recommendations.	59

1 Introduction

1.1 Overview: why use microstructural models?

This report is a survey of microstructurally-based modeling and simulation methods for predicting the properties of materials made with Advanced Manufacturing Technologies (AMTs). This report focuses on a limited set of technologies likely to be applied to nuclear reactor structural components, outlined in Section 1.3 below. Microstructural models relate the final material properties directly to the material's microstructure – either using physics-based simulations or correlations to microstructural data. Microstructural models contrast with traditional empirical models that correlate property data directly.

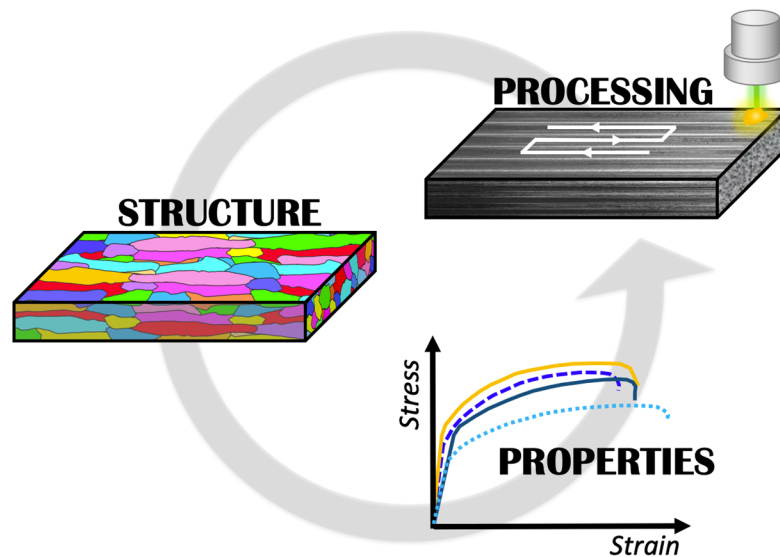


Figure 1.1. Schematic of a processing-structure-properties model.

Why use microstructural models, particularly for AMTs? The main long-term objective is to include microstructural models in complete processing-structure-properties models to accelerate the qualification of new manufacturing methods and material types (see Figure 1.1). A processing-structure-properties model takes as input the material processing parameters and information about the raw material feedstock and from that information predicts the properties of the resulting finished material. These models accomplish this by first predicting the microstructure resulting from the processing step and then relating that microstructure to the final material properties. The microstructural models covered in this report form half of a complete processing-properties model. Section 1.3 describes the relation of this report to an earlier, companion report produced by the same authors, covering processing-microstructure models. Taken together, these two reports describe progress developing complete processing-structure-properties models for AMTs.

An ideal processing-structure-properties model could predict the properties of AMT material without extensive testing of the final material or components. The report details the near-term obstacles to such ideal *ab initio* models. Their direct application to material qualification is unlikely in the near-term and validation testing will be required for safety-critical applications.

However, when combined with experimental test programs, processing-structure-properties models could accelerate the qualification of new AMTs and new materials produced with AMTs by reducing the amount of testing required to qualify a new material or process. This advantage is especially significant for applications requiring long-term material properties, like changes in material properties caused by long-term exposure to the component operating environment or for materials in elevated temperature service.

Additionally, even partly-accurate processing-structure-properties models could be used to optimize AMT processes and focus developers on promising technologies, regions of processing-space, and materials. Given target material properties, for example from component design engineers, solving an inverse optimization problem through a processing-structure-properties model gives the material processing parameters needed to achieve those properties. Solving these types of inverse problems is challenging. However, the processing flexibility permitted by AMT processes suggests the future possibility of a “material-by-design” Integrated Computational Materials Engineering (ICME) approach for which processing-structure-properties models would be a key component.

Even without a complete processing-structure-properties model, microstructural models can be more effective than traditional empirical models in predicting material properties for conditions outside of the database of experimentally measured properties. A key tenant of material science is that the material microstructure controls the final material properties. A microstructural model that represents this fundamental connection tends to be more accurate than a purely empirical model when attempting to make predictions outside the available experimental property database. An example might be a model for predicting the long-term creep rupture of a material in elevated temperature service. A purely empirical model, for example the classical Larson-Miller correlation [1] might miss a mechanism shift that occurs at relatively the low stresses found in operating components but rarely tested because of the correspondingly long rupture times. By contrast, a microstructural model can capture this mechanism transition and lead to better predictions for long-term properties [2]. A similar concept applies to other material properties where direct test data is sparse.

Microstructural modeling will be especially important for AMTs. These manufacturing techniques are relatively new and so extensive material property databases are unavailable. Conventional qualification through extensive testing would impose a large delay between the development of a promising new technology/material and actually putting that material into service. This will be especially true for materials applied in high temperature reactors, where the component design is often determined by long-term material properties, like creep strength, thermal aging, and creep-fatigue damage. However, reducing long-term testing requirements could also impact the adoption of AMTs for light water reactors. While the base component design of LWRs is often based on time-independent material properties, long term environmental effects like radiation embrittlement and stress corrosion cracking significantly affect components in service. Furthermore, the different processing methods, in particular the rapid heating and cooling, used in certain AMTs means that experience with conventional wrought and cast materials may not be directly applicable. Additionally, the processing flexibility allowed by AMTs means that component-to-component or even build-to-build variability in microstructure, and hence, final properties, is likely to be more of an issue when compared to conventional materials produced in large, central locations. Microstructural models could help alleviate this potential qualification problem by

providing direct predictions of batch-to-batch material properties, given some microstructural characterization of each build.

1.2 The purpose of this report

This report is one of a series aimed to assist the NRC in developing the technical information, knowledge, and tools required to assess future licensing proposals using AMT material. The NRC anticipates the use of AMT components in operating reactors in the near future, both in new construction to take advantage of the enhanced flexibility of AMT processes and in fabricating difficult-to-obtain replacement parts [3]. Indeed, an AMT component (a thimble-plugging device) was recently put into service in an operating LWR [4]. As such, the focus of this report is on nuclear applications of AMTs.

This report then surveys the current state of the art in microstructurally-based modeling for AMTs and identifies key gaps and recommendations. Based on guidance from the NRC, the report focuses on nuclear structural materials and not on potential fuel applications. That said, as described in the technical chapters of this report, there have been few direct applications of AMT to nuclear structural materials thus far. Therefore, the literature review includes a wider range of materials. The aerospace industry has largely been driving the development of AMTs and so there is a more extensive body of knowledge on aerospace materials, especially titanium alloys and nickel-based superalloys [5]. Some of this work could be transferred directly to typical nuclear structural materials.

1.3 Relation to the companion report

This report is the second in a collection of two by the same authors. The first report [6] covers processing models aimed at predicting the initial material microstructure. This report covers modeling and simulation methods taking the initial microstructure and predicting key material properties. As described above, taken together these two reports describe complete processing-structure-property models for AMTs. Each separate report also details potentially-relevant aspects of individual processing or microstructural models, again focusing on potential nuclear applications.

To avoid duplication, this second report does not repeat some basic background material contained in the first report on processing models. That report contains a general overview of the different AMTs that may be applied to reactor structural components (described in Table 1 of the companion report), an overview of the materials most of interest for reactor structural applications, and a list of key microstructural features of AMT materials, both as an indication of the key microstructural characteristics to capture in a model and to highlight the differences between conventionally-processed materials and AMT materials. The first report also contained a more detailed description of the potential nuclear applications of AMTs.

The technologies of interest, identified in the companion report, are Powder Bed Fusion (PBF), Directed Energy Deposition (DED), electron beam (e-beam) welding, Power Metallurgy/Hot Isostatic Pressing (PM/HIP), and, to a lesser extent, binder jet and cold spray processes. For

convenience, both reports divide the technologies into fusion-based (PBF, DED, e-beam welding) and diffusion-based (PM/HIP) categories.

1.4 Organization

Chapter 2 contains an overview of crucial material properties for nuclear structural materials and the microstructural features controlling those properties. This chapter then describes the types of structure-properties connections that successful models must include. Chapters 3 and 4 are the key technical content of the report. Chapter 3 covers physically-based microstructural models applied to AMTs and Chapter 4 covers data-driven approaches. Both chapters survey the current literature and then synthesize those surveys into a gap analysis targeting potential issues applying this approach to reactor structural components. Chapter 5 briefly outlines various modeling and simulation software packages available for microstructurally-based simulations of AMT material properties. The focus here is on freely available and widely used tools, though, as the chapter notes, many of these simulations in the literature survey were actually performed using in-house, custom research codes. Chapter 6 summarizes the key gaps and recommendations developed in Chapters 2-5 and formulates a concise list of specific recommendations. Finally, Chapter 7 provides a brief summary of the complete report.

2 Material Properties and Microstructural Connections

AMTs generate unique microstructures that are very different from traditionally manufactured materials, with the added complexity that they can significantly change for the same material and technique due to the variation in processing parameters. The following section delves into the particular microstructural features and mechanisms that affect the key material properties in structural materials of interest for the nuclear community and, where possible, highlights the main differences in material properties between traditional and novel materials due to changes in the microstructure and the underlying processing parameters.

2.1 Monotonic Loading Properties

2.1.1 *Tensile*

The tensile properties of materials are highly dependent on the grain size distribution of the microstructure, which in turn is affected by the build parameters of materials that are manufactured via AMTs. As an example, for Directed Energy Deposition (DED) SS316 the yield and tensile strengths decrease with increased laser power and decreasing scanning speed because this combination results in slower cooling rates and, therefore, larger grains [7]. Additionally, the size of the grains is affected by the location relative to the build. At locations close to repeated passes or a heated base, where high temperatures are held for longer times, the grains are coarser. Locations with faster cooling rates, such as at the top of the build or near a cold baseplate, produce a finer microstructure [7], [8].

In addition to grain sizes, the build parameters can also determine the final grain morphology observed in AMT materials [9] (Figure 2.1). In general, the velocity and the temperature gradient dictate how and when the grain morphology changes from equiaxed to dendritic [10]. A proper selection of these processing parameters can result in evenly distributed dendritic grains without any damaging columnar-to-equiaxed transitional grains, which in turn will result a stronger material with a possible transversely isotropic behavior. As an example, dendritic DED 304L will have a lower ductility in the longitudinal build direction than in the transverse build direction, while the tensile and yield strength will remain isotropic in both directions [11].

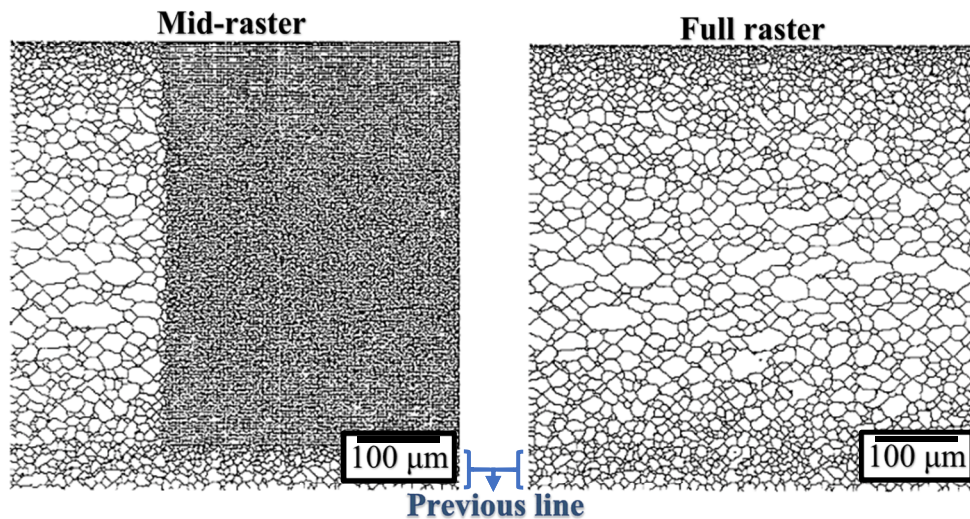


Figure 2.1. Coarsening in a deposition layer at mid- and fill-raster of a laser beam during fabrication. The laser raster direction is to the right and the strip at the bottom of the figure is the previously deposited line. Reproduced from [9].

AMT manufacturing can improve the tensile properties of the material. For SS316L Selective Laser Melting (SLM), a form of laser powder-bed fusion, the strength properties are higher than the corresponding properties of the rolled material due to Hall-Petch grain refinement [12]. In particular, the yield strength is higher than that of wrought SS316 (almost twice the value), while ductility remains high enough to be used for design applications [12]–[14]. Usually, an increase in the yield strength translates into a severe decrease in ductility, limiting the usage of the material. These improved material properties from AMT mean that the designer can not only have the freedom to design complex geometries, but also is able make material savings and weight reductions due to stronger tensile properties [13].

However, the designer must pay attention to the material phases that are generated in the selected material, as a finely equiaxed grain microstructure generated from high-energy AMTs like DED may not necessarily guarantee a stronger material, which would be otherwise the case for an equiaxed microstructure generated via PM-HIP. As an example, in SS304L both the tensile strength and the elongation properties of a DED manufactured material are lower than those of wrought 304L. This is because the transformation from austenite to martensite that provides the macroscopic strain hardening in 304L does not occur in AMTs due to the different thermal histories. In this scenario, phase transformations play a stronger role than microstructural orientations in the tensile properties of the material [11].

Microstructural features like porosity also strongly affect the strength of the material. In SS316, the Young's modulus increases as porosity is reduced, with the material exhibiting 2x the mechanical properties of the base material in the absence of porosity [15]. Furthermore, the shape of porosity also plays a part, with angular porosity affecting the Young's modulus more than round porosity. Therefore, the designer needs to aim for a low porosity with a spherical geometry. Additionally, the designer needs to be careful when selecting the methodology to reduce porosity in the material to ensure that the other mechanisms that improve tensile strength remain largely unaffected. As an example, Hot Isostatic Pressing (HIP) needs to be used with caution because it can reverse the beneficial material properties from AMTs. In the case of Powder Bed Fusion (PBF)

SS316L, the heat treatment in HIP can homogenize the microstructure to grain sizes and shapes resembling those of traditionally manufactured SS316L [16], therefore bringing the tensile strength down to the level of the traditional material. On the other hand, if a design calls for homogenous material properties rather than a material with very high tensile strength (which may be the case for components that need a resistance to impact loads), then performing HIP ensures a dense material with equiaxed and coarse grains [17].

2.1.2 Fracture

The fracture mechanisms of AMT materials can differ greatly than those of traditionally manufactured materials mostly because microstructurally weak features and defects that initiate fracture can be more easily generated during the build process. In materials built with powder-based AMTs such as PBF, DED, and others, the porosity and partially melted powders are usually the location where the cracks initiate. To a lesser extent, the interface of layer depositions are the source of crack initiation, however they are usually a sign of poorly selected build parameters [12] and, unlike porosity, can be easily avoided. Therefore, they are not a large cause for concern for the fracture properties of powder-based AMTs. Additionally, fracture can be linked to internal residual stresses in the material, which can be significantly higher for AMT materials due to the higher thermal gradients and the presence of stress concentrators such as pores and particles.

The fracture toughness may greatly vary for the same material given different AMTs, as is the case for Ti-6Al-4V which exhibits a lower fracture toughness for SLM than for Electron Beam Melting (EBM), especially if the component was annealed afterwards [18]. The microstructure is the cause of this difference: while EBM prevents the creation of a martensitic microstructure and dissolves alloying elements, SLM with annealing actually creates the opposite microstructure, which heavily impacts the fracture toughness of Ti-6Al-4V. It is interesting to observe, however, that if HIP is performed on an SLM component, both the martensite and alloying elements are forced to dissolve back into the microstructure, therefore improving its fracture properties [18] to resemble that of its EBM counterpart. It should be noted that SLM Ti-6Al-4V without annealing performs poorly, and usually annealing is suggested to make the material perform to a reasonable standard.

The fracture behavior will vary greatly for the same AMT given different materials due to the unique microstructural features that dictate the fracture mechanisms in each material. As an example, for SLM Ti-6Al-4V, both horizontal and vertical builds show a similar transgranular fracture surface with mixed brittle and ductile deformation, where the interaction of the porosity with the constituent particles plays a key role in the tensile fracture behavior of Ti-6Al-4V. On the other hand, SLM PH1 stainless steel exhibits widely different fracture surfaces on the horizontal and vertical builds, with both directions exhibiting cleavage fracture. The fracture of samples built in the vertical direction are dominated by brittle fracture and intergranular macro cracks, whereas the tensile samples built in horizontal direction are dominated by the coalescence of micro-cracks and micro-voids [19]. The anisotropic tensile fracture behavior of SS PH1 may be attributed to the directional distribution of porosity, with the grain morphology playing a secondary role. As a result, for SS PH1 the designer has to concentrate on the interaction of pores with the grain boundaries instead of the evolution of phases that dominate the fracture behavior of Ti-6Al-4V.

To improve the mechanical performance of AMT components and lessen the anisotropic fracture behavior that is often observed in AMT materials, designers usually utilize a combination of heat treatments, hot isostatic pressing and surface treatments [20], [21] to bring the performance of the

AMT material up to the level of its traditionally manufactured counterpart [17]. With proper use of these post-processing treatments, AMT components are capable of exhibiting ductile fracture in directions both parallel and perpendicular to the build, with a fracture surface similar to that of traditional material (Figure 2.2) [13], [22]. The designer must be careful when using these post-processing techniques because, while HIP/surface/heat treatments minimize porosity and remove residual stresses, this series of postprocessing methods are not only detrimental to the manufacturing chain in terms of costs and time, but also are difficult to apply on parts with complex geometries or internal features.

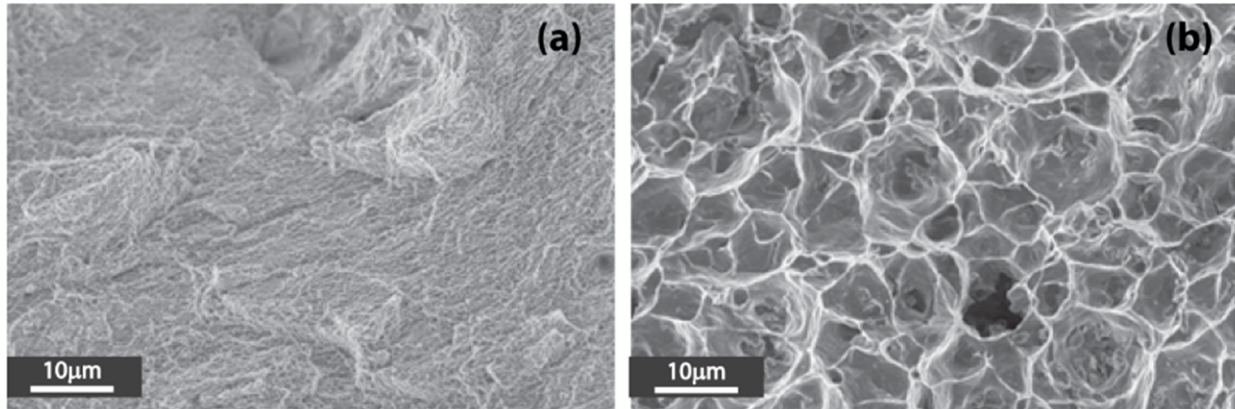


Figure 2.2. SEM images of an SLM aluminum alloy fracture surface (a) before heat treatments and (b) after annealing heat treatment. Taken from [21].

To avoid the use of costly and complex post-processing techniques, engineers are focusing more on the microstructure generated via AMT as a feature that can be tailored to control the behavior of mechanical properties such as tensile fracture. Even in the presence/absence of pores, the microstructure dictates the distributions of stresses and strains, both of which affect material failure. As an example, we can look at SLM Ti-6Al-4V, a material with a complex multi-phase microstructure that is very sensitive to thermal processes. In Ti-6Al-4V, the former β phase boundaries that enclose microtextured regions and the α phase major axis orientations help localize strains inside the Widmanstätten microstructures. To counteract this strain localization, the manufacturer has to decrease the size of β grains during the solidification process, which can be achieved by both reaching higher cooling rates and by creating a building strategy that minimizes the reheating of the material [23].

2.2 Cyclic loading properties and fatigue

2.2.1 Fatigue strength and degradation

The special microstructures of AMT materials induce variability in the damage formation and evolution mechanisms of fatigue. Usually, fatigue damage evolution has three stages: fatigue crack initiation, microstructurally small crack growth, and long crack growth. For AMT materials, the fatigue crack initiation usually occurs at large pores (and in some cases at partially melted powder particles) located near the specimen's surface [24] (Figure 2.3). For AMT components that either cannot undergo final machining (i.e. the inner surfaces and overhangs of complex geometries), or are manufactured with techniques that are capable of generating final geometries relatively even surfaces (PM-HIP, binder jetting, EBM, etc.), the crack initiation will be mainly dominated by the surface roughness [25], where the ridges act as a notch that concentrates stresses and can therefore

be directly considered as a large crack problem, and where the different ridges can initiate multiple cracks at once, therefore lowering the fatigue endurance of the component [26]. In the absence of significant surface roughness, the small cracks initiated by pores or partial melts will grow and coalesce in the microstructurally small crack regime, where the microstructure plays an important role in determining the direction and speed of the microcrack. The microstructural cracks eventually transform into a major critical crack that follows macroscale mechanical behaviors (modes I, II, and III) and eventually fractures the material. We can observe these transitions from Scanning Electron Microscope (SEM) surface micrographs, which show three surface transitions: a sharp fracture surface that indicates the location where cracking initiated (which is usually at a pore), followed by clear surface patterns (such as striations and steps) that indicate a microstructural influence on the crack as it grows outwards, and finally a rough and relatively flat surface that exhibits the Mode I behavior of a large crack under tensile loading [27].

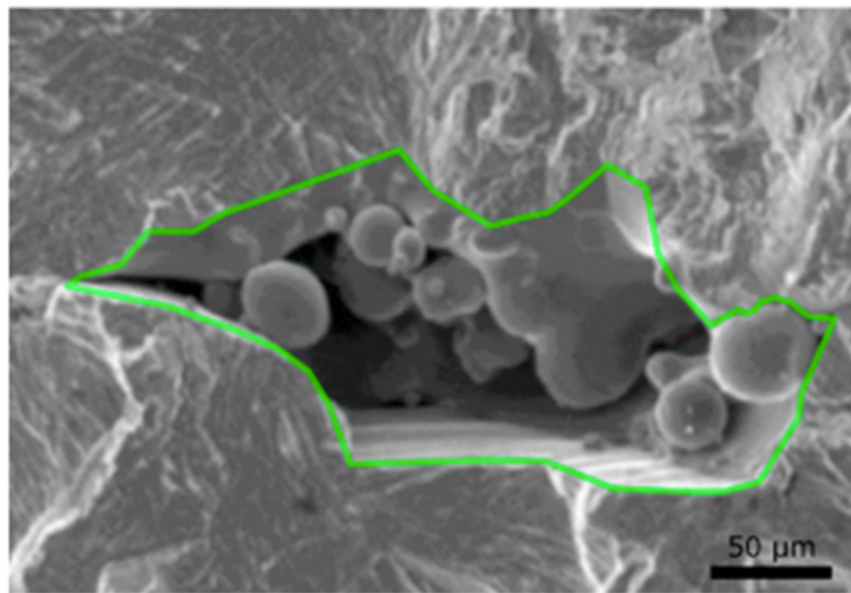


Figure 2.3. SEM image of fatigue crack origin in SLM Ti-6Al-4V. Taken From [24].

During the onset of cracking, we need to pay special attention to porosity in AMT materials because they are largely responsible for the initiation stage, and this stage comprises a large fraction of the overall fatigue life (>70%). In particular, we need to pay attention to the shape of the pore itself, since their geometry combined to the proximity to a free surface dictates the stress concentrations that the material will experience at that pore and, as a consequence, dictates the onset of crack initiation [27], [28]. Since most AMTs result in porous materials, the deposition parameters need to be optimized such that the distribution, shape, and size of the pores is tailored to the distribution of applied stresses in the AMT components [28].

During the small crack growth stage, the microstructure ahead of the crack is the main factor that drives its direction and growth. Depending on the type of material, a small crack may exhibit different propagation mechanisms. All of these mechanisms aim to minimize the amount of energy required to propagate the crack. For Body Centered Cubic (BCC) materials, a small crack will propagate according to the pencil-glide model, and will cross grain boundaries as long as the slip directions where it propagates have a minimal burgers vector. In other words, that the slip

directions are well aligned and pose a minimal expense of energy for the crack to propagate from one slip direction to the next [29].

In the case where slip cracking is energetically too expensive, the crack will tend to grow along the grain boundaries. In this situation, the small crack growth will be influenced by the type of grain boundary (high energy vs low energy), as well as any obstacles or drivers encountered throughout the grain boundary such as particles or pores. In the case of AMTs, it is likely that small crack growth will occur along grain boundaries for AMT materials where a poor selection of parameters will result in weakened grain boundaries where damaging elements and particles have diffused. As a result, intergranular cracking for both small and large crack growth will be observed for AMT materials, which may have been otherwise absent in their traditionally manufactured counterparts [22].

Lastly, during the long crack growth stage, the coalescence of small cracks as well as the macro-mechanics are the driving mechanisms behind the growth rate. Given that the fatigue life of a material is governed by the initiation and growth of cracks, there has been an interest in predicting the growth of small cracks in AMT materials using analytical/FEA representations of long crack growth rates that can account for the high variability in the cyclic fracture toughness of the material [24], [30].

2.3 Time-dependent

2.3.1 Creep

Given the novelty of AMTs and the time required to perform high-temperature experiments, the investigation of high-temperature materials for use in AMTs has mostly focused on aerospace materials such as titanium and nickel-based superalloys [31]. For other nuclear materials of interest, such as stainless steels, the material data is limited to either short qualitative analyses or a few datapoints [32], [33] because the experimental characterizations are costly and time-consuming, and most of the work that studies creep in AMTs is driven by the aerospace industry. The silver lining is that this sector has been studying high-temperature alloys from a microstructural standpoint before AMT was implemented, which has resulted in both a better understanding of the effect that microstructural features have on creep as well as on a microstructural approach to most studies that relate to aerospace components manufactured through AMTs.

One of the most commonly used Ni-base superalloys in aerospace is IN718, the mechanical performance of which is controlled by secondary phase fractions. In particular, the creep behavior of IN718 is affected by the fraction and the level of dispersion of the γ' and γ'' particles, and the orientation of grains within the microstructure. Researchers have shown that the creep performance of SLM IN718 is better than that of wrought IN718, regardless of the post-processing heat treatment used [34] and irrespective of the grain sizes in the SLM material, which means that an increased grain size of the SLM material cannot be responsible for the superior creep strength [35].

The main cause for such an improvement in material properties in IN718 is the very strong $\langle 001 \rangle$ texture that SLM (or any other AMT, for that matter) generates, where regardless of the build direction, as long as the microstructure shows a strong $\langle 001 \rangle$ texture relative to the creep loading direction, the AMT material will exhibit a better creep performance than the wrought counterpart. In addition to the microstructural orientation, the large thermal gradients that SLM generates

permits all initial secondary phases to remain dissolved during solutionizing, which in turn transform into the very needed γ'' particles during aging [34], [36]. Researchers have stressed that designers need to carefully select the processing parameters of AMTs to achieve the desired level of texturing in the microstructure while minimizing material defects. Otherwise, initial defects such as porosity may cause cracks and serrated grain boundaries that may lower the creep performance of the material. A big issue, however, is that the traditional heat treatments to improve material performance in conventional IN718 do not work for SLM IN718, and therefore specialized methods such as HIP + aging need to be implemented to remove pores and improve creep performance [36].

Other works have studied relatively simpler materials, such as 15-5Ph stainless steel generated via SLM [19], [37]. For this material, the AMT generated a much smaller grain size than its traditionally manufactured counterpart. Most interestingly, the AMT generated round particles and highly misoriented grain boundaries that usually do not exist in wrought 15-5PH SS. Most of the material parameters: the microhardness, the tensile strength, and the creep rupture life, were higher for the AMT material than for the traditionally manufactured counterpart, mainly because of the microstructural orientations and the newly found secondary particles. A work focusing on high-temperature properties [37] concluded that the unique microstructural features generated via AMT (particles) are the main reason behind this SS retaining its high mechanical properties at elevated temperature. This selective addition or suppression of phases and microstructural features may prove useful in improving the creep performance of SS 316, which exhibits undesirable phases such as carbides and intermetallic compounds in the δ phase, and ferrite/austenite interfaces at high temperatures [38].

2.3.2 Creep-fatigue

Creep-fatigue behavior is of major importance in high temperature applications as it is often the property that controls the component service life. As a result, creep-fatigue tests are common benchmarks for the aerospace and nuclear industries. Just like in pure creep studies, most of the creep-fatigue tests are limited to a few materials such as nickel and titanium superalloys, with limited information available for nuclear AMT materials. Most as-fabricated materials from raster AMTs such as DED, SLM, or EBM fall in the lower range of the performance when compared to parts manufactured via traditional methods [39].

For creep-fatigue properties, the microstructure plays a major role in the performance of the material. Fortunately, AMTs can be used to tailor the grains in such a way that both creep and fatigue are improved in the material. Given that a coarser grained microstructure is typically better for creep strength, and a finer-grained microstructure is similarly preferred for better fatigue life [40], a recent study of SLM IN718 developed a novel microstructural design that uses the processing parameters of AMTs to control the grain size in the material, where the core is coarse and the outside shell has a fine-grained microstructure (Figure 2.4) [41], [42]. This designed microstructure allowed for the best trade-off between the creep and fatigue performance of the AMT material. A downside was the formation of brittle particles during the AMT (i.e. NbC and Laves-phase particles), which are known to nucleate cracking due to their brittle nature. Therefore, the material has to undergo post-processing heat treatments to remove these undesirable microstructural features. A side benefit of the heat treatments is that the Laves phase particles can

be converted into needle-like $\text{Ni}_3\text{Nb}-\delta$ precipitates that help the creep properties of the material by acting as a barrier to dislocation motion.



Figure 2.4. Schematic of functionally fabricated SLM Inconel 718 using variable processing parameters.

Given the limited information regarding creep-fatigue on AMT materials, we can look at older weld studies to further investigate the creep-fatigue behavior of other materials of interest, such as SS316L. A study showed that SS316 weld metal has a higher creep-fatigue endurance compared to the base metal, with the life being directly related to the hold time [43]. Analyses of the microstructure showed that the greater creep-fatigue life of the weld metal was mainly due to the δ phase -boundaries generated during welding, which helped deflect the crack growth in the material and therefore enhanced its creep-fatigue life. This work also noted that for SS316L, at lower strain rates and long hold times at high temperatures, oxidation influences the creep-fatigue life of the material irrespective of whether it is a base material or a weld, with the differences in creep-fatigue being attributed to crack propagation differences between the base and the weld metals.

Similar studies of 9Cr-1Mo weld metals show that cyclic softening during creep-fatigue occurs in the material because the high dislocation density initially present in the martensitic lath structure rearranges into cells and sub-grains. Unlike in the base metal, the softening of the weld metal has a lower cyclic stress response (lower allowable peak tensile stresses during cycling), which ultimately translates into a lower life for the weld material, due to its heterogeneous microstructure and its soft intercritical region in the heat affected zone (that is, the region at the boundary of the weld). This zone also is responsible for crack initiation and a lower creep-fatigue life, possibly because the strain localization combined with the sub-surface creep cavities in this region work together to initiate and enhance the propagation of cracks [44]. Similar to SS316L, oxidation of the surface plays a part in the reduction of creep-fatigue life when the material is exposed to compressive loads.

In a study of nickel-base A617 welded with gas tungsten arc (GTA), the weld metal showed a dendritic microstructure, with creep-fatigue cracking being interdendritic and occurring only within the weld metal (Figure 2.5) [45]. Although the weld contained some porosity, it was not observed to interfere with the crack path, which could mean that either there was not enough porosity in the material (which is common when welding is performed with a filler wire), or the microstructure plays a stronger part in the development of creep-fatigue failure. In general, the weld metal has a lower creep rate and strain to rupture compared to the base metal, and similar to SS316L, the tensile hold time is directly related to the life of the weld metal. Interestingly, the base metal has a clear saturation in creep-fatigue life after a hold time of ~ 30 minutes [45].

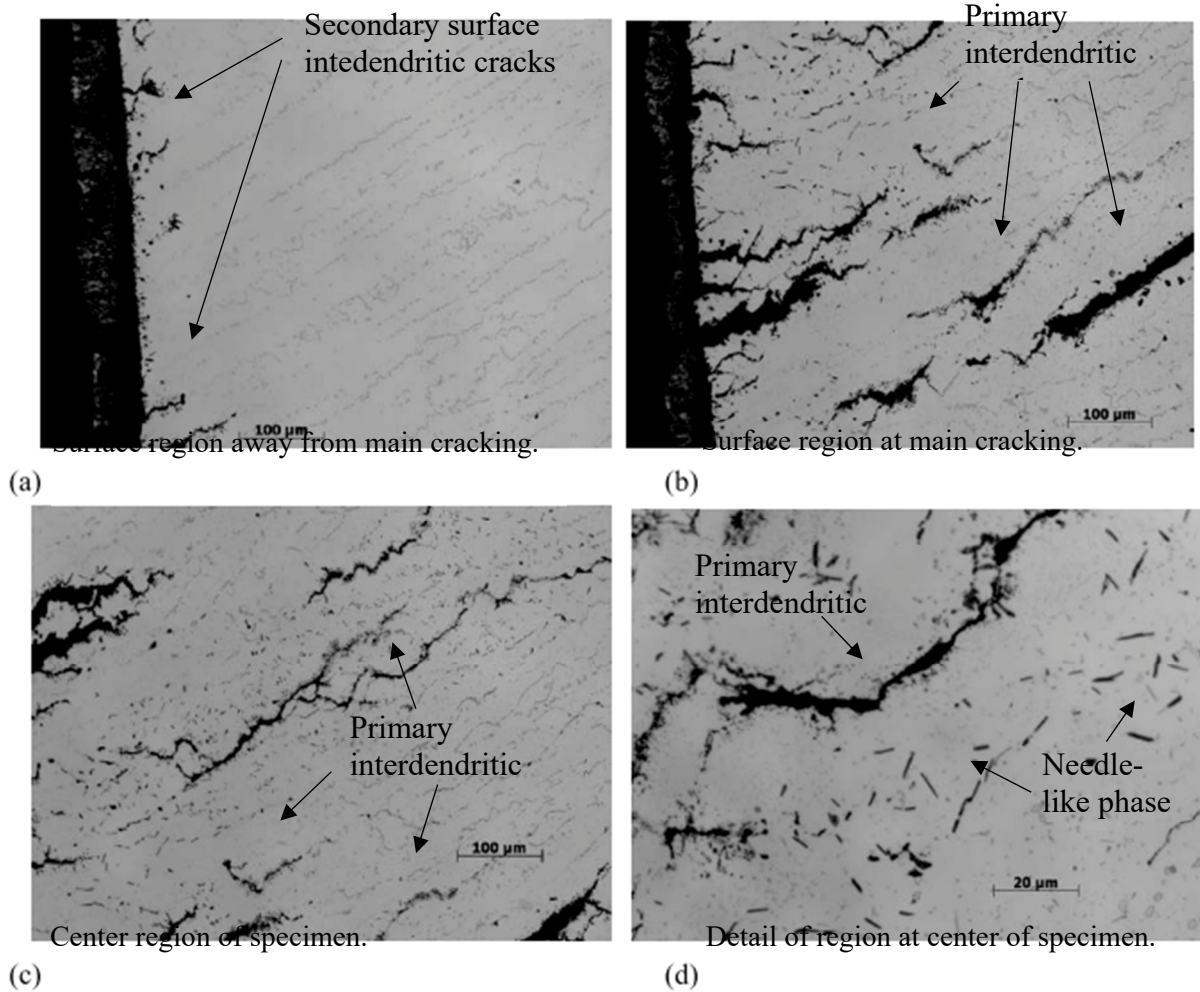


Figure 2.5. Optical post-mortem micrographs of a creep-fatigue A617 GTA specimen (at weld section) that was tested at 950°C, 1.0% total strain, and a 9,000 sec hold time at peak tensile strain. The specimen showed 103 cycles to failure. Taken from [45].

2.4 Environmental Degradation

2.4.1 Thermal aging

Thermal aging describes changes in the material properties caused solely by time-temperature effects. It can be thought of as “in-service” heat treatment of the material. In traditional steels, the strength decreases and the ductility increases with increasing thermal exposure due to the tempering of martensite. During this process, the carbon diffuses out of the martensite, meaning that the distortion of the martensite phase is reduced and thus lowers the residual stresses and strength of the material. If precipitation hardening elements such as copper or aluminum are introduced into dual-phase steels, the opposite occurs and the material is actually strengthened with increasing thermal exposure [46].

Usually, thermal aging is investigated for commonly used materials that benefit from the process, such as austenitic stainless steels, and some other materials that have a severe detrimental effect

such as SS welds and Cast Austenitic Stainless Steels (CASS) [47], [48]. In some instances of austenitic SS, thermal aging is desirable since it increases the tensile strength, yield strength, and elongation to fracture of the material. Although thermal aging is usually studied as a post-processing technique, it is sometimes analyzed as an event that occurs during the life of the component, oftentimes by analysis of the Larson Miller Parameter (LMP). As an example, we have a study of 12% chromium ferritic stainless steel, where the researchers observed that the thermal aging of the material (measured via the LMP) increased as the carbide precipitate sizes increased. As a result, the most aged samples contained very coarse carbide precipitates widely spaced between each other, and the dislocation density in the material decreased. Overall, the study concluded that a decrease in matrix strength from the precipitates, rather than a reduction of grain-boundary strengthening effects, was primarily responsible for the macroscopic softening behavior observed during thermal exposure [49].

When investigating thermal aging in AMT materials, most of the information available comes from studies of PM-HIP materials. For PM-HIP austenitic stainless steels, neither the effect of porosity nor the phase fraction play a significant role in the thermal aging behavior of the material. This in contrast to conventional processing techniques where the phase fractions are used to tune the properties. The researchers verified this insensitivity to phase fractions by observing that the yield and ultimate tensile strengths of different PM-HIP steels increased with a higher aging temperature, regardless of the phase fractions. This behavior is attributed to precipitation hardening from the presence of copper and stress relief from carbon diffusion and tempering of the martensite. Also, researchers found that at some point over-aging occurs at higher temperatures because the carbide precipitates coarsen and causes a decrease in strength. The ductility was also observed to increase slightly with aging due to tempering of the martensite [46].

To a lesser extent, a few scan-based AMTs (L-PBF and DED) have been studied under the influence of thermal aging. One of these studies mainly concentrated on the effect that different types of energy beams have on the microstructure and the thermal aging of DED Ti-6Al-4V. For a DED build processed using a pulsed beam, the microstructure exhibited smaller and more uniform α -lath widths due to rapid cooling within the melt pool, which in turn resulted in reduced thermal aging and a higher performing material [50].

2.4.2 Corrosion

Several materials used in nuclear applications are susceptible to environmental damage such as general corrosion, localized corrosion, and stress corrosion cracking because they work in high temperature water. Each of these behaviors are affected by different mechanisms, and are rarely studied in AMT materials due to the novelty of the technique [51]. For all of these behaviors, corrosion damage is usually affected in varying degrees by factors such as temperature, residual strains and stresses, local chemistry, oxide inclusions, porosity, electrochemical potential, etc. [52]–[54]. In the case of AMT materials, the main factors that designers need to be concerned about are high residual strains/stresses present from the large thermal gradients, the porosity throughout the material, and the highly variable microstructure generated by the processing parameters. This section discusses how these microstructural factors affect the corrosion behaviors.

All corrosion behaviors in AMT materials are generally worse than in their traditionally manufactured counterparts because of challenges unique to AMTs. Materials produced via

rastering techniques such as SLM, PBF, DED, etc, have a dendritic microstructure with unusually large/small fractions of secondary phases present due to the rapid solidification process, which will result in highly anisotropic physical and electrochemical properties throughout the material. As a result, the microstructure (and thus the corrosion behavior) will vary at any point in all directions, meaning that behaviors such as localized corrosion are inevitable (Figure 2.6) [55] and may cause a problem for AMT materials whose corrosion resistance is usually described by general corrosion rates [51]. Both the anisotropy and undesirable secondary phases can be removed from the material using post-processing heat treatments. However, heat treatments may negatively affect the material geometry and elevate the manufacturing cost of the AMT component [56],

therefore the engineer must be cautious during both the design and the manufacturing process of an AMT component subjected to a corrosive environment.

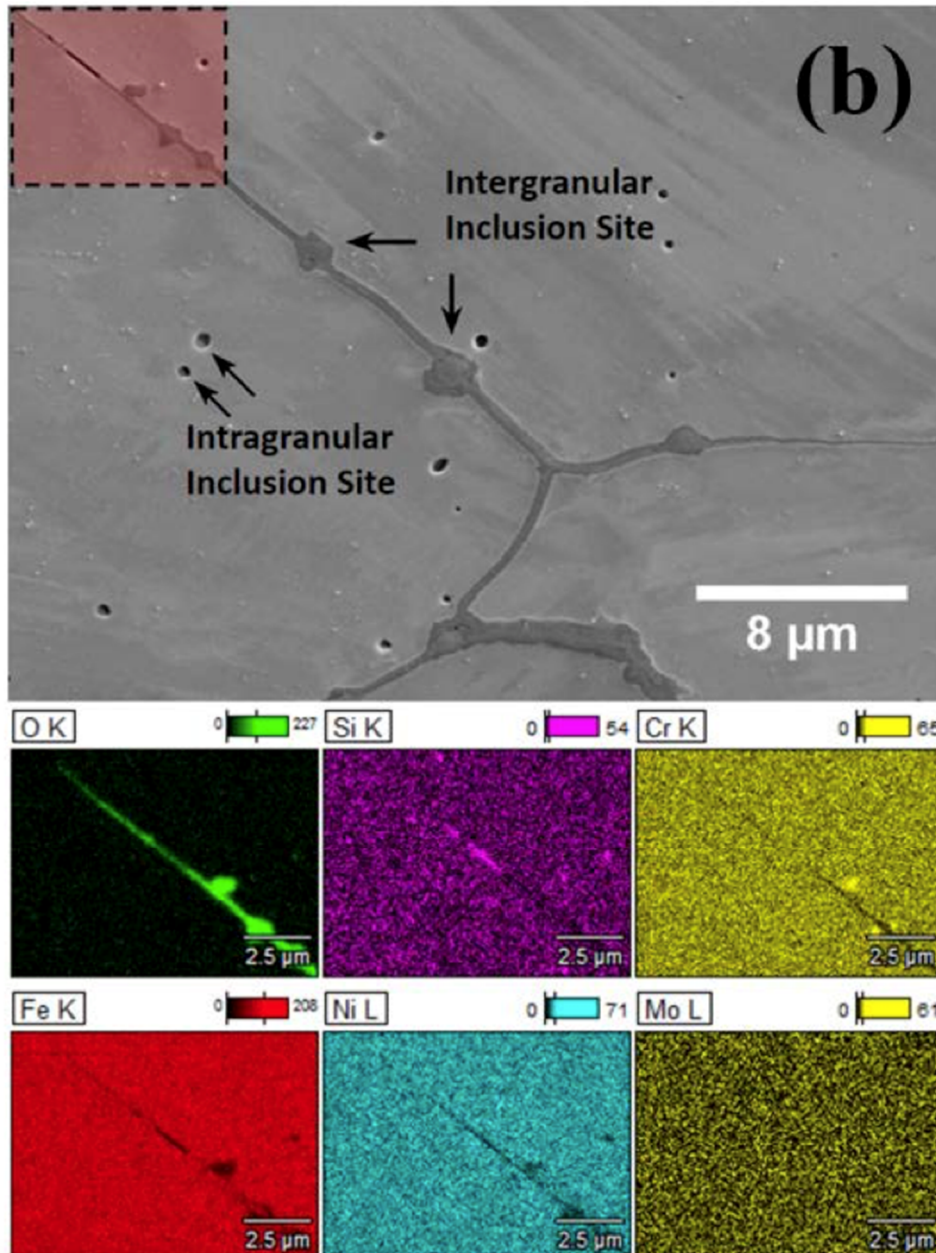


Figure 2.6. High magnification SEM (a) and EDS (b) image of corrosion damage nucleation at secondary phases (inclusions) in AMT SS 316L. The secondary phase may generate localized corrosion due to a different electrochemistry relative to the microstructure. Taken from [55].

In the study of stress corrosion cracking of SS316L manufactured via L-PBF, the researchers found that stress corrosion cracking is driven by the anisotropic microstructure, where the crack followed the material build direction. To a lesser extent, the porosity affected the growth rate, and it was found that relieving stresses did not significantly improve the resistance of the material to stress corrosion cracking. Therefore, to ensure that SS316L performs as well as its wrought counterpart

when exposed to high-temperature water, the material needs to be annealed at high temperatures to ensure proper recrystallization into an equiaxed microstructure [52].

Unlike any other material property, resistance to all types of corrosion is heavily dependent on the chemical composition of both the matrix and the secondary phases in the AMT material. Since AMTs generate vastly different thermal histories than those of traditional manufacturing methods, we can expect different distributions and compositions of the secondary phases inside AMT microstructures. In fact, the high thermal gradients in AMTs can encourage the segregation of corrosion-resistant phases into weak zones in the microstructure. For full density samples of SS 316L manufactured via DED, ferrite can migrate to the grain boundaries, which is uncommon for SS 316L generated via traditional methods since ferrite usually dissipates into the rest of the microstructure. As a result, intergranular localized corrosion is slower for 316L AMT components [22]. Inversely, these high thermal gradients can prevent the segregation of elements, such as Cr and Mo, into the grain boundaries due to the rapid cooling. A side benefit to using AMTs is that high-energy sources can evaporate impurities such as carbides, creating a homogenous microstructure that is more resistant to localized pitting [57].

Several secondary environmental parameters of AMTs may also lead to the degradation of general corrosion properties of the material. As an example, a nitrogen gas environment in AMTs at full pressure will react with SS316L and create chromium nitride, which will locally deplete the material of chromium and thus make it more susceptible to general corrosion. A solution to this depletion is using a partial pressure environment that prevents the material from reacting with the environment [57]. Another study of corrosion in SS316L shows that the parameters of the energy source can also affect the susceptibility of the material to corrosion. The SLM-generated material experienced higher general corrosion and higher density when a higher laser power density was used [58] and it is possible that the higher hardness indirectly translates into a finer grain size and a greater amount of carbides in the material, which would partially explain the material's increased susceptibility to general corrosion. In short, the overall corrosion behavior of the material is closely linked to the local chemistry of the material, and the designer must be careful in selecting which microstructural features remain in the material given the desired performance of the component. For example, while carbides may be desirable for the mechanical performance of the material, they may be undesirable from a corrosion perspective.

2.4.3 Radiation

After long term exposure to radiation in nuclear reactors, nuclear materials will generate a large amount of radiation defects and by-products. These features will result in bubbles, swelling, and radiation hardening that will ultimately alter the mechanical properties of nuclear materials [59], [60]. Additionally, the unique microstructures generated via AMTs will not only cause changes in the material properties, but will also affect the material's resistance to radiation. Therefore, it is important to study the behavior of AMT materials under reactor-representative radiation environments from a microstructural perspective.

One of the materials most regularly studied under radiation is 316L SS. Some ex situ studies of PBF 316L have focused on analyzing the microstructure and properties before and after being exposed to proton irradiation [61] and helium ion irradiation [62]. Neither studies showed the generation of any secondary phases when exposed to radiation. Other in situ studies of L-PBF 316L have focused on studying the underlying mechanisms and microstructure of the material

under heavy ion irradiation [63]. In all three studies, the researchers showed that microstructural features unique to AMTs such as cellular structures, sub-grain boundaries, and nano-inclusions act as defect sinks (Figure 2.7), therefore alleviating the void swelling in the material and improving its performance under irradiated environments.

Under helium irradiation, researchers did not see any significant change to the microstructure developed during the AMT process, and observed that fewer He bubbles were generated during irradiation of the AM-fabricated 316SS material [62]. They attributed these changes to the fact that the AMT material has stable cellular sub-grains and nano-inclusions even after radiation, which increased the fraction of interfaces and consequently influenced the size of the He bubbles as well as their density. The lower density in the AMT material resulted in a lower hardness and swelling after radiation, which meant that the SS 316L generated via AMT shows a better tolerance to helium radiation than the traditional material.

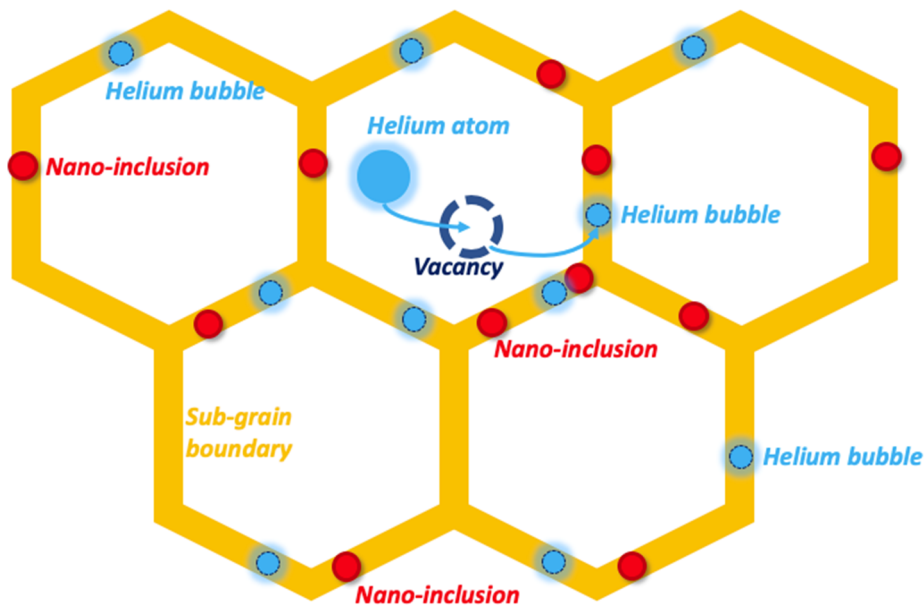


Figure 2.7. Schematic diagram of the effects of sub-grain boundaries and inclusions to radiation defects and He bubbles.

Under heavy ion Kr^{++} irradiation [63], the AMT material only showed a slight increase in dislocation loop density throughout the microstructure, but the microstructure itself remained largely unchanged. In fact, this in situ study showed that the loop density in conventional 316 SS was nearly four times as much as that in the irradiated AMT 316 SS across all dose levels (0–5 dpa). More interestingly, the trapped dislocations in the cellular walls were relatively stable at high temperatures during the in-situ irradiation, which is not commonly seen in conventional 316L. Just like the helium irradiation study, the unique microstructural feature from AMT, that is, the cellular walls with high-density dislocations, acted as defect sinks that reduced the dislocation loop density in the AMT material and therefore improved its resistance to radiation.

Under proton irradiation [61], the microstructure of the AMT material changed due to irradiation-induced dislocation loops, voids, and γ' precipitates. Additionally, the cell structure and dense dislocation walls in the stress-relieved AMT materials recovered and exhibited recrystallization after irradiation, possibly because irradiation is known to enhance diffusion. This study also

investigated the effect on post-processing techniques on the radiation resistance of AMT materials, and found that HIP enhanced the radiation tolerance of PBF 316L because it eliminated the anisotropic mechanical behavior and irradiation-assisted stress corrosion cracking susceptibility of the material, which is associated with the texture of the microstructure. Regardless of the post-processing technique used (stress relieving vs HIP), the AMT material showed a higher density and smaller size of dislocation loops than the traditionally manufactured material, which resulted in the absorption of both interstitials and vacancies and suppression of swelling.

3 Current State of the Art: Physics-based Modelling and Simulation

3.1 A hierarchical description of metallic materials

Looking at a metal alloy with the naked eye it appears to be homogeneous – the color, density, stiffness, and other properties of the material seem to be uniform. Oftentimes, particularly for untextured materials, the properties on this engineering scale are also isotropic – the same in all directions. However, in actuality metals are fundamentally inhomogeneous and, on small length scales, their properties can be quite anisotropic. The apparent uniformity of the material is the product of the vast difference in length scale between the material microstructure and the scale of an engineering component. This jump in length scale conceals the underlying material inhomogeneity and anisotropy by averaging the material’s microscale properties over a vast number of subscale units (for example, atoms or grains). However, the key material physics, which ultimately dictate the engineering properties of the material, lies at the microscale in this inhomogeneous, anisotropic response.

AMTs can produce a large variety of metal alloys so no brief summary can be comprehensive. However, Figure 3.1 illustrates a typical hierarchy of material features in a metal alloy. This hierarchy starts at the scale of individual atoms. Atoms in most metallic materials are arranged in a regular structure – an atomic lattice. Therefore, on this finest scale, metals are crystalline and are composed of a repeating arrangement of atoms. This basic crystal structure determines a number of properties of the material, particularly elastic, electronic, and thermal properties ([64] as an example of a particular method, there are innumerable papers titled “Elastic, electronic, and thermal properties of X,” c.f. [65]–[68] among literally hundreds of others). Alloys can be single-phase; in which case they predominately contain a single type of crystal structure with a roughly consistent chemistry. Alternatively, they can have multiple phases, where two or more crystal structures and associated chemistries coexist on the microscale. Even in single phase materials, the crystal structure of the material can change as a function of pressure and temperature. These phase changes often significantly affect the material’s properties.

Interspersed in this atomic lattice are a large number of defects. These defects can be viewed as breaks in the regular, repeating atomic lattice. There are numerous categories of defects, only a few of which are illustrated in the figure. One of the great discoveries of 20th century material science was the realization and confirmation that these defects determine the inelastic properties of the material [69].

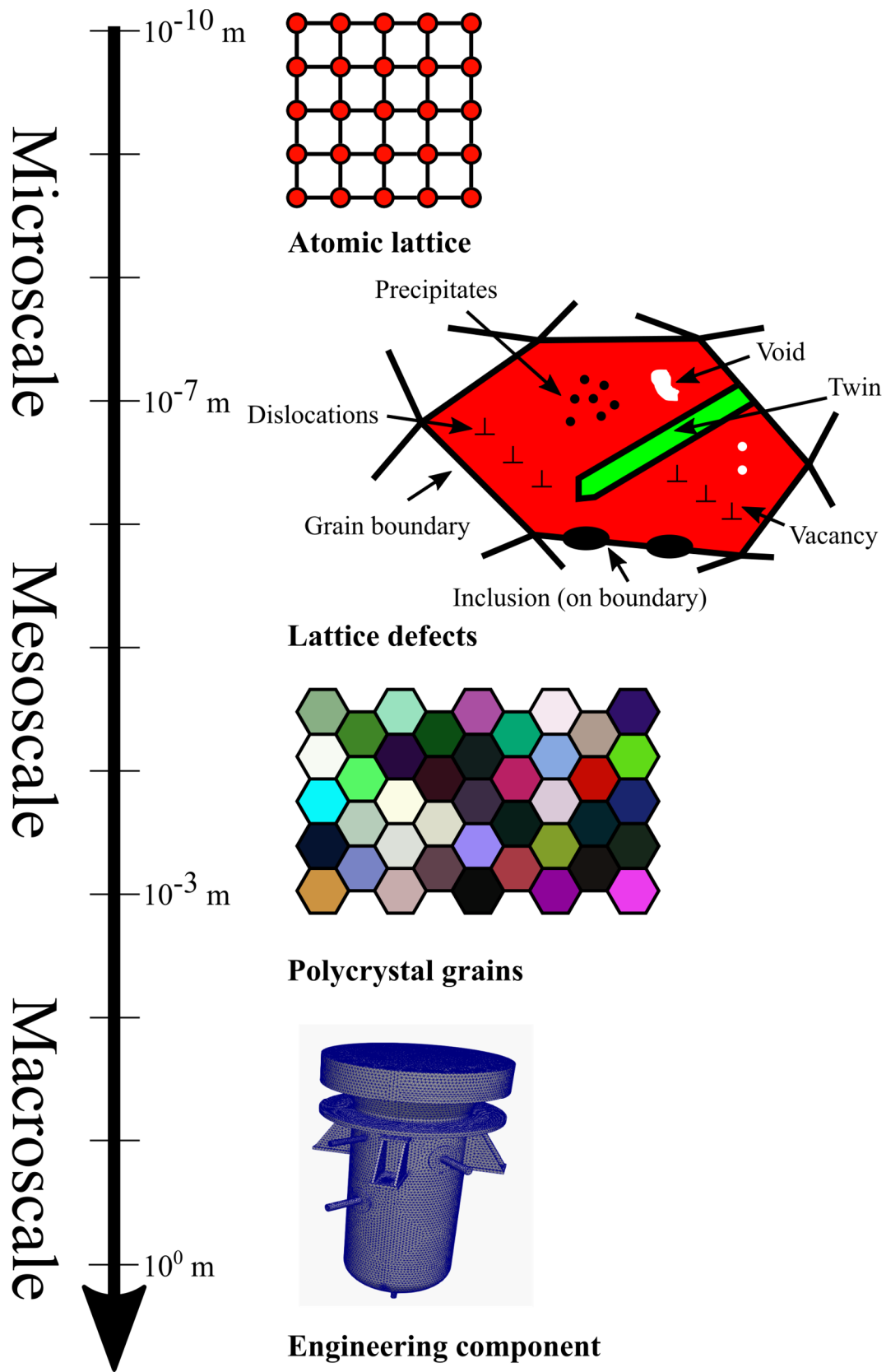
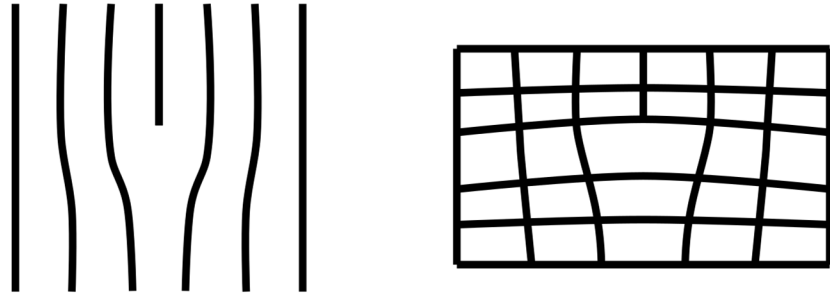


Figure 3.1. Typical multiscale material hierarchy for a metal alloy.

In particular, the figure highlights five types of defects. The first, and perhaps most important, is the dislocation. There are two fundamental types of dislocations – screw and edge (see Figure 3.2) – but both are missing half-planes of atoms [70]. The key feature of a dislocation is that this missing half plane of atoms allows the material to slide through itself – a process called slip – with much less resistance than what would be required to break a plane of atomic bonds in a perfect crystal. In many metal alloys, it is the motion of these dislocations and their interaction with other defects that controls material inelasticity and therefore most of the critical engineering material properties.



Edge dislocation

Screw dislocation

Figure 3.2. Idealized representation of a pure edge and screw dislocation. Actual dislocations are typically a mixture of these two idealized types.

The second form of defect is the vacancy or void. A vacancy is a missing atom in the atomic lattice. The change in the lattice stress associated with this type of defect make it mobile, much like the dislocation, and so the motion of voids through the material through diffusion is another source of inelasticity [71]–[73]. Typically, the time-scale for these diffusional processes is much longer than the time scale associated with dislocation motion and so vacancy-mediated inelasticity is typically more significant for higher component temperatures and longer times, i.e. in the creep regime. A collection of multiple vacancies is a void – a hollow region of material. These voids, either originally included in the material microstructure or grown during service through

dislocation or diffusion mediated mechanisms, often determine when and how the material will fail.

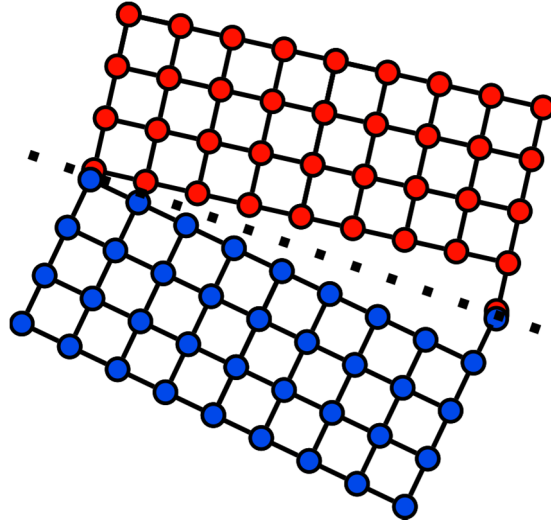


Figure 3.3. A lattice view of a 2D grain boundary.

The third type of defect highlighted in Figure 3.1 is the grain boundary. This is a uniform rotation of the crystal lattice – on either side of the planar boundary the material has the same crystal structure, but the two lattices are rotated relative to one other (Figure 3.3). Grain boundaries, as the name suggests, divide the metal into regions of roughly-uniform atomic lattice called grains. The size and shape of these grains is another critical microstructural feature as, for example, grain boundaries act as barriers to dislocation motion but promote vacancy diffusion [74]. The figure shows a single-phase material. For multi-phase materials, borders between regions with different phases are another type of grain boundary.

A twin boundary can be viewed as a special type of grain boundary where the lattices on either side of the boundary are somewhat coherent resulting in a subset of atomic positions coinciding on the boundary (see Figure 3.4). This feature of a twin means that it can be created with a relatively low amount of energy. Many materials develop these twin boundaries during thermal processing. However, some materials can form deformation twins – twins can form through the combination of thermal activation and mechanical force in the lattice, i.e. stress on the engineering scale. In these materials twinning is another deformation mechanism contributing towards

inelasticity [75]. Twin boundaries are especially significant because they are so coherent – they are, for example, very strong barriers opposing dislocation motion.

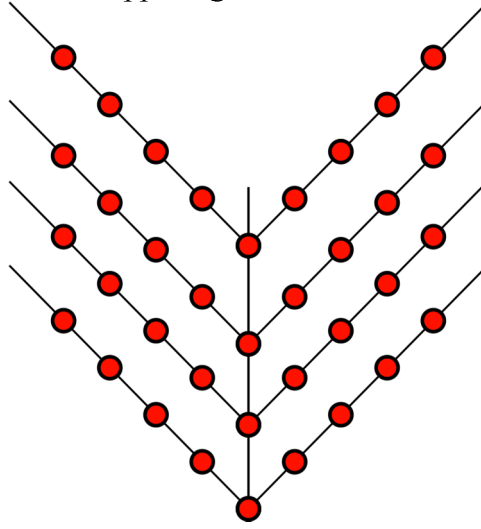


Figure 3.4. A coherent twin boundary. Note the coincidence of the lattice positions on the boundary plane.

The final type of defect illustrated in Figure 3.1 is an inclusion. These are volumes of material with a different chemical composition and, often, crystal structure, than the base material. As indicated in the figure, these precipitates can be small or large and can have preferential locations. These types of defects are alternately called “inclusions” or “precipitates.” As with grain boundaries and the other defects summarized here, these precipitates can contribute to macroscale inelasticity by providing obstacles to dislocation motion and deformation twinning (precipitate hardening [76]). Additionally, stiff inclusions can crack and form nucleation sites for void growth [77].

These defects encompass many individual atoms and so can be thought of as existing on a higher length scale from the base, undisturbed atomic lattice. Of course, just like all the material features mentioned in this section, they are ultimately an arrangement of atoms. However, as discussed below, treating the defects themselves as discrete or continuous features is often useful for modeling.

Each of these defects, with the exception of grain boundaries, can exist within an otherwise-perfect single crystal grain. The next highest length scale often considered in metallic materials is a collection of a large – say thousands – of grains, each containing their appropriate defects. The response of each grain is anisotropic and the material is clearly inhomogeneous. However, the aggregate response of many thousands of these grains is often nearly homogenous and often isotropic. The scale of an individual grain is so small that the engineering properties of the material is the average response of many grains, which often appears to be approximately homogenous. The final scale illustrated in Figure 3.1 is then the engineering scale, where the key material properties for engineering design are measured.

The length scales included in Figure 3.1 are approximate. The descriptions of “microscale,” “mesoscale,” and “macroscale” are likewise approximate. One convention might be that the “mesoscale” begins where the material can be treated as a continuum – resolving the response of

individual atoms and defects is no longer required to determine the response of the material. Note this definition means that “microscale” does not correspond to the classical 10^{-6} m length.

This summary and the illustration in Figure 3.1 portray metallic materials as hierarchical. In the end, material properties of interest are determined by the arrangement of atoms on the finest scale. In practice, modelers think of the material on several different length scales, from the individual atoms all the way to the scale of the engineering component to abstract the details of the material deformation and formulate tractable, useful material models.

3.2 Brief summary and description of modeling techniques

Given that the structure of metallic materials is hierarchical, a comprehensive model of that material should likewise be hierarchical. Different types of modeling and simulation techniques are best suited for capturing the material’s response on different scales. While in principle all material properties originate at the atomistic level, in practice multiple types of models on successively larger length scales are required because a complete atomistic model of a material is computationally intractable. For example, a steel vessel weighing on the order of 1 metric ton contains on the order of 10^{28} atoms. On the other hand, simulations on higher length scales typically require empirical properties describing the response of the system. A multiscale approach builds a hierarchical model of the material starting from a lower¹ length scale [78], [79]. The objective of such an approach is to minimize the number of empirical parameters in the complete formulation by calibrating models on a higher length scale against results from the lower length scale, less empirical models.

There are several flavors of models that need to be categorized. A multiscale model is simply one that encompasses descriptions of the problem at multiple length scales. This definition includes the full multiscale physics modeling approach, denoted in this work simply as “multiscale,” but also classical homogenization (discussed in Section 3.2.3.1) and even numerical methods like multigrid solvers [80]. Both classical homogenization and multigrid methods are multiscale in the sense that they consider the problem at two different length scales. However, they do not apply the multiscale philosophy of using lower length scales to bootstrap the parameters of higher length scale models to reduce empiricism. In particular, in the classical multigrid approach solves the same partial differential equation (PDE) on each scale – all the material parameters are already determined.

A multiphysics model is then one where the model encompasses more than one type of physical model. This includes problems where a single scale includes multiple types of physics– for example a coupled heat transfer/structural continuum mechanics problem – as well as multiscale problems where different physics are solved on different length scales. Our definition of multiscale includes the latter approach. Even here, there are two subcategories. Each length scale might resolve entirely different physics – for example quantum mechanics on the finest scale transitioning to classical energy/momentum equilibrium on higher length scales. Or the physics might fundamentally be the same, but the description of the problem might change. An example

¹ In the multiscale modeling community “lower” is often used to refer to a model on a smaller length scale and “higher” used to refer to a model on a larger length scale. This phrasing is nearly ubiquitous and likely stems from viewing models (as in this section) as hierarchical, starting from smaller length scales on the “bottom” and proceeding through scales to higher length scale models on the “top.”

would be a scale transition between an atomistic, molecular dynamics description of a collection of atoms and a corresponding, higher-length-scale, continuum mechanics description. Both problems solve momentum, mass, and energy balance equations but the problem formulations on the two length scales are so different as to be essentially different physical descriptions.

Another contrast is a physically-based model versus an empirical model. A physically-based model references, in the extreme case, only fundamental laws of physics. By contrast, a purely-empirical model is calibrated entirely against experimental data. Physically-based models are typically better than empirical models at predicting material properties for experimentally unknown conditions. A complete physical model captures all of the relevant material physics and the laws of physics are invariant at different temperatures, pressures, time scales, and environmental conditions. Most models, however, involve a combination of physically-based and empirical components.

A microstructural or microstructurally-informed model is a model whose parameters are a description of the material microstructure, rather than a set of empirical, calibrated coefficients. As described in Chapter 1, this report focuses on these types of models in particular. However, microstructural models need not be multiscale or even physically-based. An example would be a model *correlating* grain size to flow strength. This model is microstructural – it relates a material property to a microstructural feature – but it is neither multiscale nor physically based. Several of the data-driven methods discussed in Chapter 4 fall into this category.

Even without a physical basis microstructural models tend to be more predictive than simple empirical models. A fundamental tenant of materials science is that material microstructure controls material properties. The hope is that by explicitly modeling this connection the model extrapolates better, for example outside the experimental conditions used to calibrate the model. The full multiscale, multiphysics approach is a complete application of this approach where all of the parameters are microstructural and the model determines the material properties *only* from the material physics.

However, as in many of the models described in this chapter, even models that aim for the full multiscale approach typically fall short. Ideally, a “true” multiscale model would require no calibration against experimental data. Experimental data would only be required to validate the model, either on the engineering or the lower scales. In practice, models typically incorporate experimental data on all length scales and hence the property predictions do not derive only from first principles physics. A model that only incorporates first principles physics is called an *ab initio* model. While the vast majority of material models fall short of being truly *ab initio*, even hybrid multiscale models that incorporate experimental data on the lower length scales have a better chance of extrapolating outside the experimental database and yielding better material property predictions when compared to purely empirical models. Such hybrid models are still microstructural physically-based to some extent.

There is a final distinction between a discrete and a continuum model. Discrete models represent the behavior of discrete structures – for example individual atoms or individual defects. Continuum models use a field approximation to smooth out this discrete physics. A continuum model might consider, for example, a distribution of defects across a volume of material. At least

for the typical multiscale hierarchy in metals, the lower length scale models tend to be discrete while the higher length scale models tend to be continuum representations.

To summarize: the ideal microstructural model is an *ab initio*, physically-based description of the key material processes. The ideal multiscale framework assembles such a model by starting at a very small length scale, where *ab initio* modeling is feasible, and transitioning up a hierarchy of physically-based models at larger and larger length scales, propagating the required material information from the lower length scale models. Typically, these models are multiphysics in the sense that different length scales either incorporate different physical phenomena (e.g. quantum mechanics versus solid mechanics) or use different descriptions of the physical phenomena at different scales (e.g. molecular dynamics versus dislocation dynamics). Very few, if any, models actually achieve this idealized modeling framework. Typically, models incorporate experimental data at various stages in the multiscale hierarchy. However, these models are still microstructurally-based and so have a significant advantage over classical empirical modeling approaches.

This section briefly describes a collection of modeling techniques that often contribute to multiscale models of metallic materials. Additionally, Chapter 5 (Table 5.1) contains a survey of software implementing some of the techniques described here. As the focus of this report is on the application of such methods to AMT materials, the section limits the description to identifying the length scale covered by the modeling method, providing a short overview of the approach with high-level references (review papers, where available) and then briefly describing the limitations of the technique. The hope is this information will help inform regulators about the potential and limitations of the various methods.

3.2.1 Discrete approaches

3.2.1.1 *Ab initio* methods: Density Functional Theory and other electronic structure methods

Material properties ultimately originate from the quantum mechanics of the individual atoms composing the material. Ultimately, the goal of these *ab initio* methods is to solve the quantum many-body problem built on the Schrödinger equation and the Pauli exclusion principle [78]. However, in practice models based directly on the wave equations resulting from the interaction of nucleons and electrons are intractable. Approximations based on the density of the electrons, i.e. Density Functional Theory (DFT), are more practical [81], [82].

These types of models are truly *ab initio* – they require no experimental data or empirically-correlated parameters. The ultimate result of these calculations, at least in the context of multiscale modeling, is the effective interatomic potential as described in Section 3.2.1.2. As such DFT provides a first-principles point of entry to the multiscale hierarchy. A model (solely) based on underlying DFT calculations requires no calibration.

However, the limitations of DFT (and other *ab initio* quantum mechanics methods) is the extreme difficulty of solving the quantum many-body problem for realistic systems. This means the method can only be applied to extremely simple atomic species (by limiting the number of electrons and nucleons in the calculation) or through approximations like DFT. In practice then, accurate

interatomic potentials are seldom created solely using direct *ab initio* calculations, but typically will also require fitting the potential to experimental data.

3.2.1.2 Atomistics: Molecular Dynamics and Kinematic Monte Carlo

3.2.1.2.1 Molecular Dynamics

The *ab initio* methods described in the previous section model the interaction of discrete electrons and nucleons. This next category of atomistic methods models the discrete interaction of individual atoms or molecules.

Molecular Dynamics (MD) simulations solve the n -body problem of the dynamic interactions of n atomic or molecular species. The information required to run a simulation is the initial position of the atomics, the atomic mass of each species, and the force between any two pairs of atoms. MD simulations use an interatomic potential to describe these force pairs. Given these three ingredients, very efficient numerical algorithms have been developed to propagate the atomic positions forward in time using high performance, massively parallel computers (e.g. [83]).

MD simulations can provide comprehensive information about the material. Simulation methods exist that can maintain the ensemble of atoms at fixed total energy, fixed pressure, or fixed temperature. MD calculations under these conditions are in thermodynamic equilibrium [84]–[86]. More complicated methods can be used to impose specified average conditions on periodic cells of atoms, for example an imposed average Cauchy stress (e.g. [87]). Preprocessing and postprocessing software can initialize and identify defects in the simulated atomic lattice [88]. Dislocations [89], voids [90], and even (simple) grain boundaries [91], [92] can also be represented.

The primary challenge in simulating the material response using MD is defining the interatomic potential. Focusing on metals, a huge body of work aims to develop accurate potential for a various single and multi-atom systems (e.g. [93]–[95] among a vast number). An additional body of work seeks to develop more accurate forms for the interatomic potential. Early work on liquids used simple Lennard-Jones forms [96] while more modern simulations on metals apply Embedded Atom Models (EAM) [97] and more sophisticated potentials, including Modified Embedded Atom Models (MEAM) [98].

In principle, MD potentials can be completely determined using *ab initio* methods like DFT. In practice, fitting an accurate potential that accounts for all the key features of the material system is extremely challenging and often requires incorporating physical property data, for example thermal, elastic, and electronic properties as well as the observed material phase diagram [94], [99]. Deriving accurate potentials becomes even more challenging as the number of atomic species increases. Accurate potentials for realistic alloy chemistries are not available. Instead, models typically use potentials encompassing the main atomic species. The higher length scale models then account for the effect of the minor elements in the alloys, often in an ad hoc manner.

Given an accurate interatomic potential, the main challenges in applying MD to predict useful, macroscale material properties are the length and time scale issues. Real engineering components contain far too many atoms to represent directly in MD calculations. Instead, typically the MD simulation encompasses a “representative” volume that samples the bulk material response of a single crystal grain, plus associated defects. Again, the higher length scale models must then

account for grain-grain interactions. However, even a single grain in a metal alloy contains more than 10^{12} atoms. This is beyond the limit of even the most advanced current high-performance computers. Despite recent work looking at huge numbers of atoms [100] this limitation on the number of representative atoms means that the continuum material response – even the single crystal response – cannot be directly modeled using MD simulations.

Additionally, the MD method can only directly examine very short time scales. The integration algorithms used to advance the dynamic state of the ensemble impose limitations on the maximum computational time step size [101]. As the time integration cannot be parallelized, this imposes a severe limitation on the time scale resolvable by MD simulations. Typical MD time scales must start on the order of the period of atomistic vibrations, around 10^{-15} s. Simulations can propagate the dynamics of the system through many thousands or even millions of time steps, but this still leaves total simulation times on the order of 10^{-9} s. This means that direct MD simulations can only examine material processes occurring on very short time scales. MD approaches are then directly relevant only to extreme loading events, of the type not typically found in nuclear components. The main use of MD then is to extract parameters for higher length scale models.

3.2.1.2.2 Kinetic methods

Kinetic methods are a way to overcome some of the length- and time-scale challenges associated with MD. Rather than considering the direct motion (dynamics) of discrete atoms, these approaches consider probability densities [78]. This concept can be applied to either the spatial or temporal components of atomistic models. If applied to the spatial location of molecules, kinetic methods work with the probability distribution of particle locations, providing a direct bridge between discrete atomistic and continuum approaches. However, these methods are not commonly applied to metals because of the difficulty in modeling realistic particle-particle interactions [78].

When applied to the temporal component of an MD model, the kinetic method works with the probability of atoms transitioning states, rather than direct integration of the n -body system. The Kinetic Monte Carlo (KMC) method is one approach for propagating such simulations forward in time [102]. KMC is notable here because it allows a discrete atomistic simulation of metals on long time scales, capturing diffusional processes [103]. As such, it can be applied to examine processes like vacancy diffusion [104] and dislocation climb [105], [106], which are key microscale components of multiscale models for creep, thermal aging, and other long-term material processes.

The limitation of KMC is that it considers only very long time scales where events occur solely through diffusional processes. This means that it cannot represent events on intermediate time scales where interactions occur through non-thermal processes, i.e. those most relevant to material properties controlled by non-diffusional processes in metal alloys used in nuclear reactor components.

3.2.1.3 Defects: Discrete Dislocation dynamics

Ab initio methods represent discrete electrons and nucleons, while MD and the KMC method represent discrete atoms. A logical next model, at a yet longer length scale, is a model that looks at discrete defects in the atomic lattice. Given the importance of dislocations in determining the

properties of metallic materials, Discrete Dislocation dynamics (DD) models are often used to bridge length scales in models of metal alloys.

As the name suggests, DD methods treat dislocation lines as discrete objects in a simulation [107]. These dislocation lines move according to rules derived from the mechanics of a single dislocation embedded in an elastic continuum [70]. Moreover, when dislocation lines meet they can react with one another to model junction formation, annihilation, and other dislocation/dislocation interactions [108], [109]. The method has been extended to model the interaction of dislocations with grain boundaries [110], [111], inclusions [112], and other obstacles to dislocation motion. As with discrete MD simulations, the initial configuration of defects can affect the simulation results [113]. Pre- and post-processing software exists to aid in setting up and interpreting simulation results. Simulations, at least in the multiscale framework, often use a periodic simulation cell with an imposed strain or stress on the cell face(s).

The advantage of DD modeling over the other discrete approaches discussed so far is that it can simulate events on a higher length scale. The simulations have no difficulty in representing the grain bulk response of a material, and special configurations can examine isolated grain boundaries, precipitate interactions, and other events of interest. The main disadvantage of DD is that again the dynamics of dislocation motion and the (typically) explicit integration algorithms limit the time step size. Typical time steps in DD simulations are around 10^{-11} seconds – much better than atomistic calculations but still very small. Therefore, as with MD calculations, DD simulations are directly relevant only to fast material processes, which are not typically found in reactor structural materials.

3.2.2 *Mesoscale continuum approaches*

3.2.2.1 *Field Dislocation theories*

As noted in 3.2.1.2.2, kinetic methods are seldom applied to spatially upscale discrete simulations of metallic materials because of the difficulty in formulating an adequate theory for atom-atom interactions. However, these types of theories are the natural bridge between discrete and continuum theories for simple materials like gases or elastic solids.

A direct analog of this approach for metals might be to develop a kinematic (i.e. a statistical mechanics) theory to link discrete dislocation motion to the evolution of a probability density field describing the dislocation density. There have been several attempts to develop such theories (c.f. [114]). While field dislocation theories have been successfully applied in many specialized situations [115], [116], no theory has become widely used in a multiscale framework. The reason likely lies in the difficulty in formulating a general theory encompassing the evolution of the density of both statistically-stored and geometrically-necessary dislocations [117]. There are also difficulties in formulating stable numerical methods for the theories, which often have a strong advection term [118]. However, given the potential for field dislocation methods to overcome the challenges associated with bridging the discrete-to-continuum gap, discussed in 3.2.3.2 below, these methods are a promising direction for future research.

3.2.2.2 *Crystal Plasticity*

Crystal plasticity methods are often the lowest length-scale continuum model in a multiscale model of a metal. Crystal plasticity describes the continuum deformation of a single metal crystal [119]–

[122]. Because this is a continuum theory, standard discretization techniques for partial differential equations can be used to represent large volumes of material consisting of many different grains in a polycrystal [123], [124]. This approach is sometimes called a “fully resolved” or “full field” simulation. Figure 3.5 shows a typical full-field crystal plasticity finite element method (CPFEM) simulation, which fully-resolves the grain and grain boundary structure of the material using a finite element discretization (figure reproduced from [125]). An alternative approach uses the fast Fourier transform to spatially discretize the model (CPFFT). Alternatively, the theory can be used in concert with classical homogenization techniques to represent the average response of the polycrystal without fully-discretizing the domain. One of the more common frameworks for homogenized crystal plasticity modeling is the self-consistent, viscoplastic

(VPSC) [126], which applies the self-consistent, effective medium approach based on Eshelby's solution to viscoplastic crystal plasticity material models.

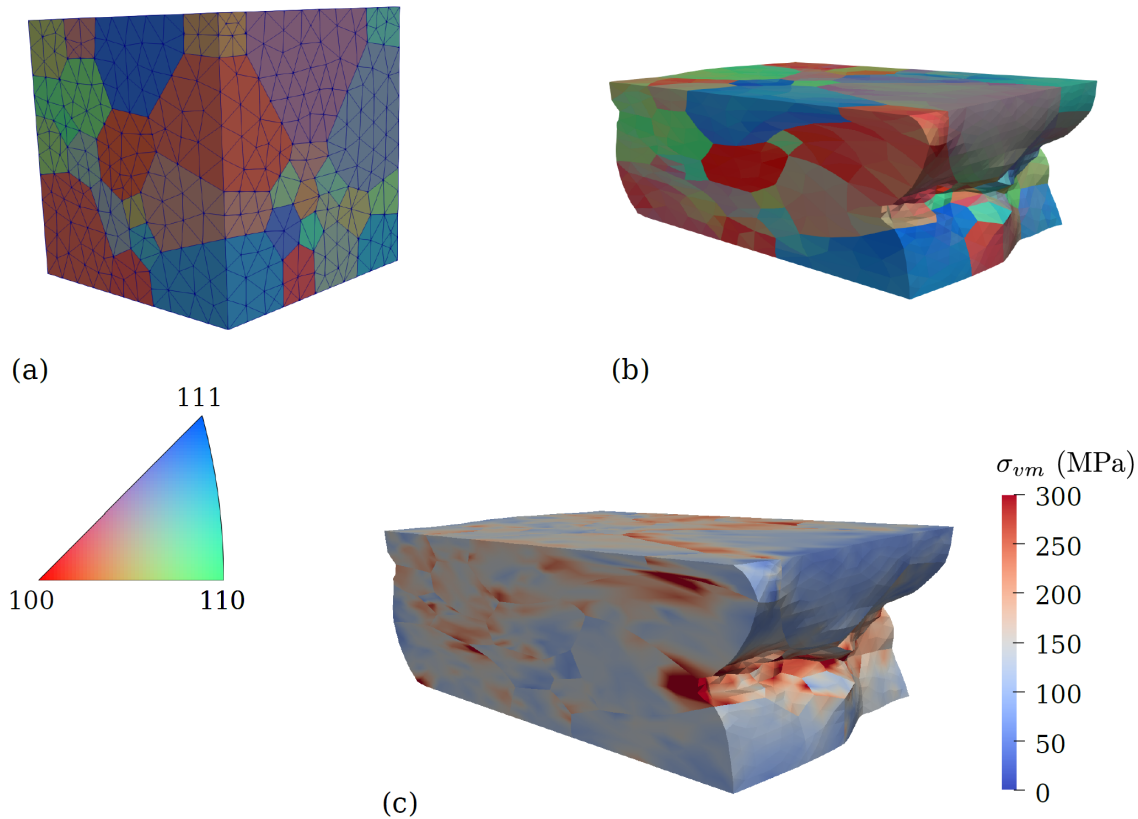


Figure 3.5. A typical crystal plasticity finite element simulation. (a) The initial mesh, showing the orientation of each grain using an inverse pole figure map. (b) The deformed geometry after 50% rolling strain. (c) The von Mises stress in the deformed configuration. (Figure reproduced from [113]).

Crystal plasticity has been very successful in representing material deformation and damage mechanisms in metal alloys (see [127] for a review). Several factors contribute to its widespread use:

- It is a continuum theory and so it can be used to represent essentially arbitrary volumes of material with arbitrary resolution. It works with standard homogenization and discretization schemes. This means it can, for example, be implemented in commercial finite element software with little-to-no modifications. Because it is a continuum theory and solves the same conservation equations as in macroscale structural analysis, upscaling from crystal plasticity simulations is an exercise in classical, formal homogenization (see 3.2.3.1).

- It provides a framework representing the key kinematics of deformation through slip and deformation twinning. Physically-based slip and twin system deformation rules have been developed, often linked to lower length scale simulations.
- It simulates material processes on a scale that can be directly observed using electron microscopy, high energy diffraction, and other modern characterization techniques.

At the same time, crystal plasticity methods have several disadvantages;

- There is no formal connection between lower length scale models, like MD or DD simulations, and crystal plasticity. Field dislocation theories are an attempt at formalizing this connection, but current crystal plasticity models are based on an *ad hoc* kinematic theory that represents slip deformation in single crystals, rather than a formal connection to dislocation mechanics.
- The scale of high-performance computing still limits the scale of fully-resolved crystal plasticity calculations. Simulations of more than 1,000 grains have been completed, particularly using discretization schemes based on the fast Fourier transform. However, this is still far less than the number of grains in a typical metallic component. As such, homogenization, often based on statistical or representative volume elements (S/RVEs) must be used to upscale, with challenges associated with the size of the RVE, applying external boundary conditions, and free surfaces.

3.2.2.3 Damage modeling on the microscale

Full-field crystal plasticity methods provide a continuum description of the grain bulk response. The discretization of the momentum balance equation provides at least a reasonable representation of the mechanical conditions on grain boundaries. However, additional models are required to represent detailed grain boundary physics and to represent damage in the grain bulk or on the grain boundary. These additional models are often embedded as interface-cohesive formulations (on the grain boundaries) [128] or as continuum damage models (in the grain bulk) [129], [130]. Depending on the size of the damaged region, direct representations in a fully-resolved framework are also possible [131].

The form of these models depends on the material – the models capture the physical processes leading to the degradation and failure of the material in service. For metals, typical grain bulk failure mechanisms include cavitation [132], cleavage [133], and fatigue damage [29]. Grain

boundary mechanisms include sliding [134], cavitation [135], and diffusion-assisted cavitation, particularly in creep conditions [2], [136], [137].

Section 3.3 describes damage models used specifically to capture failure mechanisms in AMT materials. Beyond the context of AMTs, there are numerous different models, each tailored to a different type of material. However, these models all share a few common advantages:

- There is a direct analog between damage models of this type and the development of damage/fracture models on the macroscale. Many of the models used in full-field simulations are extensions of models originally developed for macroscale continuum finite element simulations.
- The models are compatible with the length scales represented by mesoscale continuum simulation methods. They can be applied to relatively large volumes of material;

and disadvantages:

- The construction of models is ad hoc, tailored for specific material systems. There is no universal framework for constructing an adequate model.
- There is no direct connection between damage models of this type and finer-scale representations. Models are often developed to be physically based, but the construction of such a model relies on the developer, rather than a formal connection to the subscale physics.

3.2.3 Macroscale modeling: Homogenization and the multiscale method

So far, this section has bypassed discussing how multiscale models transition between scales, focusing rather on describing modeling approaches for each scale in isolation. This subsection covers methods for transferring model information between scales.

3.2.3.1 Formal homogenization techniques

Formal homogenization is the mathematical problem of relating the solution of a mathematical operator (e.g. a linear or nonlinear system of partial differential equations) with rapidly oscillating

coefficients to the solution of an operator with smoothly varying coefficients [138], [139] over the same domain. As an example, consider the linear operator

$$L_\varepsilon u_\varepsilon = f \text{ in } \Omega$$

with L_ε being a linear operator with oscillating (periodic) coefficients with period ε , u_ε the solution over domain Ω , and f the source term. Formal homogenization seeks the coefficients of the linear operator

$$\bar{L}u = f \text{ in } \Omega$$

for $u = \lim_{\varepsilon \rightarrow 0} u_\varepsilon$. That is, mathematical homogenization aims to find a smoothly-varying equivalent description of the problem.

There is a huge body of literature describing formal methods for accomplishing this task (and extending the problem to nonlinear operators, integral operators, etc.). See [140] for a review. These methods are useful in the multiscale context for transferring results between continuum models – for example between a mesoscale crystal plasticity simulation and macroscale effective properties. For fully-resolved mesoscale simulations this approach often uses a representative or statistical volume element (R/SVE) with appropriate boundary conditions meeting the Hill-Mandel conditions [141] and with constraints/external boundary conditions matching the effective macroscale conditions. Other approaches can be used to relate reduced descriptions of the micromechanical problem to effective macroscale material properties [142].

A key challenge for multiscale methods is scale bridging in situations that do not fit the definition of mathematical homogenization – for example bridging between discrete and continuum simulation methods. Kinetic methods and statistical mechanics are the tools for a formal connection (see Section 3.2.1.2.2), but rigorous mathematical methods and standard frameworks are not yet available for metallic materials. Instead, a variety of heuristic methods are employed. The most common is expert intervention – an expert examines the results of the lower length scale calculations and somehow calibrates the higher scale model to that data set. This process often involves optimization of the higher scale model parameters (for example [143]), even employing machine learning techniques (see Chapter 4), but the process is still guided by expert intervention.

3.2.3.2 Multiscale frameworks

This section describes the multiscale process – lower length scale models inform higher length scale models until the simulation framework reaches a scale that can directly model the material properties of interest. Oftentimes scale bridging is simply direct intervention by an expert, in the form of calibrating models to lower length scale data.

Multiscale models can be divided into concurrent multiscale approaches where the highest scale model calls the lower scale hierarchy “live” during the simulation [144]–[146] and non-concurrent models where each of the simulations on each scale are run individually and consecutively and the results transferred in the form of model parameters to the higher length scale models. Only in the context of concurrent multiscale methods does a framework – mathematical or software – for multiscale simulation make sense. For non-concurrent multiscale models, the individual scale model can use entirely separate simulation tools and scale bridging is often done with custom software developed for the task at hand. Concurrent multiscale methods applied to metallic

materials include the FE² approach, where a fine scale finite element model with appropriate boundary conditions provides the constitutive model directly for a coarse scale simulation [147] and various sampling approaches [148]. However, these concurrent approaches are seldom used for metallic materials for anything except model problems because of the very high computational cost. Additionally, these approaches do not address the problem of bridging between discrete and continuum models.

Overall, the development of a multiscale model is often guided by manual expert intervention between each scale. For example, an MD expert might provide a database of simulation results looking at the motion of individual dislocations. A DD expert might then take these simulation results, formulate a DD model, and provide a database of single crystal simulation results to an experiment in crystal plasticity methods. This expert would then calibrate a single crystal constitutive model. At this point formal homogenization can be used to deduce the material's macroscale effective stress/strain constitutive model – which is then sufficient for engineering design [149]. The development of concurrent methods to replace some of this manual hierarchy is a topic of active research. This research has yet to develop an automatic framework for developing constitutive models for metallic materials, particularly starting from *ab initio* calculations.

3.3 Applications to AMTs

This section summarizes the application of microstructurally informed models to predict the properties of AMT materials. As described in Chapter 1, this report focuses on the AMTs of most interest for future nuclear reactor applications and on nuclear reactor structural materials. However, as there has been comparatively little work on these materials, this section includes work on other materials, in particular aerospace alloys, in order to better describe the potential applications to future nuclear systems. Also excluded are examples of multiscale/microstructural process modeling, as opposed to property prediction. As described in Chapter 1, these types of models were covered in a companion report. This survey also excludes a vast number of papers that make qualitative connections between the material microstructure and the resulting material properties as well as models that empirically correlate processing parameters directly to measured properties, focusing only on work on developing physical models linking material microstructure to the resulting material properties. Models that *correlate* microstructure to properties are covered in this report in Chapter 4.

3.3.1 Comprehensive models

Our literature search identified a few attempts at developing complete processing-structure-properties models for AMT materials. These kinds of models span the topics covered by both this and the companion report. The focus in this subsection is on the structure-properties link. However, this subsection highlights these works as the most complete attempts to date at accomplishing the modeling goals described in Chapter 1.

Yan et al. [150] is a high-level overview of a framework for developing process-structure-property models for AMT materials. The approach recommends using design of experiments to select key conditions to model with physical, microstructural models. The framework, as presented in the reference, includes process modeling of SLM powder spreading, melting, and solidification, and property-prediction using crystal plasticity modeling. It advocates using data mining techniques

to then build surrogate models for process/material optimization. This paper provides a good overview of the goals of developing physically-motivated processing-structure-property models.

Ge et al. [151] uses self-consistent crystal plasticity modeling to predict the stress/strain flow curve of a duplex DED Ti alloy. Of particular note, they develop a complete, albeit vastly simplified, comprehensive model spanning from processing parameters (laser power, scan speed, etc.) all the way to predicting the material flow curves. The property prediction part of their model is quite simple, a self-consistent mixing of alpha- and beta-phase flow models with no other microstructural parameters beyond the phase fraction. It is unclear how they calibrate the individual phase models, but the final result accurately matches experimental data drawn from the literature.

Lindgren et al. [152] is another example of an attempt at developing a complete modeling framework starting from processing parameters. The authors develop a model for generic fusion-based manufacturing (i.e. PBF or DED) of Ti-6Al-4V and Inconel 718. The model predicts flow curves, with a relatively simple microstructurally-based model for the flow stress. This work is an application of previous generic models for the effect of thermal processing on the flow curve of the two materials [153], [154], rather than a model specifically aimed at AMT material. Like Yan et al., the model includes processing components for melting and solidification in PBF processes. The framework uses very simple micromechanical models for predicting macroscale flow curves.

Yan et al. [155] describes an ambitious integrated model spanning from process modeling to a homogenized CP model for the material flow curve. Almost uniquely in the context of fully-integrated models, the authors then develop this model further to predict fatigue crack initiation, using a standard fatigue indicating parameter (FIP), in conjunction with the CP stresses. The model (including the introduction of experimentally-observed porosity) reasonably captures the experimentally-observed low cycle fatigue curve. Interestingly, the model predicts a mechanism shift in the predicted fatigue curve for very high cycle fatigue, though this prediction is not validated against experimental data.

Reference [156] is one of the better-validated complete modeling frameworks surveyed in this report. It summarizes a full process-structure-performance model for PBF Ti-6Al-4V. The structure-performance link is via full field CPFEM, including the effect of α/β phase morphology. The model reproduces key macroscale data (e.g. the measured yield stress) but also demonstrates good correlation with microstructure-property trends, for example the correlation between the α grain thickness and the flow stress.

3.3.2 Models targeting flow curve predictions

The next set of models target simulating material flow curves (i.e. stress/strain relations) given underlying microstructural information. For the most part, these are either CPFEM or CPFEM models using standard homogenization techniques to upscale the CP results to the macroscale flow curve or simpler models relying on classical Taylor type homogenization to transition from the grain to the engineering scale.

Hayes et al. [157] is one of the most complete and well-validated models of this type. Their framework produces a microstructural model for the flow curve of DED Ti-6Al-4V using simple Taylor-factor type flow stress contributions related to key microstructural parameters. The flow curve model is quite comprehensive, including the effects of solid solution strengthening, the size

of the alpha laths and colonies, texture, and basic Taylor hardening. The model captures broad trends in processing/microstructure/performance connections and the authors demonstrate it captures the measured yield strength from a large experimental database reasonably well (84% of the data lies within a 5% prediction bound).

The model described in [158], [159] is an interesting example of a micromechanical model for the properties (flow curves) of PBF 316L stainless steel. The model is a CPFEM representation of a realistic AMT microstructure. The model represents individual melt tracks of material, each consisting of randomly-generated Voronoi grain structures. Cohesive models represent delamination failures between melt pools. The modeling framework includes introducing voids on the melt track boundaries to represent prescribed values of porosity. The author uses the model to predict macroscale flow curves. The model is heavily calibrated against experimental data, and yet serves as an example of how a microstructural framework can be used to explain and, to a lesser extent, predict the effect of PBF processing characteristics on the resulting mechanical properties.

Reference [160] produces a very similar model to the one described in the previous paragraph. This model is likewise for PBF 316L stainless steel. Again, the simulation discretizes the grain structure of individual melt tracks and applies a simple crystal plasticity model to predict the final flow curves. Like the other model, the results are 2D only. Additional work [161] extends this model to examine the effects of damage (cracks) on the melt track boundaries. Cunningham et al. [162], by some of the same authors, is a similar approach but looking at the differences in critical pore size between PBF Ti-6Al-4V with and without HIP postprocessing.

Kergaßner et al. [163] is an excellent example of applying a sophisticated microstructural model (a gradient-enhanced crystal plasticity model accounting for slip transmission through grain boundaries) to capture grain size effects in columnar grained Inconel 718 manufactured with electron beam melting. They calibrate the model against a single experiment and were able to reproduce the experimental flow curve in two different loading directions.

The authors of [11] build a simple microstructural Hall-Petch model linking the grain size of DED 304L stainless steel to the yield strength of the material. The results show a large scatter, with errors between the model and the measurements of up to 30%.

Mulay et al. [164] applies homogenized crystal plasticity modeling to predict the flow curve of Ti-6Al-4V. While the paper compares mill-annealed material to PBF material the authors were only able to apply the crystal plasticity modeling to mill-annealed materials, as the crystal model could not capture the complicated grain structure of the PBF material. This is then an example of a negative result: current crystal plasticity simulation methods could not capture the complex microstructure of AMT material. The same authors further develop the polycrystal model in [165], though that work focused on modeling the β phase of generic Ti-6Al-4V rather than developing a model for AMT material.

Zhang et al. [166] describes a semi-empirical model for the mechanical properties of PBF Ti-6Al-4V. The model correlates the parameters of a Ramberg-Osgood flow model to key microstructural characteristics, including the α/β phase fractions and the lath thickness. The model is calibrated

and validated against two sets of experimental results and adequately in predicts the flow curves in the validation set.

The modeling framework described in [167] builds a full-field CPFEM model for the response of HIP and SPS processed ultra-fine-grained nickel. The model incorporates the experimentally-measured microstructure, including grain morphology and texture as measured through EBSD. The model predicts macroscale flow curves and is heavily calibrated to data. The final model predicts the macroscale, experimentally-observed Hall-Petch effect starting from a microstructural Hall-Petch model. The HIP data used in [167] comes from an earlier study by one of the authors [168]. This earlier work develops a simpler self-consistent viscoplastic model for the HIP material flow curves.

Ghorbanpour et al. [169] describes a comprehensive crystal plasticity model for the response of PBF Inconel 718. The paper focuses on the causes of anisotropy in the PBF material. The CP results suggest anisotropy stems from the grain structure and tension/compression asymmetry from non-Schmid effects and latent hardening. Model validation is limited to flow curve comparisons at different temperatures.

3.3.3 Models predicting fatigue initiation

The majority of the models identified in the literature focus on aerospace materials. As such, fatigue prediction is an emerging trend in the most recent work on microstructural models for AMT materials.

The work described in [170] is a call to arms for applying advanced, microstructurally-informed modeling techniques to predict fatigue properties of AMT materials. Interestingly, the authors argue against the use of conventional correlations developed for traditionally-processed alloys, warning that classical approaches could produce poor predictions for complex AMT microstructures.

Veerappan et al. [171], [172] describes the development of a CPFEM model for Inconel 718 and validation against diffraction data. The focus is on using the validated model to examine the critical fatigue pore size in the material by inserting pores of various sizes into the CP representation.

3.3.4 Models including grain residual stresses

The properties predicted by the remaining models do not fit into any of the prior categories. One general theme is models to predict the effect of the grain-level residual stress developed during the manufacturing process on the final macroscale materials properties. These models are interesting because they can be validated against direct residual stress measurements taken via X-ray or neutron diffraction.

Reference [173] describes an integrated experimental/simulation framework for including the effects of grain residual stress developed during processing on the final properties of Ti-6Al-4V fabricated with PBF. The model uses a CPFEM approach and was validated directly against high

resolution digital image correlation data on the grain scale. The authors conclude that incorporating the grain-level residual stresses improved the model predictions.

The work of [174] describes a full-field CPFEM simulation of PBF 304L stainless steel. The focus of these simulations was on predicting grain-level residual stress evolution during annealing, but the study is noteworthy for a detailed comparison to neutron diffraction studies.

3.3.5 *Summary*

This report identifies only around 20 applications of microstructurally-informed property modeling applied to AMTs. By contrast, the companion report describes over one hundred examples of microstructural process modeling. A recent review paper [175] reflects this dichotomy. That review calls for additional work in property modeling, stating “there is a critical need for integrating microstructure information of the material into the model at the macroscale ... in particular for the additively manufactured material.” A separate review paper [176] echoes this sentiment, while noting that while physically accurate multiscale models are needed for ICME

of AMT processes, in the end fast model surrogates will be needed for practical design optimization.

Table 3.1 summarizes the advantages and drawbacks on the modelling and simulation techniques surveyed in this section, focusing only the method used to predict material properties from microstructure and not process modeling, if included in the simulation framework.

Table 3.1. Summary of property-prediction modeling techniques.

Modeling technique	Predicted properties	Advantages	Disadvantages
Full field crystal plasticity	Flow curves, tensile, creep, and fatigue damage	<ul style="list-style-type: none"> Fully physical model for inter and intra granular interactions. Physically-based model for second-phase interactions 	<ul style="list-style-type: none"> Computationally expensive Requires detailed microstructural data
Homogenized crystal plasticity	Flow curves, simplified tensile, creep, and fatigue damage	<ul style="list-style-type: none"> Fully physical model for intergranular interactions Reduced computational cost Works with simplified microstructural information 	<ul style="list-style-type: none"> Simplified treatment of grain/grain interaction Simplified treatment of second-phase interactions
Simple microstructural correlations	Flow curves, including yield and ultimate strength	<ul style="list-style-type: none"> Very computationally inexpensive. Only requires simple microstructural information. 	<ul style="list-style-type: none"> Vastly simplified physics, can often be partly empirical
Fatigue indicating parameters	Fatigue initiation	<ul style="list-style-type: none"> Simple way to represent the initiation of fatigue damage Some models have a strong physical basis. 	<ul style="list-style-type: none"> Some models are largely empirical No agreement on appropriate FIPs in literature
Continuum damage	Creep damage, creep, fatigue, or creep/fatigue crack growth, tensile ductility	<ul style="list-style-type: none"> Simple method for implementing damage propagation in full-field models Well-developed literature 	<ul style="list-style-type: none"> Often only has a tenuous connection to physical processes Discretization issues (mesh-dependence)

3.4 Gap analysis: Limitations of current models

One key gap is the relative lack of work on the structure-properties side of complete processing-structure-properties models. There are two potential reasons why there is less active research in this area compared to process modeling:

1. Researchers regard structure-properties modeling as a “solved problem.” This seems unlikely given the state of the general field summarized in Section 3.2. The development of *ab initio* and fully concurrent multiscale models even for standard, well-characterized materials, remains a significant research challenge.
2. General work on microstructural property models for non-AMT materials will transfer directly to AMT materials. This explanation seems more likely. For example, there is little to no property prediction work specific to AMTs using electronic structure or MD calculations. This is because, at this scale, AMT and non-AMT materials are the same. Exceptions exist for very fine-structured AMT materials, like nanocrystalline materials [177], where AMT specific MD models might be employed.

Another key gap is that most of the existing work has examined aerospace materials and, in particular, Ti-6Al-4V and aerospace Ni-base superalloys. The aerospace industry has been an early adopter and significant driver of AMT research, so this focus makes sense. However, it means that many of the material-specific aspects of current work will not transfer directly to reactor structural materials. The exception is the work on austenitic stainless steels, specifically 304L and 316L steel. Some of the work on Ni-superalloys may transfer to Ni materials slated for use in future advanced reactors.

A similar gap is that most of the work identified here focuses on determining quasi-static material properties, like flow curves, and on fatigue initiation. These properties are certainly relevant to the design of nuclear reactors, particularly LWRs. However, other properties like fracture toughness, ductility, corrosion-resistance, and radiation damage (though not a focus of this report) are critical to reactor design and have received comparatively little attention. Looking ahead to high temperature advanced reactors, there has been little work on physically-based models for crucial time-dependent material properties like creep strength, creep-fatigue resistance, or thermal aging. These properties are significantly more challenging to predict with *ab initio* models given the time scale issue discussed in Section 3.2.

The validation strategy adopted by the authors of the various works surveyed here varies greatly. Formal validation would be necessary for models used to predict design properties of AMT materials seeing nuclear service. This validation might be accomplished by retaining some portion of the available data – macroscale or microscale – from the model calibration process. This “blind” data could then be used to fairly assess the predictive power of the model. Only a few papers adopted this approach.

There are two reasons for the relative lack of formal validation. The first is simply that data is scarce, particularly detailed microstructural characterization that can be used to validate the subscale models in a multiscale framework. Retaining some of this data for validation may not leave sufficient data to fit an accurate model. The second reason is that for some of these studies, the microstructural predictions are the entire point of the study. In this context, the multiscale model is not being used to make property predictions but rather to explain the microstructural

cause of observed macroscale properties. Chapter 6 of this report contains a dedicated subsection on validation and verification which explores these issues in further detail.

Surprisingly, few works highlight the role microstructural modeling (or even process-structure-property modeling in general) can play in hastening the qualification of new materials and AMTs. The introduction to this report lays out a general vision, but further peer-reviewed work on establishing qualification frameworks is necessary to develop a community consensus on how microstructural structure-property models will play a role in qualification.

Finally, we did not identify any *ab initio* modeling work for AMTs nor any concurrent multiscale property-prediction modeling. This is not surprising as these types of models are exceedingly rare, even for conventionally-manufactured materials. Given the limitations of current *ab initio*, multiscale models regulators should not expect to see multiscale modeling used to support the qualification of a new AMT material without direct testing in the near future. There are many challenges to first overcome, as outlined in Section 3.2 above. Most notable are the computational difficulties of concurrent multiscale methods and the theoretical difficulties in transitioning between discrete and continuum models of metallic materials. Much more likely is an approach that uses microstructural models to improve the quality of material property predictions for well-characterized materials in regions where direct property measurements are difficult. Examples might include long-term creep modeling of materials where short-term test data is available. As described in the introduction to this report, these types of microstructural models are likely significantly more accurate than conventional, empirical extrapolation techniques.

However, there have been a number of notable successes for microstructural/multiscale modeling applied to AMTs. For example, the model described in [157] for DED Ti-6Al-4V was well-validated and explains most of the variation in the measured yield stress over a wide set of processing conditions. More generally, all of the models summarized here at least qualitatively contribute to our understanding of microstructure-properties connections (and, as a result, processing-structure-property linkages). This qualitative understanding could be used by license applicants to focus their experimental and validation efforts on particular regions of processing space likely to yield desirable final material properties. This approach is the most likely near-term application of microstructural, physically-based models to AMTs.

4 Current State of the Art: Data-driven microstructure-property relationships

4.1 Introduction

The development of structure-property relationships is a critical step in the optimization of additive manufacturing processes for improved reliability and performance. As described in previous sections, this might be achieved through phenomenological or physics-based modeling approaches. While typically simple and quick to evaluate, phenomenological approaches require significant effort to develop and may have limited applicability outside of the target material system and microstructural domain. On the other hand, physics-based computational approaches hold promise for extensibility and accuracy, yet also require significant development effort and often incur massive computational expenditures. In contrast to these well-established approaches, data-driven structure-property relationships are more quickly formulated and can be evaluated with low computational expense. This opens the door to inverse protocols for the design of microstructure for target properties and therefore identification of appropriate processing parameters resulting in that microstructure. Furthermore, data-driven approaches may be calibrated with either experimental or simulated data. In all likelihood, future inverse design tasks will use some form of data-driven approach. This is because inverse design protocols often require many evaluations of the model chain, which in the case of physics-based modeling may be computationally infeasible. Instead, machine learning can be used to construct surrogates of the expensive physics models or directly build models based on experimental information. The remainder of this section introduces a number of studies that suggest solutions to this problem with various degrees of completeness. Due to the novelty of this field, there is no clear organization of the existing studies other than the materials/methods or ML techniques employed.

4.2 Literature survey

In 2014, Collins et al. described an in-progress methodology for constructing processing-microstructure-property linkages for e-beam manufacturing of Ti-6Al-4V [178]. The authors described a multi-physics heat and mass transfer finite element model to simulate e-beam heating of the sample surface and compositional changes of the sample. They identified phase-field models that depend on local composition and thermal history as their preferred approach to simulate complex microstructure features. Microstructure predictions would be validated with experimentally characterized AMT samples. Finally, machine learning approaches were described to automatically identify physics-informed constitutive equations for the yield strength of the material. Input features to the constitutive model, such as phase volume fractions, and grain-boundary thicknesses, would be identified through stereological approaches. The ideal constitutive model was identified by searching through the combinatorial space of all potential models with genetic algorithms, where the fitness of a particular constitutive model would be evaluated based on similarity to a neural network surrogate of the yield strength as a function of microstructural parameters. Finally, a Monte Carlo sampling approach was employed to propagate uncertainty from the assumed distribution of the inputs to the constitutive model to its outputs, resulting in an extreme value distribution of yield strengths critical to design applications.

This was followed up in 2017 by Hayes et al., where they applied some of the techniques in the 2014 work to develop models for the yield strength of a variety of Ti-6Al-4V electron beam AMT manufactured specimens in uniaxial tension [157]. Specifically, they demonstrated the development of constitutive equations for yield strength using the previously described neural

network and genetic algorithm approach, only in this work incorporating a strength knock-down effect for soft textures, and a strong impact of Taylor hardening. In contrast to the 2014 framework, AMT- $\alpha+\beta$ stress relief, AMT- $\alpha+\beta$ HIP, and AMT- β annealed samples were produced and the microstructures experimentally characterized as inputs to the machine learning approach. As a result, yield strength predictions were within approximately 5% accuracy and cumulative distribution functions were produced that would be useful for determining the chances of the material not meeting minimum design allowables.

In 2016, Miranda et al. presented a detailed processing-property analysis for 316L stainless steel using an analysis of variance (ANOVA) approach on top of the response surface methodology (RSM) [179]. In this work they studied the effects of laser power, scan speed, scan spacing, and part orientation on shear strength, hardness, and density through 96 experiments and a quadratic regression model. While density was considered in the analysis, the effect of processing variables on the microstructure was not studied beyond qualitative correlations through the analysis of micrographs. Note that all 48 samples for each orientation were used in fitting the quadratic model, so there was no external validation dataset.

In 2018 Mutua et al. developed a processing-structure map for L-PBF of maraging steel [180]. In that work they studied the impact of processing parameters including laser power, scan speed, pitch, and spot diameter on relative density, surface morphology (e.g. balling, shrinkage, and undermelting), and mechanical properties. Mechanical properties were characterized via Vickers microhardness for a large number of conditions, and by standard tensile tests for as-built and solution-treated/aged conditions. This map was entirely experimentally constructed and required a large number of experiments. This study resulted in a processing-structure map that identified zones of varying structure optimality (and associated defects) for scan speed versus laser power.

In 2018, Kappes et al. developed processing-structure relationships for L-PBF of Inconel 718 powder based on a massive dataset of experimentally characterized samples [181]. In this work, a total of 3630 samples were produced and evaluated, representing a range of coupon positions, orientations, recycled powder feedstock fractions, and laser incidence angles. All other processing parameters, including laser settings, atmosphere, and powder layer thickness were maintained at the manufacturer recommended settings. Electron microscopy and X-ray computed tomography were employed to characterize statistics of the sample porosity. These microstructure features included volume, equivalent diameter, neighbor distances, volume fractions, and sphericity. This work employed the random forest (RF) ML technique to connect processing parameters to the porosity statistics because of its ability to accommodate examples where one or more input feature is not available. While the study revealed a number of interesting trends with respect to powder quality (e.g. recycling and presence of undersized powder) and porosity morphology, the RF regressor did not reveal strong correlations between the processing variables and porosity statistics of interest.

In 2018, Yan et al. developed a physics-based multi-scale framework for processing-microstructure-property modeling of metallic additive manufacturing. At the lowest length-scale, electron or photon interactions with the material causing local heating were modeled. The authors described a model chain consisting of micro-scale models of heating due to photon/electron-material interactions, meso-scale models for powder and microstructure evolution, and a macro-scale model for the whole build. Mechanical properties including strength, fracture, and fatigue would be evaluated experimentally to validate numerical simulations. As a demonstration of

mechanical modeling capabilities, the authors generated synthetic 3-D microstructures made of columnar grains typical of metal AMT, and compared CPFEM results to those from an accelerated self-consistent clustering analysis machine learning technique [182]. This resulted in a reduction of computational cost of 2500x with 1% error when compared to the CPFEM simulations. Finally, the authors proposed that machine learning surrogates for processing-structure or structure-property relationships could reduce computational cost and enable accelerated design and optimization of AMT.

In 2019, Gan et al. published a machine learning approach that resulted in a full processing-microstructure-property linkage for DED of Inconel 718 [183]. This work is unique in that it leveraged diverse experimental and computational approaches. The authors related processing variables including laser power and mass flow rate to dendrite arm spacing and Vickers microhardness. From the computational perspective, the authors simulated the DED process resulting in energy densities and cooling rates, with which the dendrite arm spacing and microhardness could be estimated using mechanistic models from the literature. The authors also produced samples via DED and characterized their structure and hardness. All of the processing variables, derived processing characteristics (cooling rates and energy density), the dilution, and micro-hardness were used as inputs to a Self-Organizing Map (SOM) [184]. SOMs are an unsupervised machine learning approach similar to feed-forward neural networks that perform dimensionality reduction on the inputs. It is common to create a 2-dimensional map for ease of visualization. In general, the resulting map represents the training examples such that neighboring examples are similar and far apart examples are dissimilar. From the self-organizing map, the

authors suggested processing parameters resulting in desirable dendrite arm spacing and microhardness. Figure 4.1, reproduced from [183], describes the method adopted in this paper.

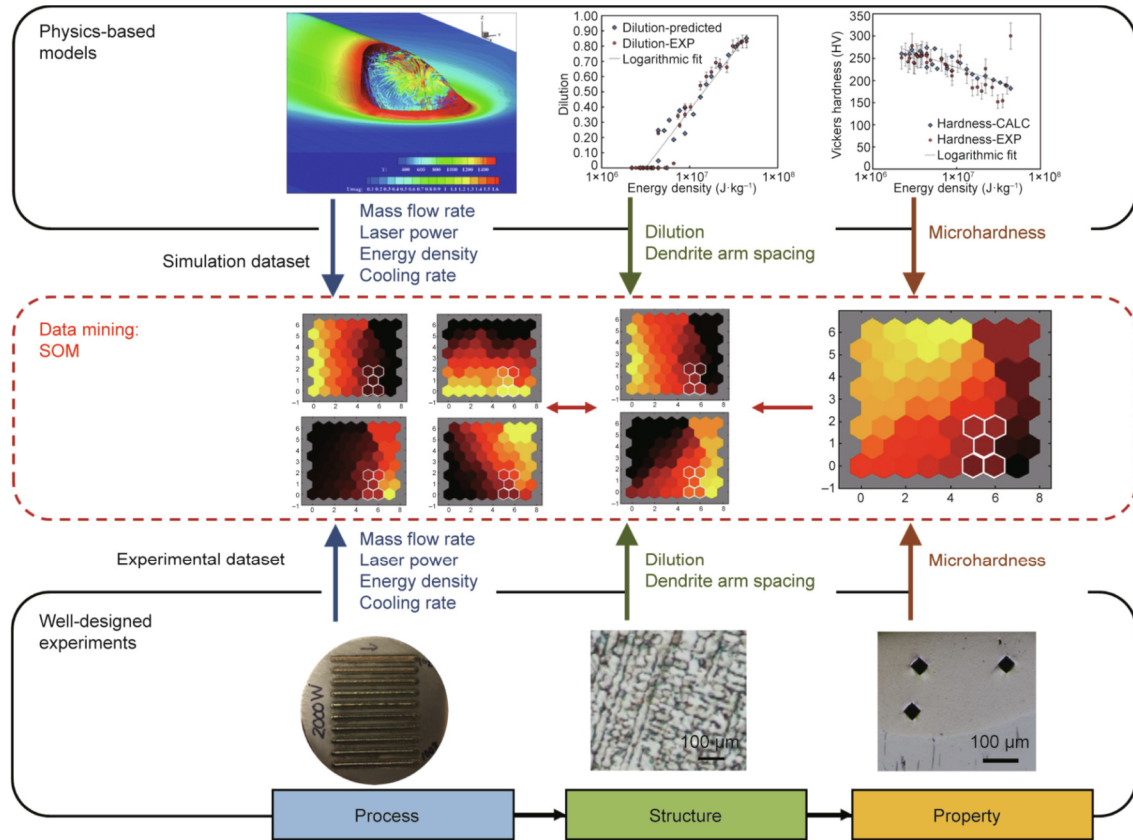


Figure 4.1. Method adopted by Gan et. al to relate processing parameters to the material Vickers hardness. (Image reproduced from [171]).

A 2020 work by Kusano et al. developed ML linkages between microstructure and mechanical properties of L-PBF and heat treated Ti-6Al-4V [185]. In this study, cylindrical tensile specimens were produced with constant processing parameters, and were subsequently heat treated with different times, temperatures, and air/furnace cooling conditions. Microstructures were characterized via SEM and X-ray CT, and mechanical properties were evaluated via uniaxial tensile testing. Sixteen microstructure features, including the volume fractions and averaged maximum and minimum Feret diameters of the prior β and α grains, were extracted from the SEM images using the FIJI software package with the random-forest based Trainable Weka Segmentation plugin [186]. Multiple linear regression was then employed to correlate these features with the mechanical properties of interest. Yield and ultimate tensile strengths were predicted to within 2% mean absolute percent error, but predictions for elastic modulus and % elongation were not successful.

4.3 Outlook and summary

As discussed in the introduction, the development of structure-property relationships in metals AMT is a new field with studies dating back to 2014 at the earliest. As such, limited works are available and address the multiple considerations with varying degrees of completeness. The simplest approaches do not address the microstructure at all, and instead connect processing

directly to properties (sometimes including porosity as a property instead of a structural characteristic). At the next level, studies develop linkages that connect some microstructure quantities (generally volume fractions and grain sizes) to properties of interest (generally strength and elongation/stiffness in some cases). In this category, the two approaches are to use a fully machine learning based linkage with little physical meaning beyond the selected features, or to try to develop constitutive equations in the spirit of those previously used for cast/wrought materials. It is too early to say definitively, but it appears that approximately 5% accuracy can be expected from such an ML approach for a given materials system and AMT. It is not so clear that this approach will work for elastic properties, elongation to failure, creep, or fatigue properties. In future studies, the community should expect a greater variety of machine learning formalisms applied to even more generally defined materials systems and a wider variety of properties. Furthermore, all such studies should provide plots illustrating predicted versus experimental/simulated properties as evidence of the efficacy of the machine learning approaches.

5 Software Tools for Predicting Material Performance

5.1 Summary and overview

This chapter surveys widely or freely available software tools for predicting material properties starting from microstructure. The survey includes formal multiscale frameworks, which are uncommon and, as described in Chapter 3, not often used in actual modeling, but also individual physics solvers often incorporated into multiscale models. The list, shown as Table 5.1, was generated by examining each AMT-specific example of microstructural modeling cited in Chapters 3 and 4, identifying the software tools used in the work, consolidating the list, and eliminating any in-house research codes. Because of the relative lack of discrete atomistic and defect modeling specific to AMTs, we supplemented the list with commonly used simulation suites of this type.

One trend is that many researchers use custom software developed within their research group. For multiscale coupling this is likely because most of the models surveyed here are non-concurrent and so a variety of approaches were used to connect scales. For the single-scale physics, the state of the art in subscale (i.e. micro or meso-scale) simulation methods rapidly evolves, and so commercial software is unlikely to keep up. Furthermore, many researchers have dual roles both as developers of new multiscale simulation methods and in applying microstructurally-informed modeling to specific material systems.

The software type “continuum physics” represents a generic finite element solver that could be used to solve a variety of physical problems (at least structural and thermal, and often more). As noted in Chapter 3, these solvers can be used in the context of CPFEM to simulate the mesoscale response of metal polycrystals. However, the underlying solver technology is the same as the standard macroscale FE analysis. Therefore, see the companion report for a detailed overview of ALE3D, COMSOL, ABAQUS, and MOOSE. Note however that ALE3D and MOOSE both built in crystal plasticity solvers. For the commercial codes (COMSOL and ABAQUS) the researcher supplies the CP constitutive model response with a user material subroutine.

Table 5.1. Survey of physics solvers/multiscale frameworks.

Software	URL	Type	References
COMSOL Multiphysics	https://www.comsol.com/	Continuum physics	[187]
ABAQUS	https://www.3ds.com/products-services/simulia/products/abaqus/	Continuum physics	[156], [158]–[161], [166], [167], [171], [173]

EVP-CPFFT	https://public.lanl.gov/lebenso/	Crystal plasticity	[156], [162]
Dream.3D	http://dream3d.bluequartz.net/	Preprocessing	[162], [172], [173]
ALE3D	https://wci.llnl.gov/simulation/computer-codes/ale3d	Continuum physics	[164], [165]
VPSC	https://public.lanl.gov/lebenso/VPSC7c_manual.pdf	Crystal plasticity	[169]
MOOSE	https://mooseframework.org/	Continuum physics	[174]
MUI	https://github.com/MxUI/MUI	Multiscale framework	[148]
ParaDiS	http://paradis.stanford.edu/	Discrete dislocation	[188]
LAMMPS	https://lammmps.sandia.gov/	MD	[83]

5.2 Overview of particular software tools

This subsection provides an overview of five particular codes. These five were selected to sample different types of systems (multiscale frameworks, discrete and continuum models, and preprocessing tools).

5.2.1 MUI

The authors have no experience using this multiscale coupling framework, but we include it in this summary as an example of an open-source, freely-available concurrent multiscale framework. The software is a library for linking individual physics solvers together into a concurrent multiscale hierarchy – not a physics solver by itself. It aims to simplify the task of linking solvers and, in particular, handling the details of parallel communication through multiple simulation instances.

As previously described, there are very few true concurrent multiscale models described in the literature and none that were directly applied to AMTs. However, this library is an example of how concurrent multiscale coupling works. Typically, in the authors' experience, individual research groups develop their own coupling codes so this is an admirable attempt at standardization

providing a system that can be used to couple individual physics solvers without requiring bespoke software.

5.2.2 LAMMPS

LAMMPS is the canonical MD code. The reference cited in the table ([83]) is the original paper, but many researchers have since contributed to the framework (see <https://lammmps.sandia.gov/authors.html>). Sandia National Laboratories maintains the framework, which is free and open source. LAMMPS is a framework for running an MD simulation and encompasses a vast number of particular simulation types. For metals it is commonly used to run MD simulations of atoms. It supports a range of interatomic potentials, including those most commonly used for metallic materials (https://lammmps.sandia.gov/doc/Intro_features.html). A main focus of the software is on efficient parallel simulation, and the code is essentially a benchmark problem for high performance computing systems (c.f. [189]).

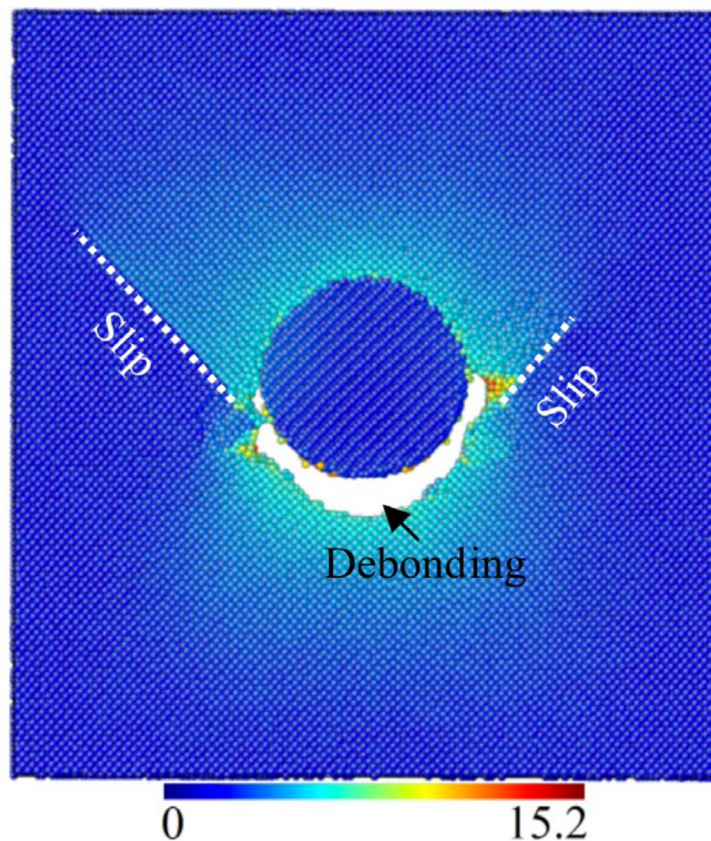


Figure 5.1. Typical raw MD simulation result: the position of atoms. Here the simulation is of debonding from a Si inclusion in a Cu matrix. Colors show the magnitude of the atomic displacement from the initial lattice position. Figure reproduced from [178].

The raw output of an MD simulation is simply the positions of the atoms in the ensemble. Figure 5.1 (reproduced for [190]) shows a simulation result of this type. Of course, visualizing millions of atoms is not a profitable post-processing method. The particular post-processing technique varies depending on the objective of the simulation, but tools exist, for example, to identify and

categorize dislocations and other defects (for example, <https://gitlab.com/stuko/crystal-analysis-tool/-/starrers>).

5.2.3 EVP-CPFFT

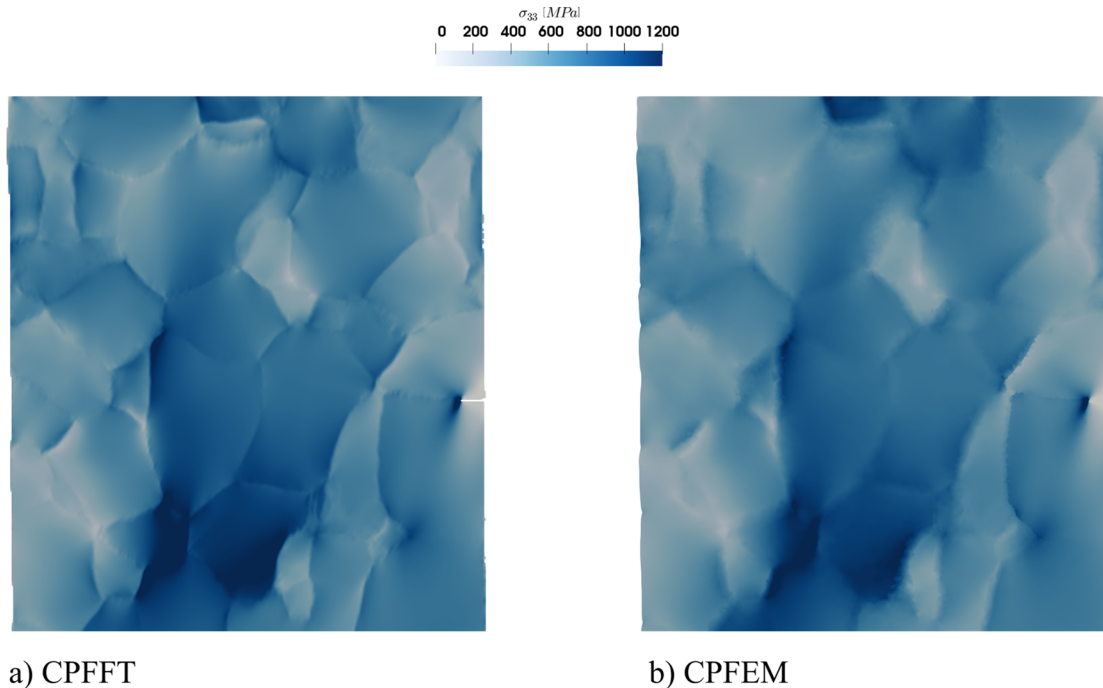


Figure 5.2. Comparison between CPFFT (a) and CPFEM (b) stress fields for a cracked polycrystal.

EVP-CPFFT [124], [191] (elasto viscoplastic-crystal plasticity fast Fourier transform) is a competitor to CPFEM. This particular software is maintained by the originator of the method, at least applied to crystal plasticity, and is developed at Los Alamos National Laboratory. It is a full-field simulation technique and so produces the complete mesoscale displacements, strains, stresses, and so on for a fully-discretized polycrystal. Essentially it competes with CPFEM for these types of simulations. Without delving into a detailed comparison, CPFFT methods tend to be faster than equivalent CPFEM calculations, while CPFEM simulations have more geometric flexibility (i.e. FFT methods require regular discretizations). However, both methods will produce the same answer for equivalent problems [192]. As with MD calculations, the raw field data is only so useful. Typically, further post-processing is applied to the full field results. The advantage of continuum methods is that standard tools (for example, <https://www.paraview.org/>), can be used for this task.

Figure 5.2, adapted from [192], shows the typical results of both CPFFT and CPFEM simulations. This figure is a 2D slice of a 3D microstructural simulation giving the stress distribution in grains of a Ti55531 alloy near a crack. The figure illustrates the level of detail represented in full-field microstructural simulations – the results are the full deformation, strains, stress, etc. distributions within each individual grain in the microstructure. The figure also demonstrates the equivalence between the CPFFT and CPFEM methods – both produce the same results and, at least for a subset

of problems, produce essentially the same results given the same discretization of the microstructure.

5.2.4 DREAM.3D

DREAM.3D is a preprocessing tool [193]. It can be used to generate statistically-consistent representative microstructures, given a description of an experimentally-characterized sample. The base capability of DREAM.3D is to take a stack of images representing slices through a 3D sample of material and reconstruct a volumetric description. An example would be feeding the software a stack of serially-sectioned EBSD characterizations of a volume of material, with the output being a 3D reconstruction of the sample grain structure (see Figure 5.3). The software outputs this 3D reconstruction directly for further use (for example, in a full-field simulation of the sample), generate statistics that describe the material microstructure (for example, grain size distributions, the sample texture), or uses those statistics to create representative, synthetic microstructures (again see Figure 5.3).

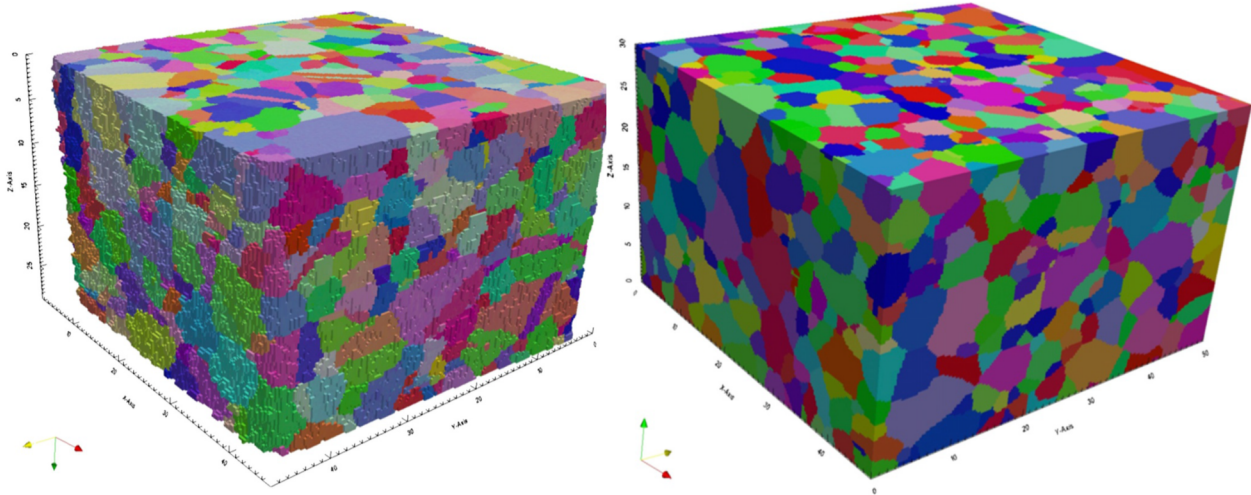


Figure 5.3. Left: reconstructed microstructure using EBSD images for a Ni-based superalloy. Right: synthetic constructed microstructure with statistics matching the original sample. Image reproduced from [181].

Competing software to DREAM.3D includes the neper package (<http://www.neper.info/>), though this package focuses solely on generating microstructures and not on gathering statistics from experimental data [194]. Representing microstructural statistics, using those statistics, and generating statistically-equivalent microstructures is an active area of research and new methods and tools continue to be developed.

5.2.5 ParaDiS

ParaDiS is a discrete dislocation simulation code jointly developed at Lawrence Livermore National Laboratory (LLNL) and at Stanford (<http://paradis.stanford.edu/>) [188]. There are differences between the LLNL and the openly-available Stanford version, but this description is broad enough to apply to both versions. The software simulates the motion and evolution of networks of dislocations. Dislocation lines are discretized into straight segments connected at nodes. The simulation calculates the forces on these straight segments caused by the other dislocation segments in the simulations, dislocation line tension, and image forces caused by

boundary conditions and explicitly updates the location of all the dislocation segment nodes via configurable mobility models. ParaDiS uses advanced numerical algorithms to scale this basic dynamic update process to billions of dislocation segments on large-scale HPC. In addition to the basic positional update and various methods used to applied external boundary conditions, the code also must handle dislocation-dislocation interactions when segments intersect. Developing these interaction models is a topic of active research (e.g. [195]), but the software provides a framework for implementing appropriate rules for what happens when segments interact.

6 Gap Analysis and Recommendations

6.1 Overview of this chapter

This chapter synthesizes the literature survey and gap analysis in Chapters 2-5 into a set of recommendations focusing on future potential issues on applying microstructurally-based models to AMT materials. One key issue will be on how to validate the application of these methods to new AMT materials, particularly given that one of the potential advantages of microstructurally-based modeling is in its ability to reduce the direct testing required to qualify new materials. As such, this chapter first summarizes current work on validating microstructural approaches and multiscale models for AMT materials.

6.2 Survey of verification and validation approaches

While there is a plethora of software and codes in the literature that investigate important mechanisms that affect the final performance of an AMT component, complete examples of validation and verification against experimental data are rare. Of course, individual studies include model validation, but a formal approach, for example a blind application of the model to a validation data set withheld from the initial modeling training/development process, is very uncommon. The scarcity stems from the unavailability of experimental data itself, as acquiring data is time-consuming, complex, and costly, and there is comparatively little data available for AMTs in the literature, as many of the manufacturing processes are relatively new. As a result, most of the robust validation and verification efforts come from government agencies that provide research groups in academia, industries, and national laboratories with high-quality experimental information (Figure 6.1) that the research groups then use as input for their predictions [196]. At the same time, the validation study withholds a set of challenge data that can be used to assess the various model inputs. The validation program sponsor then performs an impartial assessment where they compare the different predicted results against the known, withheld, experimental results.

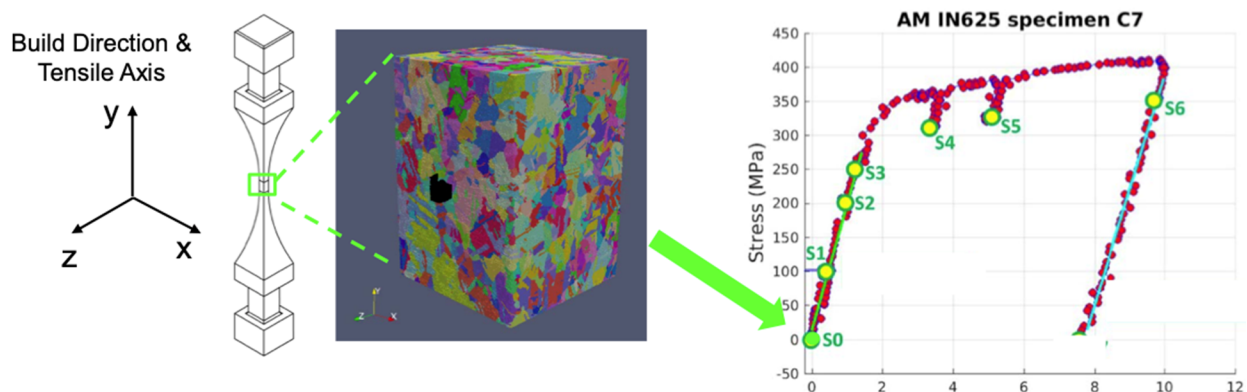


Figure 6.1. Example of some of the datasets provided by AFRL for their modeling challenges. The reconstruction of this type of data requires a team of experts in XRD scanning and reconstruction. Reproduced from [183].

The Air Force Research Laboratory (AFRL) released the Additive Manufacturing (AM) Modeling Challenge Series, which is a part of a larger program focused on including material heterogeneity in design systems for AMTs at both the micro- and macro-structure level. This challenge series

will help develop solutions that are focused on validating/improving the accuracy of model predictions for AMTs [197]. AFRL publicly released data packages containing information of IN625 produced via AMT. Depending on the challenge selected, the participants were tasked with either making process-to-structure predictions, where processing details would be used to predict geometries, microstructural details, and residual strains; or structure-to-property predictions, where the models of representative or explicit microstructures would be used to predict stress-strain behaviors in the material.

In 2020, a team from SIMULIA was awarded the first-place prize (out of 6 submissions) for predicting macroscale residual elastic strains from processing details in a IN625 component, which was the goal for challenge problem 1 of the AFRL Challenge Series: macro-scale process-to-structure predictions [198]. The team used AMT process simulation apps from SIMULIA and 3D Printing preparation apps from DELMIA and the CATIA in this challenge. They used the DELMIA PBF app to recreate the scan path used in the AMT machine, and they used the SIMULIA Additive Manufacturing Scenario app to perform a coupled thermo-mechanical analysis of a high-quality FE mesh where elements were progressively activated to simulate the deposition process.

Similarly, the National Institute of Standards and Technology (NIST) released the Additive Manufacturing Benchmark test series (AM-Bench) in response to the several challenges of AMTs, where NIST publicly releases a series of highly controlled benchmark tests for AMTs that are used to validate the simulation tools of AMTs given different modelling challenge problems [199]. In the metal alloy category, NIST has two types of benchmark tests: The AMB-01 test, which consists of a bridge structure manufactured via PBF that seeks to investigate the residual stress, the part distortion, and the developed microstructure, and the AMB-02 test, which consists of individual laser scan tracks made on a IN625 plate using three different power and speed combinations, with the goal of investigating the melt pool length and the cooling rate of the solidifying material via in-situ measurements.

In 2018, another team from SIMULIA in collaboration with TWI Ltd was awarded the first-place prize of the NIST challenge for predicting the residual stresses within an as-built IN625 bridge structure [200], [201]. Similar to the AFRL challenge, the team used the SIMULIA Additive Manufacturing Scenario App to perform a coupled thermo-mechanical analysis of the AMT component with local activation of elements. Their results led to a publication that highlighted the abilities of their software for the prediction of mechanical responses (Figure 6.2) [202]. Within the same benchmark, the PRISM research group from the university of Birmingham was awarded the first-place prize for predicting the phase evolution during residual stress annealing of an as-built IN625 bridge structure [201]. The group used a computer coupling of phase diagrams and electrochemistry (CALPHAD)-based approach to capture the dendritic segregation of the alloying elements on the precipitation behavior of the IN625 material. The model was able to capture the precipitation kinetics during annealing considering Nb-rich and Nb-depleted regions in a leg of the component.

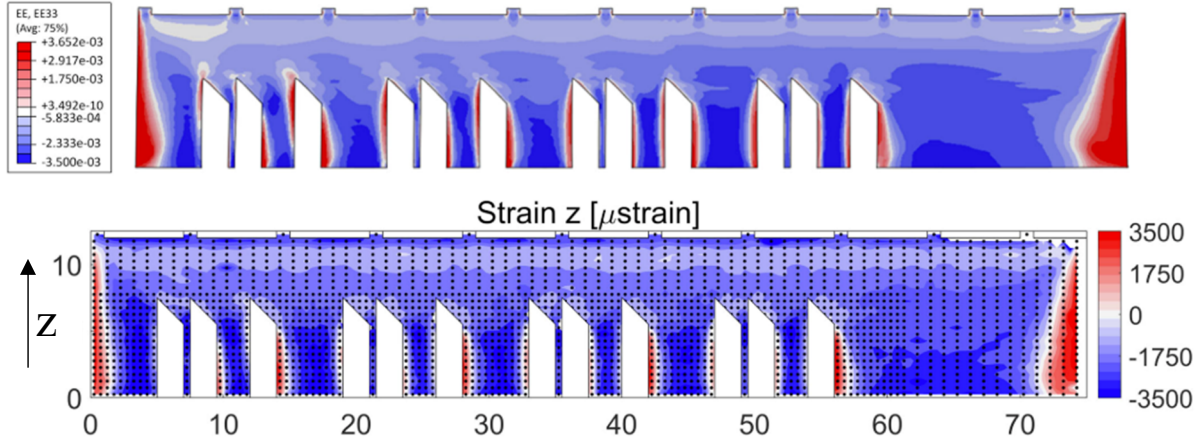


Figure 6.2. Comparison between predicted (top) and experimental (bottom) residual strains in a PBF bridge structure, modeled using SIMULIA. Reproduced from [189].

Under the second benchmark test of the NIST challenge, Applied Organization Inc. (AO) received a second-place award for predicting the grain structure within three single laser tracks on a bare plate of alloy Inconel 625 (IN625). They used the Additive Manufacturing Parameter Predictor (AMP²) software [203], which is an Integrated Computational Materials Engineering (ICME) suite of software developed by their company, to predict the melt-pool geometry, cooling rate, solidification grain shapes, and the microstructure of each scan [204]. Their melt pool width and depth predictions showed a good agreement with the AM-Bench experiment data, whereas their cooling rate was overpredicted. Their dendritic spacing and overall grain shapes were also in good agreement with the experimental EBSD scans.

Currently, there are ongoing efforts by both NIST and AFRL to perform additional challenges in 2021-2022. The resulting validation and verification of the different software used during the challenges can shed some light onto their limitations, their opportunities, and the overall path that we need to take to accurately recreate an AMT component from a multi-scale and a multi-physics approach.

6.3 Key recommendations

Table 6.1 summarizes and prioritizes the key gap and recommendations developed in this report. The recommendations in this table are aimed at the wider research community, not just to the NRC. The subsequent text expands on this summary.

Table 6.1. Summary of key gaps and recommendations.

Rank	Topic	
High	New validation approaches will be needed to realize the potential of microstructural modeling for AMT materials	
	<i>Ranking Rationale</i>	Validation by comparison to direct testing will significantly delay the qualification of AMTs
	<i>Discussion</i>	<ul style="list-style-type: none"> • Comparison to long-term testing is incompatible for rapid qualification of AMTs • Staged qualification might be an option

Rank	Topic	
Low	Improved, more automatic scale bridging methods are required, particularly in spanning between discrete and continuum methods	
	<i>Ranking Rationale</i>	Significant issue in applying the full-multiscale method, but current partial models can be used
	<i>Discussion</i>	<ul style="list-style-type: none"> • Scale bridging between discrete and continuum model is necessary in a full multiscale hierarchy, but current models rely on ad hoc approaches • Formal approaches would greatly reduce the difficulty in constructing full multiscale models
Low	Direct discrete methods must overcome the time-scale issue to be directly applicable to nuclear structural materials	
	<i>Ranking Rationale</i>	Addressing this issue would be a key development, but it is likely a long-term research goal
	<i>Discussion</i>	<ul style="list-style-type: none"> • DFT, MD, and DD simulation time scales are too short to directly address key material issues for nuclear materials • These models can be used to address key mechanisms in higher length scale models, albeit in a way that requires expert intervention
Medium	Additional research needs to focus on nuclear structural materials	
	<i>Ranking Rationale</i>	Reactor vendor economic decision will hopefully guide DOE and other funding organization investment in key materials and technologies
	<i>Discussion</i>	<ul style="list-style-type: none"> • Most current research focuses on aerospace applications and materials
Medium	New methods and additional research will be needed to accurately predict long-term properties	
	<i>Ranking Rationale</i>	Long-term property predictions will be required for high temperature reactors and could be useful for certain LWR applications
	<i>Discussion</i>	<ul style="list-style-type: none"> • Models currently focus on predicting stress-strain flow curves. • Other long-term properties are importance for certain reactor types
High	Qualification methods partly relying on modeling and simulation to replace long-term testing should be developed and validated	
	<i>Ranking Rationale</i>	Increased emphasis on M&S is likely in future qualification approaches, particularly for AMTs
	<i>Discussion</i>	<ul style="list-style-type: none"> • M&S can at least partly replace long-term testing • Integrated approaches including testing, monitoring, and modeling are likely in the near future
Medium	Methods for integrating data-driven modeling approaches into qualification frameworks should be developed	
	<i>Ranking Rationale</i>	Machine learning and other data-driven approaches are increasingly popular, supplementing traditional physics-based modeling
	<i>Discussion</i>	<ul style="list-style-type: none"> • Data-driven approach are often supplementing, complementing, or even replacing traditional physics-based modeling

Rank	Topic
	<ul style="list-style-type: none"> • Applications to AMTs are likely as large dataset are available (for example from in-situ process modeling)

Regulators are unlikely to see applications of the full multiscale method to new AMT materials in the near future

The long-term goal of microstructurally-informed property prediction methods for AMTs is to form a complete process model that predicts the final material properties of interest starting from the input processing parameters. In theory, such a model could predict the final performance of a component assembled using a new combination of AMT/base material chemistry without any direct experimental testing. This approach could revolutionize the material qualification process by drastically reducing the time required to qualify a new material by greatly reducing the required experimental data.

In practice, regulators are unlikely to see this qualification approach pursued in the near future. As described in Chapters 3 and 4, there are significant research challenges that would need to be overcome before this approach could be applied to AMTs. This section highlights some of these challenges, which include the development of a more automated multiscale model development processes, new methods for predicting relevant long-term properties, and the challenge associated with the time scale of discrete atomistic approaches. Significant effort will be devoted to research overcoming these challenges, but it is unlikely anything like an automated multiscale, microstructural model for AMT materials will emerge in the next several years.

However, one of the main attractions of a complete processing-structure-properties model is in solving the inverse problem of determining the processing parameters leading to a target set of material properties. AMTs are particularly good targets for this type of ICME process, as they offer significant processing flexibility. Moreover, the processing-structure models used for tailoring a new material need not be as accurate as a model used to qualify a material. For example, a reactor vendor might use ICME to design a new material for some particular application and then use a conventional or accelerated (see below) qualification approach to qualify it for nuclear service. Regulators should then be aware of the ICME methods in order to better understand the development of the new material, but need not rely on new approaches to directly qualify the material.

Regulators are likely to see applications of microstructurally-based models to extend experimental data on new AMTs and to help qualify new materials and processes

While regulators are unlikely to see *ab initio* modeling used to qualify materials in the near future, they are likely to see increasing applications of microstructural models in aiding material qualification. This approach might combine experimental testing and microstructural modeling, with the goal of reducing, but not eliminating, the testing required to qualify a new AMT material. Of particular importance to vendors would be reducing long-term test requirements. For some high temperature reactor applications, qualifying a material for a 60 year service life requires a 20 year test. This would severely limit the impact of rapidly-evolving AMTs on the nuclear industry

and so there will be a strong research focus on replacing, as much as possible, tests with modeling and simulation.

The most likely applications of this approach for nuclear materials will address radiation and environmental damage and long-term high temperature structural properties. The former could apply to both existing LWRs and new advanced reactors, the latter more likely to apply to future high temperature reactor designs.

The current qualification methods for these types of properties involves dedicated long-term tests. For example, a dedicated set of in-reactor radiation damage experiments might be used to qualify the material for in-service radiation conditions. As another example, long-term creep tests are used to determine the material rupture strength used for component design. Oftentimes this testing is accelerated – for example testing at higher fluence or testing at higher temperature. However, some long-term testing is still required. This significantly increases the time between the development of a new material or manufacturing process and putting it into nuclear service.

As described above, microstructural modeling could be used to reduce this long-term testing requirement and therefore reduce the time required to qualify the material. The key idea, expounded above, is that microstructural models are more likely to remain accurate when extrapolated outside the conditions directly tested by experiments. These models might still be partially calibrated to data but this increased model accuracy might reduce the required length of direct long-term testing needed to qualify the material by extending the acceptable extrapolation period.

Regulators are likely to see these types of applications in the near future, particularly for AMTs where the existing experimental database does not include long-term tests on these new material and manufacturing processes. Regulators will then need ways to assess the accuracy of microstructural models (see the next recommendation). However, combined approaches using experimental data supplemented by modeling predictions represent a bridge between conventional qualification and qualification predominantly accomplished through modeling. In the hybrid approach, some properties, for example those that only require short-term testing, might be qualified through conventional approaches, and some direct test data might be incorporated into the microstructural models used to qualify long-term properties.

The community will need to develop new validation approaches to realize the potential of microstructural modeling and AMT materials

Microstructural modeling approaches for qualifying new AMT materials will need to be validated. However, validation through direct testing, particularly for long-term properties, defeats the main purpose of using microstructural models to reduce the time required to qualify new materials and manufacturing processes. Regulators will then need to consider new validation approaches.

The gold standard for validation remains comparison to a blind dataset. For example, the model developers might retain a subset of the available data from the model calibration process for a data-driven formulation. They might similarly not consider a subset of the data when developing a physically-based model. The most rigorous approach, typified by the AFRL and NIST benchmarks described in Section 6.2, keeps a set of validation data entirely secret from the model developers. These formal benchmark studies can then be presented as round robins, where various models/research groups attempt to accurately predict the withheld data. These types of studies

could build regulator confidence in the general approaches used by the community, though they will not necessarily be helpful in evaluating a particular application.

An additional challenge with these formal validation benchmarks for AMT materials is that they cannot be applied, at least in the near future, to long-term properties. AMT processes are too new to have an extensive long-term property database already established. Moreover, new AMT methods are continually being developed and applied to new materials. One option would be to perform a benchmark study on an existing, non-AMT material with an available long-term property database. Again, these types of studies would not be directly applicable to particular applications of AMT materials in future nuclear components, but could be used to build regulator confidence in the approach.

Future qualification programs might consider a staged qualification approach, particularly for long-term properties. Here, state-of-the-art approaches could be used to predict the relevant long-term material properties used in the reactor design. The component design and construction could go ahead using these predicted properties. But at the same time a long-term testing program would be established with a staggered test schedule designed to produce validation data in the future at regular intervals. This data could then be used to validate the predicted properties and the component operating conditions altered, or the component repaired or retrofitted, if needed.

A staggered qualification plan is a variant of this approach. Here the staggered testing program would precede the component design by some period of time so that a portion of the test data would be available to develop models for “bootstrapping” the direct property tests out to longer-periods of time. Again, the remaining staggered tests could then be used to evaluate the predicted properties.

Another, potentially complimentary, variant of this type of validation plan would involve in situ monitoring specimens. These test specimens would be exposed to the actual reactor operating environment (temperature, radiation dose, coolant chemistry, etc.) and periodically removed and tested to establish the staggered validation data. There are additional complications for in situ monitoring of specimens, notably the development of a robust and representative test article and the logistics of inserting and removing specimens from operating reactors, but the additional complication might be justified for reactors that expose structural materials to a harsh operating environment.

Emulating existing materials is an additional qualification approach for AMTs that could avoid long-term testing, albeit at the cost of sacrificing some of the advantages of AMT methods. Here the goal would be to tune the AMT process to deliver a material with a microstructure, and hence properties, comparable to some well-studied and qualified conventional material. Component design could then proceed using the qualified properties for the conventional material. This approach could be used to rapidly qualify AMT components and retain the geometric flexibility of AMTs. However, it could not be used to take advantage of the control offered by AMT processes

to improve the properties of the base material compared to conventional manufacturing approaches.

Data-driven models will play an increasing role in qualification methods, both by themselves and in conjunction with physically-based models

Chapter 4 summarizes current applications of data-driven approaches to microstructural models for AMTs. The current body of literature is small, given that both AMTs and the current emphasis on data-driven methods are both relatively new. However, this type of approach is likely to continue to increase and so regulators should continue to remain aware of developments in the field.

In principle, validating data-driven approaches is the same as validating physically-based methods. However, given that these methods rely on interpolating and extrapolating from an underlying dataset, additional consideration might be required in validating purely data-driven prediction methods for long-term properties.

A likely application of these techniques is in conjunction with physically-based modeling. For example, machine learning techniques might be used to develop a simplified surrogate model representing a dataset generated from a more expensive physically-based model. Data-driven modeling might be used to bridge scales in a multiscale, physically-based framework. Or physical constraints might be incorporated into data-driven models in order to increase their accuracy, particularly when extrapolating outside of the training data set. An example might be in modeling the deformation of structural materials. A simple machine learning approach might train a model on sets of experimental stress-strain-time histories. However, there would be no guarantee that the resulting model would respect physical laws, for example the Clausius-Duhem inequality (the second law of thermodynamics) or well-established material relations like yield criteria, an elastic domain, etc. Enforcing these constraints should result in more accurate models and may also improve the extrapolated model predictions away from the available experimental data.

The development, by the wider research community, of improved, more automatic scale-bridging methods would greatly simplify the implementation of multiscale modeling, particularly in spanning between discrete and continuum models

Chapter 3 notes that one challenge in applying multiscale physical models to nuclear materials, particularly *ab initio* models, is the difficulty in automatically bridging length scales. This problem is especially acute when bridging from a discrete model (for example MD or DD) to a continuum model (for example, crystal plasticity). The lack of formal frameworks for transitioning between discrete and continuum approaches means that multiscale modeling tends to be a bespoke process, manually carried out by expert intervention. This makes the development of a multiscale model for a particular material or manufacturing process a slow task and limits the application of the approach to AMTs. Partial multiscale models ameliorate this difficulty: for example, formal homogenization solves the scale bridging problem once in the length scales covered by continuum

representations. However, additional research on scale bridging methods will be required to realize the full potential of multiscale modeling for AMT materials.

The time-scale of direct atomistic and defect modeling approaches prevents their direct application to AMTs for nuclear reactor applications

Discrete atomistic and defect simulation methods can only directly access very short time scales. Explicit time integration methods formally limit the numerical time step in these methods and so they can only directly simulate very short periods of time. Implicit integration methods can be applied, for example in DD simulations, to improve this mathematical time step limit. However, even here defect-defect interactions (for example dislocation annihilation and generation reactions) physically limit the simulation time step.

These challenges are fundamental to the simulation methods and mean that these approaches are unlikely to be directly applicable to nuclear materials. The most promising direct applications of MD and DD simulations have been for extreme loading events with very rapid time scales – time scales approachable directly by discrete simulations.

However, these methods have a place in the development of multiscale models for nuclear materials. Some critical events in the material, for example individual dislocation-obstacle interactions, have time scales directly resolvable with MD and DD simulation methods. Understanding and modeling these events is a crucial component of a complete multiscale model. Moreover, kinematic methods like KMC can apply discrete atomistic simulations on a diffusional time scale, which is directly relevant for long-term material properties like radiation damage and creep rupture. So, while discrete simulation methods cannot directly resolve the critical time scales for nuclear structural materials, they can still provide critical insight into key material processes that form a part of a larger multiscale model.

There are comparatively few studies applying microstructural modeling to predict properties of AMT materials, there are almost no studies applying these techniques to likely nuclear structural materials

We identified very few studies directly considering AMT processes and materials that will likely be applied to nuclear structural components. The most relevant were studies examining PBF austenitic stainless steel, though some of the Ni-base superalloy studies on aerospace alloys might be applicable to similar alloys used in future high temperature reactors. However, we identified a broader set of studies looking at process modeling for nuclear structural materials in the companion report.

We expect more published research directly applicable to nuclear materials in the future as AMTs are applied in future advanced reactor designs and as industry begins to adopt AMT techniques for the manufacture of replacement parts in operating reactors.

Most current applications are for predicting short-term properties; predicting long-term properties will be more difficult

The applications identified here have, for the most part, focused on short term material properties, predominantly flow curves and the associated measurements of yield strength, tensile strength,

and ductility. Models targeting such properties are comparatively easy to validate because direct experiments can be used to quickly assess the model's performance.

However, the design of nuclear components often involves long-term material properties, like radiation-induced embrittlement, long-term creep strength, and other similar properties. Microstructural methods will need to be developed to model these properties to complete processing-structure-properties models for nuclear components. Validation will be one key challenge in developing these models, as discussed above. Improved physical models will be an additional challenge, as physically-based methods for predicting long-term properties are less well developed when compared to methods for predicting short-term properties like flow curves.

7 Conclusions

This report summarizes the current state of the art in microstructurally-based methods for predicting material properties for AMT materials. The report includes a broad literature survey focusing on key microstructural features, physically-based methods, and data-driven methods for AMTs of likely interest to reactor operators, developers, and vendors. Based on this literature survey, the report includes a gap analysis focusing on technological challenges applying the modeling techniques to reactor structural materials. Finally, the report synthesizes a list of key gaps and recommendations on microstructural modeling. Chapter 6 describes these key recommendations, which are:

- Regulators are unlikely to see applications of the full multiscale method to new AMT materials in the near future
- Regulators are likely to see applications of microstructurally-based models to extend experimental data on new AMTs and to help qualify new materials and processes
- New validation approaches will be needed to realize the potential of microstructural modeling for AMT materials
- Data-driven approaches will continue to increase, both by themselves and in conjunction with physically-based models
- Improved, more automatic scaling bridging methods are required, particularly in spanning between discrete and continuum models
- The time-scale of direct atomistic and defect modeling approaches prevents their direct application to AMTs for nuclear reactor applications
- There are comparatively few studies applying microstructural modeling to predict structural material properties for AMTs, there are almost no studies applying these techniques to likely nuclear structural materials
- Most current applications are for predicting short-term properties; predicting long-term properties will be more difficult

In addition, the report surveys widely available modeling and simulation tools for microstructural modeling, focusing on the software tools that have been applied to AMT materials. Chapter 6 also contains a brief summary of formal validation studies applied to AMT materials

Taken together with a companion report describing processing models to predict the initial material microstructure, these reports summarize current progress towards processing-structure-properties models for AMTs. When fully developed, these models will greatly reduce the time between the development of a new processing technology or material and qualifying that new process or material for nuclear service. Furthermore, these types of models will aid in the ICME process of tailoring a material for a particular application. These models then have the potential reduce the cost and increase the flexibility of nuclear systems. In this context, regulators should expect to see an increasing application of these models and AMTs in general, both in the repair and retrofitting of the existing reactor fleet and in the development and construction of future advanced reactors.

ACKNOWLEDGEMENTS

This report was sponsored by the U.S. Nuclear Regulatory Commission (NRC) under agreement 31310019F0057 with the U.S. Department of Energy. The authors thank Dr. Shah Malik and Dr. Amy Hull of the NRC for their helpful feedback on draft version of the report.

REFERENCES

- [1] F. R. Larson and J. Miller, "A time-temperature relationship for rupture and creep stresses," *Trans. ASME*, vol. 74, pp. 765–771, 1952.
- [2] M. C. Messner *et al.*, "Combined crystal plasticity and grain boundary modeling of creep in ferritic-martensitic steels: II. The effect of stress and temperature on engineering and microstructural properties," *Model. Simul. Mater. Sci. Eng.*, vol. 27, p. 075010, 2019.
- [3] U.S. NRC, "Revision 1 of the Action Plan for Advanced Manufacturing Technologies (AMTs)," 2020.
- [4] A. Aleshin, D. S. Huelgel, and W. Clearly, "Nuclear fuel assembly debris filtering bottom nozzle," US20180268949A1, 2018.
- [5] A. Gebhardt, *Understanding Additive Manufacturing*. Hanser, 2011.
- [6] A. Nicolas, A. Chakraborty, N. Paulson, and M. C. Messner, "Survey of Modeling and Simulation Techniques for Advanced Manufacturing Technologies Volume I –Predicting Initial Microstructure," Lemont, IL, 2020.
- [7] K. Zhang, S. Wang, W. Liu, and X. Shang, "Characterization of stainless steel parts by Laser Metal Deposition Shaping," *Mater. Des.*, 2014.
- [8] J. Yu, M. Rombouts, and G. Maes, "Cracking behavior and mechanical properties of austenitic stainless steel parts produced by laser metal deposition," *Mater. Des.*, 2013.
- [9] M. GRIFFITH *et al.*, "Laser Wire Deposition (WireFeed) for Fully Dense Shapes LDRD," Nov. 1999.
- [10] Y. Li, "Research on technical characters and microstructure of laser solid forming." Ph. D. dissertation, Northwestern Polytechnical University, 2001.
- [11] Z. Wang, T. A. Palmer, and A. M. Beese, "Effect of processing parameters on microstructure and tensile properties of austenitic stainless steel 304L made by directed energy deposition additive manufacturing," *Acta Mater.*, 2016.
- [12] M. L. Griffith *et al.*, "Understanding the microstructure and properties of components fabricated by Laser Engineered Net Shaping (LENS)," *Mater. Res. Soc. Symp. - Proc.*, 2000.
- [13] I. Tolosa, F. Garcíandía, F. Zubiri, F. Zapirain, and A. Esnaola, "Study of mechanical properties of AISI 316 stainless steel processed by 'selective laser melting', following different manufacturing strategies," *Int. J. Adv. Manuf. Technol.*, 2010.
- [14] P. A. Kuznetsov, A. A. Zisman, S. N. Petrov, and I. S. Goncharov, "Structure and mechanical properties of austenitic 316L steel produced by selective laser melting," *Russ. Metall.*, vol. 2016, no. 10, pp. 930–934, 2016.
- [15] M. S. F. De Lima and S. Sankaré, "Microstructure and mechanical behavior of laser additive manufactured AISI 316 stainless steel stringers," *Mater. Des.*, 2014.
- [16] N. P. Lavery *et al.*, "Effects of hot isostatic pressing on the elastic modulus and tensile properties of 316L parts made by powder bed laser fusion," *Mater. Sci. Eng. A*, 2017.
- [17] Y. Zhai, B. Huang, X. Mao, and M. Zheng, "Effect of hot isostatic pressing on microstructure and mechanical properties of CLAM steel produced by selective laser melting," *J. Nucl. Mater.*, vol. 515, pp. 111–121, 2019.
- [18] D. Greitemeier, F. Palm, F. Syassen, and T. Melz, "Fatigue performance of additive manufactured TiAl6V4 using electron and laser beam melting," *Int. J. Fatigue*, vol. 94, pp. 211–217, 2017.
- [19] H. K. Rafi, T. L. Starr, and B. E. Stucker, "A comparison of the tensile, fatigue, and

- fracture behavior of Ti-6Al-4V and 15-5 PH stainless steel parts made by selective laser melting,” *Int. J. Adv. Manuf. Technol.*, 2013.
- [20] S. Leuders *et al.*, “On the mechanical behaviour of titanium alloy TiAl6V4 manufactured by selective laser melting: Fatigue resistance and crack growth performance,” *Int. J. Fatigue*, 2013.
- [21] D. Manfredi *et al.*, “Additive Manufacturing of Al Alloys and Aluminium Matrix Composites (AMCs),” in *Light Metal Alloys Applications*, 2014.
- [22] M. Ziętała *et al.*, “The microstructure, mechanical properties and corrosion resistance of 316 L stainless steel fabricated using laser engineered net shaping,” *Mater. Sci. Eng. A*, 2016.
- [23] T. A. Book and M. D. Sangid, “Strain localization in Ti-6Al-4V Widmanstätten microstructures produced by additive manufacturing,” *Mater. Charact.*, vol. 122, pp. 104–112, Dec. 2016.
- [24] A. Iliopoulos, R. Jones, J. Michopoulos, N. Phan, and R. Singh Raman, “Crack Growth in a Range of Additively Manufactured Aerospace Structural Materials,” *Aerospace*, vol. 5, no. 4, p. 118, Nov. 2018.
- [25] H. Masuo *et al.*, “Influence of defects, surface roughness and HIP on the fatigue strength of Ti-6Al-4V manufactured by additive manufacturing,” *Int. J. Fatigue*, 2018.
- [26] E. Wycisk, A. Solbach, S. Siddique, D. Herzog, F. Walther, and C. Emmelmann, “Effects of defects in laser additive manufactured Ti-6Al-4V on fatigue properties,” in *Physics Procedia*, 2014.
- [27] Y. Xue, A. Pascu, M. F. Horstemeyer, L. Wang, and P. T. Wang, “Microporosity effects on cyclic plasticity and fatigue of LENSTM-processed steel,” *Acta Mater.*, 2010.
- [28] S. Tammis-Williams, P. J. Withers, I. Todd, and P. B. Prangnell, “The Influence of Porosity on Fatigue Crack Initiation in Additively Manufactured Titanium Components,” *Sci. Rep.*, vol. 7, no. 1, pp. 1–13, 2017.
- [29] A. Rovinelli, M. D. Sangid, H. Proudhon, Y. Guilhem, R. A. Lebensohn, and W. Ludwig, “Predicting the 3D fatigue crack growth rate of small cracks using multimodal data via Bayesian networks: In-situ experiments and crystal plasticity simulations,” *J. Mech. Phys. Solids*, 2018.
- [30] A. Gupta, W. Sun, and C. J. Bennett, “Simulation of fatigue small crack growth in additive manufactured Ti-6Al-4V material,” *Contin. Mech. Thermodyn.*, 2020.
- [31] W. E. Frazier, “Metal additive manufacturing: A review,” *Journal of Materials Engineering and Performance*. 2014.
- [32] T. Byun, W. Chen, F. Heidet, M. Li, K. Terrani, and X. Zhang, “Creep Resistance of Additively Manufactured 316 Stainless Steel,” in *Transactions of the American Nuclear Society*, 2020, vol. 122, no. Virtual Conference, pp. 259–260.
- [33] T. Byun *et al.*, “Testing and Evaluation of Additively Manufactured TCR Core Materials,” 2020.
- [34] F. Brenne, S. Leuders, and T. Niendorf, “On the Impact of Additive Manufacturing on Microstructural and Mechanical Properties of Stainless Steel and Ni-base Alloys,” *BHM Berg- und Hüttenmännische Monatshefte*, 2017.
- [35] M. Pröbstle *et al.*, “Superior creep strength of a nickel-based superalloy produced by selective laser melting,” *Mater. Sci. Eng. A*, 2016.
- [36] Y. L. Kuo, T. Nagahari, and K. Kakehi, “The effect of post-processes on the microstructure and creep properties of Alloy718 built up by selective laser melting,”

- Materials (Basel)*., 2018.
- [37] D. Roberts, Y. Zhang, I. Charit, and J. Zhang, “A comparative study of microstructure and high-temperature mechanical properties of 15-5 PH stainless steel processed via additive manufacturing and traditional manufacturing,” *Prog. Addit. Manuf.*, 2018.
 - [38] D. J. Chastell and P. E. J. Flewitt, “The formation of the σ phase during long term high temperature creep of type 316 austenitic stainless steel,” *Mater. Sci. Eng.*, 1979.
 - [39] W. J. Sames, F. A. List, S. Pannala, R. R. Dehoff, and S. S. Babu, “The metallurgy and processing science of metal additive manufacturing,” *Int. Mater. Rev.*, vol. 61, no. 5, pp. 315–360, 2016.
 - [40] M. Moiz, “The influence of grain size on the mechanical properties of Inconel 718,” Linköping University, 2013.
 - [41] V. A. Popovich, E. V. Borisov, V. Heurtebise, T. Riemslog, A. A. Popovich, and V. S. Sufiiarov, “Creep and thermomechanical fatigue of functionally graded inconel 718 produced by additive manufacturing,” in *Minerals, Metals and Materials Series*, 2018.
 - [42] V. A. Popovich, E. V. Borisov, A. A. Popovich, V. S. Sufiiarov, D. V. Masaylo, and L. Alzina, “Functionally graded Inconel 718 processed by additive manufacturing: Crystallographic texture, anisotropy of microstructure and mechanical properties,” *Mater. Des.*, 2017.
 - [43] S. L. Mannan and M. Valsan, “High-temperature low cycle fatigue, creep-fatigue and thermomechanical fatigue of steels and their welds,” in *International Journal of Mechanical Sciences*, 2006.
 - [44] V. Shankar, R. Sandhya, and M. D. Mathew, “Creep-fatigue-oxidation interaction in Grade 91 steel weld joints for high temperature applications,” *Mater. Sci. Eng. A*, 2011.
 - [45] J. K. Wright, L. J. Carroll, and R. N. Wright, “Creep and Creep-Fatigue of Alloy 617 Weldments,” Idaho National Laboratory, INL/EXT-14-32966, Idaho Falls, Idaho, 2014.
 - [46] J. L. Stewart, J. J. Williams, and N. Chawla, “Influence of thermal aging on the microstructure and mechanical behavior of dual-phase, precipitation-hardened, powder metallurgy stainless steels,” *Metall. Mater. Trans. A Phys. Metall. Mater. Sci.*, 2012.
 - [47] T. S. Byun, D. A. Collins, T. G. Lach, and E. L. Carter, “Degradation of Impact Toughness in Cast Stainless Steels during Long-Term Thermal Aging,” *J. Nucl. Mater.*, vol. 542, p. 152524, 2020.
 - [48] S. L. Li *et al.*, “Microstructure evolution and impact fracture behaviors of Z3CN20-09M stainless steels after long-term thermal aging,” *J. Nucl. Mater.*, 2013.
 - [49] J. Il Jang, S. Shim, S. I. Komazaki, and T. Honda, “A nanoindentation study on grain-boundary contributions to strengthening and aging degradation mechanisms in advanced 12 Cr ferritic steel,” *J. Mater. Res.*, 2007.
 - [50] A. R. Nassar and E. W. Reutzler, “Additive Manufacturing of Ti-6Al-4V Using a Pulsed Laser Beam,” *Metall. Mater. Trans. A Phys. Metall. Mater. Sci.*, 2015.
 - [51] C. Örnek, “Additive manufacturing—a general corrosion perspective,” *Corros. Eng. Sci. Technol.*, 2018.
 - [52] X. Lou, M. Song, P. W. Emigh, M. A. Othon, and P. L. Andresen, “On the stress corrosion crack growth behaviour in high temperature water of 316L stainless steel made by laser powder bed fusion additive manufacturing,” *Corros. Sci.*, vol. 128, no. February, pp. 140–153, 2017.
 - [53] X. Lou, P. L. Andresen, and R. B. Rebak, “Oxide inclusions in laser additive manufactured stainless steel and their effects on impact toughness and stress corrosion

- cracking behavior,” *J. Nucl. Mater.*, 2018.
- [54] D. Kong, C. Dong, X. Ni, and X. Li, “Corrosion of metallic materials fabricated by selective laser melting,” *npj Mater. Degrad.*, 2019.
- [55] R. B. Rebak *et al.*, “Environmental Cracking and Irradiation Resistant Stainless Steels by Additive Manufacturing,” 2018.
- [56] X. Chen, J. Li, X. Cheng, H. Wang, and Z. Huang, “Effect of heat treatment on microstructure, mechanical and corrosion properties of austenitic stainless steel 316L using arc additive manufacturing,” *Mater. Sci. Eng. A*, 2018.
- [57] T. M. Yue, J. K. Yu, and H. C. Man, “The effect of excimer laser surface treatment on pitting corrosion resistance of 316LS stainless steel,” *Surf. Coatings Technol.*, 2001.
- [58] T. Kurzynowski, K. Gruber, W. Stopyra, B. Kuźnicka, and E. Chlebus, “Correlation between process parameters, microstructure and properties of 316 L stainless steel processed by selective laser melting,” *Mater. Sci. Eng. A*, vol. 718, pp. 64–73, 2018.
- [59] T. Miura, K. Fujii, and K. Fukuya, “Micro-mechanical investigation for effects of helium on grain boundary fracture of austenitic stainless steel,” *J. Nucl. Mater.*, 2015.
- [60] O. K. Chopra and A. S. Rao, “A review of irradiation effects on LWR core internal materials - IASCC susceptibility and crack growth rates of austenitic stainless steels,” *Journal of Nuclear Materials*. 2011.
- [61] M. Song, M. Wang, X. Lou, R. B. Rebak, and G. S. Was, “Radiation damage and irradiation-assisted stress corrosion cracking of additively manufactured 316L stainless steels,” *J. Nucl. Mater.*, 2019.
- [62] X. Sun, F. Chen, H. Huang, J. Lin, and X. Tang, “Effects of interfaces on the helium bubble formation and radiation hardening of an austenitic stainless steel achieved by additive manufacturing,” *Appl. Surf. Sci.*, 2019.
- [63] Z. Shang *et al.*, “Response of solidification cellular structures in additively manufactured 316 stainless steel to heavy ion irradiation: an in situ study,” *Mater. Res. Lett.*, 2019.
- [64] M. Bockstedte, A. Kley, J. Neugebauer, and M. Scheffler, “Density-functional theory calculations for poly-atomic systems: Electronic structure, static and elastic properties and ab initio molecular dynamics,” *Comput. Phys. Commun.*, vol. 107, no. 1–3, pp. 187–222, 1997.
- [65] A. Boudali, M. D. Khodja, B. Amrani, D. Bourbie, K. Amara, and A. Abada, “First-principles study of structural, elastic, electronic, and thermal properties of SrTiO₃ perovskite cubic,” *Phys. Lett. Sect. A Gen. At. Solid State Phys.*, vol. 373, no. 8–9, pp. 879–884, 2009.
- [66] S. Goumri-Said and M. B. Kanoun, “Theoretical investigations of structural, elastic, electronic and thermal properties of Damiaoite PtIn₂,” *Comput. Mater. Sci.*, vol. 43, no. 2, pp. 243–250, 2008.
- [67] Y. Cao, J. Zhu, Y. Liu, Z. Nong, and Z. Lai, “First-principles studies of the structural, elastic, electronic and thermal properties of Ni₃Si,” *Comput. Mater. Sci.*, vol. 69, pp. 40–45, 2013.
- [68] Y. Cao, J. Zhu, Z. Nong, X. Yang, Y. Liu, and Z. Lai, “First-principles studies of the structural, elastic, electronic and thermal properties of Ni₃Nb,” *Comput. Mater. Sci.*, vol. 77, no. 59, pp. 208–213, 2013.
- [69] G. I. Taylor, “The mechanism of plastic deformation of crystals. Part I.—Theoretical,” *Proc. R. Soc. London*, vol. 145, no. 855, pp. 362–387, 1934.
- [70] J. P. Hirth and J. Lothe, *Theory of dislocations*. 1982.

- [71] R. L. Coble, "A model for boundary diffusion controlled creep in polycrystalline materials," *J. Appl. Phys.*, vol. 34, 1963.
- [72] C. Herring, "Diffusional viscosity of a polycrystalline solid," *J. Appl. Phys.*, vol. 21, no. 5, pp. 437–445, 1950.
- [73] F. R. N. Nabarro, "Creep at very low rates," *Metall. Mater. Trans. A*, vol. 33, no. February, pp. 213–218, 2002.
- [74] N. Hansen, "Hall-petch relation and boundary strengthening," *Scr. Mater.*, vol. 51, no. 8 SPEC. ISS., pp. 801–806, 2004.
- [75] J. W. Christian and S. Mahajan, "Deformation twinning," *Prog. Mater. Sci.*, vol. 39, no. 1–2, pp. 1–157, 1995.
- [76] A. J. Ardell, "Precipitation hardening," *Metall. Trans. A*, vol. 16, no. 12, pp. 2131–2165, 1985.
- [77] B. A. Senior, F. W. Noble, and B. L. Eyre, "The nucleation and growth of voids at carbides in 9 Cr-1 Mo steel," *Acta Metall.*, vol. 34, no. 7, pp. 1321–1327, 1986.
- [78] W. E, *Principles of Multiscale Modeling*. Cambridge University Press, 2011.
- [79] W. E and B. Engquist, "Multiscale Modeling and Computation," *Not. AMS*, vol. 50, no. 9, pp. 1062–1070, 2011.
- [80] S. R. Fulton, P. E. Ciesielski, and W. H. Schubert, "Multigrid methods for elliptic problems: A review," *Mon. Weather Rev.*, vol. 114, pp. 943–959, 1986.
- [81] W. Kohn and L. J. Sham, "Self-Consistent Equations Including Exchange and Correlation Effects," *Phys. Rev. A*, vol. 140, no. 4A, pp. 1133–1138, 1965.
- [82] P. Hohenberg and W. Kohn, "Inhomogeneous Electron Gas," *Phys. Rev. B*, vol. 136, no. 3B, pp. 864–871, 1964.
- [83] S. Plimpton, "Fast parallel algorithms for short-range molecular dynamics," *J. Comput. Phys.*, vol. 117, no. 1, pp. 1–19, 1995.
- [84] S. Nosé, "A unified formulation of the constant temperature molecular dynamics methods," *J. Chem. Phys.*, vol. 81, no. 1, pp. 511–519, 1984.
- [85] S. Nosé and M. L. Klein, "Constant pressure molecular dynamics for molecular systems," *Mol. Phys.*, vol. 50, no. 5, pp. 1055–1076, 1983.
- [86] H. C. Andersen, "Molecular dynamics simulations at constant pressure and/or temperature," *J. Chem. Phys.*, vol. 72, no. 4, pp. 2384–2393, 1980.
- [87] J. Z. Yang, X. Wu, and X. Li, "A generalized Irving-Kirkwood formula for the calculation of stress in molecular dynamics models," *J. Chem. Phys.*, vol. 137, no. 13, 2012.
- [88] D. Li, F. C. Wang, Z. Y. Yang, and Y. P. Zhao, "How to identify dislocations in molecular dynamics simulations?," *Sci. China Physics, Mech. Astron.*, vol. 57, no. 12, pp. 2177–2187, 2014.
- [89] S. J. Zhou, D. L. Preston, P. S. Lomdahl, and D. M. Beazley, "Large-scale molecular dynamics simulations of dislocation intersection in copper," *Science (80-.)*, vol. 279, no. 5356, pp. 1525–1527, 1998.
- [90] G. P. Potirniche, M. F. Horstemeyer, G. J. Wagner, and P. M. Gullett, "A molecular dynamics study of void growth and coalescence in single crystal nickel," *Int. J. Plast.*, vol. 22, no. 2, pp. 257–278, 2006.
- [91] A. Cao, Y. Wei, and E. Ma, "Grain boundary effects on plastic deformation and fracture mechanisms in Cu nanowires: Molecular dynamics simulations," *Phys. Rev. B - Condens. Matter Mater. Phys.*, vol. 77, no. 19, pp. 1–5, 2008.
- [92] Z. T. Trautt, A. Adland, A. Karma, and Y. Mishin, "Coupled motion of asymmetrical tilt

- grain boundaries: Molecular dynamics and phase field crystal simulations,” *Acta Mater.*, vol. 60, no. 19, pp. 6528–6546, 2012.
- [93] A. M. Guellil and J. B. Adams, “The application of the analytic embedded atom method to bcc metals and alloys,” *J. Mater. Res.*, vol. 7, no. 3, pp. 639–652, 1992.
- [94] B. J. Lee, J. H. Shim, and I. Baskes, “Semiempirical atomic potentials for the fcc metals Cu, Ag, Au, Ni, Pd, Pt, Al, and Pb based on first and second nearest-neighbor modified embedded atom method,” *Phys. Rev. B - Condens. Matter Mater. Phys.*, vol. 68, no. 14, pp. 1–11, 2003.
- [95] B.-J. Lee, J.-H. Shim, and H. M. Park, “A Semi-Empirical Atomic Potential for the Fe-Cr Binary System,” *Calphad*, vol. 25, no. 4, pp. 527–534, 2001.
- [96] H. Heinz, R. A. Vaia, B. L. Farmer, and R. R. Naik, “Accurate simulation of surfaces and interfaces of face-centered cubic metals using 12-6 and 9-6 lennard-jones potentials,” *J. Phys. Chem. C*, vol. 112, no. 44, pp. 17281–17290, 2008.
- [97] M. S. Daw and M. I. Baskes, “Embedded-atom method: Derivation and application to impurities, surfaces, and other defects in metals,” *Phys. Rev. B*, vol. 29, no. 12, pp. 6443–6453, 1984.
- [98] M. I. Baskes, “Modified embedded-atom potentials for cubic materials and impurities,” *Phys. Rev. B*, vol. 46, no. 5, pp. 2727–2742, 1992.
- [99] M. I. Baskes and R. A. Johnson, “Modified embedded atom potentials for HCP metals,” *Model. Simul. Mater. Sci. Eng.*, vol. 2, pp. 147–163, 1994.
- [100] L. A. Zepeda-Ruiz, A. Stukowski, T. Ooppelstrup, and V. V. Bulatov, “Probing the limits of metal plasticity with molecular dynamics simulations,” *Nature*, vol. 550, no. 7677, pp. 492–495, 2017.
- [101] A. K. Mazur, “Common molecular dynamics algorithms revisited: Accuracy and optimal time steps of Störmer-Leapfrog integrators,” *J. Comput. Phys.*, vol. 136, no. 2, pp. 354–365, 1997.
- [102] A. F. Voter, “Introduction to the Kinetic Monte Carlo Method,” in *Radiation Effects in Solids*, vol. 53, no. 9, K. E. Sickafus, E. A. Kotomin, and B. P. Uberuaga, Eds. Amsterdam: IOS Press, 2015, pp. 1689–1699.
- [103] A. Chatterjee and D. G. Vlachos, “An overview of spatial microscopic and accelerated kinetic Monte Carlo methods,” *J. Comput. Mater. Des.*, vol. 14, no. 2, pp. 253–308, 2007.
- [104] W. M. Young and E. W. Elcock, “Monte Carlo studies of vacancy migration in binary ordered alloys: I,” *Proc. Phys. Soc.*, vol. 89, no. 3, pp. 735–746, 1966.
- [105] W. Cai, V. V. Bulatov, J. F. Justo, A. S. Argon, and S. Yip, “Intrinsic mobility of a dissociated dislocation in silicon,” *Phys. Rev. Lett.*, vol. 84, no. 15, pp. 3346–3349, 2000.
- [106] W. Cai, V. V. Bulatov, J. F. Justo, A. S. Argon, and S. Yip, “Kinetic Monte Carlo approach to modeling dislocation mobility,” *Comput. Mater. Sci.*, vol. 23, no. 1–4, pp. 124–130, 2002.
- [107] E. Van der Giessen and A. Needleman, “Modelling and Simulation in Materials Science and Engineering Related content Discrete dislocation plasticity : a simple planar model Discrete dislocation plasticity : a simple planar model,” *Model. Simul. Mater. Sci. Eng.*, vol. 3, pp. 689–735, 1995.
- [108] K. W. Schartz, “Local rules for approximating strong dislocation interactions in discrete dislocation dynamics,” *Model. Simul. Mater. Sci. Eng.*, vol. 11, p. 609, 2003.
- [109] C. C. Wu, S. Aubry, A. Arsenlis, and P. W. Chung, “Binary dislocation junction formation and strength in hexagonal close-packed crystals,” *Int. J. Plast.*, vol. 79, pp. 176–195,

- 2016.
- [110] M. P. Dewald and W. A. Curtin, “Multiscale modelling of dislocation/grain-boundary interactions: I. Edge dislocations impinging on $\Sigma 11 (1\ 1\ 3)$ tilt boundary in Al,” *Model. Simul. Mater. Sci. Eng.*, vol. 15, no. 1, 2007.
 - [111] M. P. Dewald and W. A. Curtin, “Multiscale modelling of dislocation/grain boundary interactions. II. Screw dislocations impinging on tilt boundaries in Al,” *Philos. Mag.*, vol. 87, no. 30, pp. 4615–4641, 2007.
 - [112] A. Lehtinen, F. Granberg, L. Laurson, K. Nordlund, and M. J. Alava, “Multiscale modeling of dislocation-precipitate interactions in Fe: From molecular dynamics to discrete dislocations,” *Phys. Rev. E*, vol. 93, no. 1, pp. 1–9, 2016.
 - [113] C. Motz, D. Weygand, J. Senger, and P. Gumbsch, “Initial dislocation structures in 3-D discrete dislocation dynamics and their influence on microscale plasticity,” *Acta Mater.*, vol. 57, no. 6, pp. 1744–1754, 2009.
 - [114] A. Acharya, “A model of crystal plasticity based on the theory of continuously distributed dislocations,” *J. Mech. Phys. Solids*, vol. 49, no. 4, pp. 761–784, 2001.
 - [115] S. Puri, A. Das, and A. Acharya, “Mechanical response of polycrystalline thin films in mesoscale field dislocation mechanics,” *J. Mech. Phys. Solids*, vol. 59, no. 11, pp. 2400–2417, 2011.
 - [116] A. Roy and A. Acharya, “Size effects and idealized dislocation microstructure at small scales: Predictions of a Phenomenological model of Mesoscopic Field Dislocation Mechanics: Part II,” *J. Mech. Phys. Solids*, vol. 54, no. 8, pp. 1711–1743, 2006.
 - [117] E. Kroner, “Benefits and shortcomings of the continuous theory of dislocations,” *Int. J. Solids Struct.*, vol. 38, pp. 1115–1134, 2001.
 - [118] A. Roy and A. Acharya, “Finite element approximation of field dislocation mechanics,” *J. Mech. Phys. Solids*, vol. 53, no. 1, pp. 143–170, Jan. 2005.
 - [119] R. J. Asaro and J. R. Rice, “Strain localization in ductile single crystals,” *J. Mech. Phys. Solids*, vol. 25, no. 5, pp. 309–338, 1977.
 - [120] R. Hill and J. R. Rice, “Constitutive analysis of elastic-plastic crystals at arbitrary strain,” *J. Mech. Phys. Solids*, vol. 20, no. 6, pp. 401–413, Dec. 1972.
 - [121] J. R. Rice, “Inelastic constitutive relations for solids: an internal-variable theory and its application to metal plasticity,” *J. Mech. Phys. Solids*, vol. 19, pp. 433–455, 1971.
 - [122] R. J. Asaro, “Crystal plasticity,” *J. Appl. Mech. Trans. ASME*, vol. 50, no. 4, pp. 921–934, 1983.
 - [123] P. Bate, “Modelling deformation microstructure with the crystal plasticity finite-element method,” *Philos. Trans. R. Soc. A Math. Phys. Eng. Sci.*, vol. 357, no. 1756, pp. 1589–1601, 1999.
 - [124] R. A. Lebensohn, A. K. Kanjarla, and P. Eisenlohr, “An elasto-viscoplastic formulation based on fast Fourier transforms for the prediction of micromechanical fields in polycrystalline materials,” *Int. J. Plast.*, vol. 32–33, pp. 59–69, 2012.
 - [125] A. Rovinelli, M. C. Messner, Y. Guosheng, and T.-L. Sham, “Initial study of notch sensitivity of Grade 91 using mechanisms motivated crystal plasticity finite element method,” 2019.
 - [126] R. A. Lebensohn and C. N. Tomé, “A self-consistent viscoplastic model: prediction of rolling textures of anisotropic polycrystals,” *Mater. Sci. Eng. A*, vol. 175, no. 1–2, pp. 71–82, 1994.
 - [127] F. Roters, P. Eisenlohr, L. Hantcherli, D. D. Tjahjanto, T. R. Bieler, and D. Raabe,

- “Overview of constitutive laws, kinematics, homogenization and multiscale methods in crystal plasticity finite-element modeling: Theory, experiments, applications,” *Acta Mater.*, vol. 58, no. 4, pp. 1152–1211, 2010.
- [128] P. Zhang, M. Karimpour, D. Balint, J. Lin, and D. Farrugia, “A controlled Poisson Voronoi tessellation for grain and cohesive boundary generation applied to crystal plasticity analysis,” *Comput. Mater. Sci.*, vol. 64, pp. 84–89, 2012.
- [129] L. Feng, K. shi Zhang, G. Zhang, and H. dong Yu, “Anisotropic damage model under continuum slip crystal plasticity theory for single crystals,” *Int. J. Solids Struct.*, vol. 39, no. 20, pp. 5279–5293, 2002.
- [130] J. B. Kim and J. W. Yoon, “Necking behavior of AA 6022-T4 based on the crystal plasticity and damage models,” *Int. J. Plast.*, vol. 73, pp. 3–23, 2015.
- [131] W. H. Liu, X. M. Zhang, J. G. Tang, and Y. X. Du, “Simulation of void growth and coalescence behavior with 3D crystal plasticity theory,” *Comput. Mater. Sci.*, vol. 40, no. 1, pp. 130–139, 2007.
- [132] C. A. Hernandez Padilla and B. Markert, “A coupled ductile fracture phase-field model for crystal plasticity,” *Contin. Mech. Thermodyn.*, vol. 29, no. 4, pp. 1017–1026, 2017.
- [133] O. Aslan, N. M. Cordero, A. Gaubert, and S. Forest, “Micromorphic approach to single crystal plasticity and damage,” *Int. J. Eng. Sci.*, vol. 49, no. 12, pp. 1311–1325, 2011.
- [134] T. Le Cheng, Y. H. Wen, and J. A. Hawk, “Diffuse interface approach to modeling crystal plasticity with accommodation of grain boundary sliding,” *Int. J. Plast.*, vol. 114, no. June 2018, pp. 106–125, 2019.
- [135] M. C. Messner, A. J. Beaudoin, and R. H. Dodds, “A grain boundary damage model for delamination,” *Comput. Mech.*, vol. 56, no. 1, pp. 153–172, 2015.
- [136] T. L. Sham and A. Needleman, “Effects of triaxial stressing on creep cavitation of grain boundaries,” *Acta Metall.*, vol. 31, no. 6, pp. 919–926, 1983.
- [137] O. Nassif *et al.*, “Combined crystal plasticity and grain boundary modeling of creep in ferritic-martensitic steels: I. Theory and implementation,” *Model. Simul. Mater. Sci. Eng.*, vol. 27, no. 7, 2019.
- [138] D. Cioranescu and P. Donato, *An introduction to homogenization*. Oxford: Oxford University Press, 1999.
- [139] G. Allaire, “Homogenization and two-scale convergence,” *SIAM J. Math. Anal.*, vol. 23, no. 6, pp. 1482–1518, 1992.
- [140] S. Saeb, P. Steinmann, and A. Javili, “Aspects of computational homogenization at finite deformations: A unifying review from Reuss’ to Voigt’s Bound,” *Appl. Mech. Rev.*, vol. 68, no. 5, 2016.
- [141] R. Hill, “Elastic properties of reinforced solids: Some theoretical principles,” *J. Mech. Phys. Solids*, vol. 11, no. 5, pp. 357–372, 1963.
- [142] S. Mercier and A. Molinari, “Homogenization of elastic-viscoplastic heterogeneous materials: Self-consistent and Mori-Tanaka schemes,” *Int. J. Plast.*, vol. 25, no. 6, pp. 1024–1048, 2009.
- [143] M. C. Messner, M. Rhee, A. Arsenlis, and N. R. Barton, “A crystal plasticity model for slip in hexagonal close packed metals based on discrete dislocation simulations,” *Model. Simul. Mater. Sci. Eng.*, vol. 25, no. 4, 2017.
- [144] R. Gracie and T. Belytschko, “An adaptive concurrent multiscale method for the dynamic simulation of dislocations,” *Int. J. Numer. Methods Eng.*, vol. 86, pp. 575–597, 2011.
- [145] M. A. Nuggchally, M. S. Shephard, R. C. Picu, and J. Fish, “Adaptive model selection

- procedure for concurrent multiscale problems,” *Int. J. Multiscale Comput. Eng.*, vol. 5, no. 5, pp. 369–386, 2007.
- [146] G. Lu, E. B. Tadmor, and E. Kaxiras, “From electrons to finite elements: A concurrent multiscale approach for metals,” *Phys. Rev. B - Condens. Matter Mater. Phys.*, vol. 73, no. 2, pp. 1–4, 2006.
- [147] F. Feyel and J. L. Chaboche, “FE 2 multiscale approach for modelling the elastoviscoplastic behaviour of long fibre SiC/Ti composite materials,” *Comput. Methods Appl. Mech. Eng.*, vol. 183, no. 3–4, pp. 309–330, 2000.
- [148] Y. H. Tang, S. Kudo, X. Bian, Z. Li, and G. E. Karniadakis, “Multiscale Universal Interface: A concurrent framework for coupling heterogeneous solvers,” *J. Comput. Phys.*, vol. 297, pp. 13–31, 2015.
- [149] N. R. Barton *et al.*, “A multiscale strength model for extreme loading conditions,” *J. Appl. Phys.*, vol. 109, no. 7, 2011.
- [150] W. Yan *et al.*, “Modeling process-structure-property relationships for additive manufacturing,” *Front. Mech. Eng.*, vol. 13, no. 4, pp. 482–492, 2018.
- [151] P. Ge, Z. Zhang, Z. J. Tan, C. P. Hu, G. Z. Zhao, and X. Guo, “An integrated modeling of process-structure-property relationship in laser additive manufacturing of duplex titanium alloy,” *Int. J. Therm. Sci.*, vol. 140, no. December 2017, pp. 329–343, 2019.
- [152] L. E. Lindgren, A. Lundbäck, M. Fisk, R. Pederson, and J. Andersson, “Simulation of additive manufacturing using coupled constitutive and microstructure models,” *Addit. Manuf.*, 2016.
- [153] B. Babu and L. E. Lindgren, “Dislocation density based model for plastic deformation and globularization of Ti-6Al-4V,” *Int. J. Plast.*, vol. 50, pp. 94–108, 2013.
- [154] M. Fisk, J. C. Ion, and L. E. Lindgren, “Flow stress model for IN718 accounting for evolution of strengthening precipitates during thermal treatment,” *Comput. Mater. Sci.*, vol. 82, pp. 531–539, 2014.
- [155] W. Yan *et al.*, “An integrated process–structure–property modeling framework for additive manufacturing,” *Comput. Methods Appl. Mech. Eng.*, vol. 339, pp. 184–204, 2018.
- [156] P. W. Liu *et al.*, “Integration of phase-field model and crystal plasticity for the prediction of process-structure-property relation of additively manufactured metallic materials,” *Int. J. Plast.*, vol. 128, no. October 2019, p. 102670, 2020.
- [157] B. J. Hayes *et al.*, “Predicting tensile properties of Ti-6Al-4V produced via directed energy deposition,” *Acta Mater.*, vol. 133, pp. 120–133, 2017.
- [158] A. Ahmadi, “A Micromechanical-based Computational Framework for Modeling the Mechanical Properties of the Metallic Parts Fabricated by Selective Laser Melting,” University of Toldeo, 2016.
- [159] A. Ahmadi, R. Mirzaeifar, N. S. Moghaddam, A. S. Turabi, H. E. Karaca, and M. Elahinia, “Effect of manufacturing parameters on mechanical properties of 316L stainless steel parts fabricated by selective laser melting: A computational framework,” *Mater. Des.*, vol. 112, pp. 328–338, 2016.
- [160] M. Taheri Andani, M. R. Karamooz-Ravari, R. Mirzaeifar, and J. Ni, “Micromechanics modeling of metallic alloys 3D printed by selective laser melting,” *Mater. Des.*, vol. 137, pp. 204–213, 2018.
- [161] M. Taheri Andani, M. Ghodrati, M. R. Karamooz-Ravari, R. Mirzaeifar, and J. Ni, “Damage modeling of metallic alloys made by additive manufacturing,” *Mater. Sci. Eng.*

- A*, vol. 743, no. September 2018, pp. 656–664, 2019.
- [162] R. Cunningham *et al.*, “Analyzing the effects of powder and post-processing on porosity and properties of electron beam melted Ti-6Al-4V,” *Mater. Res. Lett.*, vol. 5, no. 7, pp. 516–525, 2017.
- [163] A. Kergaßner, J. Mergheim, and P. Steinmann, “Modeling of additively manufactured materials using gradient-enhanced crystal plasticity,” *Comput. Math. with Appl.*, vol. 78, no. 7, pp. 2338–2350, 2019.
- [164] R. P. Mulay, J. A. Moore, J. N. Florando, N. R. Barton, and M. Kumar, “Microstructure and mechanical properties of Ti-6Al-4V: Mill-annealed versus direct metal laser melted alloys,” *Mater. Sci. Eng. A*, vol. 666, pp. 43–47, 2016.
- [165] J. A. Moore, N. R. Barton, J. Florando, R. Mulay, and M. Kumar, “Crystal plasticity modeling of β phase deformation in Ti-6Al-4V,” *Model. Simul. Mater. Sci. Eng.*, vol. 25, no. 7, 2017.
- [166] Q. Zhang, J. Xie, T. London, D. Griffiths, I. Bhamji, and V. Oancea, “Estimates of the mechanical properties of laser powder bed fusion Ti-6Al-4V parts using finite element models,” *Mater. Des.*, vol. 169, 2019.
- [167] V. T. Phan, T. D. Nguyen, Q. H. Bui, and G. Dirras, “Modelling of microstructural effects on the mechanical behavior of ultrafine-grained Nickel using crystal plasticity finite element model,” *Int. J. Eng. Sci.*, vol. 94, pp. 212–225, 2015.
- [168] Q. H. Bui and X. T. Pham, “Modeling of microstructure effects on the mechanical behavior of ultrafine-grained nickels processed by hot isostatic pressing,” *Int. J. Mech. Sci.*, vol. 53, no. 10, pp. 812–826, 2011.
- [169] S. Ghorbanpour *et al.*, “Experimental characterization and crystal plasticity modeling of anisotropy, tension-compression asymmetry, and texture evolution of additively manufactured Inconel 718 at room and elevated temperatures,” *Int. J. Plast.*, vol. 125, no. May 2019, pp. 63–79, 2020.
- [170] J. R. Yates, P. Efthymiadis, A. A. Antonysamy, C. Pinna, and J. Tong, “Do additive manufactured parts deserve better?,” *Fatigue Fract. Eng. Mater. Struct.*, vol. 42, no. 9, pp. 2146–2154, 2019.
- [171] P. Veerappan and M. D. Sangid, “The role of defects and critical pore size analysis in the fatigue response of additively manufactured IN718 via crystal plasticity,” *Mater. Des.*, 2018.
- [172] M. D. Sangid, P. Ravi, V. Prithivirajan, N. A. Miller, P. Kenesei, and J. S. Park, “ICME Approach to Determining Critical Pore Size of IN718 Produced by Selective Laser Melting,” *JOM*, vol. 72, no. 1, pp. 465–474, 2020.
- [173] K. Kapoor, Y. S. J. Yoo, T. A. Book, J. P. Kacher, and M. D. Sangid, “Incorporating grain-level residual stresses and validating a crystal plasticity model of a two-phase Ti-6Al-4 V alloy produced via additive manufacturing,” *J. Mech. Phys. Solids*, vol. 121, pp. 447–462, 2018.
- [174] R. Pokharel, A. Patra, D. W. Brown, B. Clausen, S. C. Vogel, and G. T. Gray, “An analysis of phase stresses in additively manufactured 304L stainless steel using neutron diffraction measurements and crystal plasticity finite element simulations,” *Int. J. Plast.*, vol. 121, no. January, pp. 201–217, 2019.
- [175] M. M. Francois *et al.*, “Modeling of additive manufacturing processes for metals: Challenges and opportunities,” *Current Opinion in Solid State and Materials Science*. 2017.

- [176] B. H. Jared *et al.*, “Additive manufacturing: Toward holistic design,” *Scr. Mater.*, vol. 135, pp. 141–147, 2017.
- [177] D. Wolf, V. Yamakov, S. R. Phillpot, A. Mukherjee, and H. Gleiter, “Deformation of nanocrystalline materials by molecular-dynamics simulation: Relationship to experiments?,” *Acta Mater.*, vol. 53, no. 1, pp. 1–40, 2005.
- [178] P. C. Collins *et al.*, “Progress Toward an Integration of Process--Structure--Property--Performance Models for “Three-Dimensional (3-D) Printing” of Titanium Alloys,” *JOM*, vol. 66, no. 7, pp. 1299–1309, Jul. 2014.
- [179] G. Miranda *et al.*, “Predictive models for physical and mechanical properties of 316L stainless steel produced by selective laser melting,” *Mater. Sci. Eng. A*, vol. 657, pp. 43–56, 2016.
- [180] J. Mutua, S. Nakata, T. Onda, and Z.-C. Chen, “Optimization of selective laser melting parameters and influence of post heat treatment on microstructure and mechanical properties of maraging steel,” *Mater. Des.*, vol. 139, pp. 486–497, 2018.
- [181] B. Kappes, S. Moorthy, D. Drake, H. Geerlings, and A. Stebner, “Machine Learning to Optimize Additive Manufacturing Parameters for Laser Powder Bed Fusion of Inconel 718 BT - Proceedings of the 9th International Symposium on Superalloy 718 & Derivatives: Energy, Aerospace, and Industrial Applications,” 2018, pp. 595–610.
- [182] Z. Liu, M. A. Bessa, and W. K. Liu, “Self-consistent clustering analysis: An efficient multi-scale scheme for inelastic heterogeneous materials,” *Comput. Methods Appl. Mech. Eng.*, vol. 306, pp. 319–341, 2016.
- [183] Z. Gan *et al.*, “Data-Driven Microstructure and Microhardness Design in Additive Manufacturing Using a Self-Organizing Map,” *Engineering*, vol. 5, no. 4, pp. 730–735, 2019.
- [184] T. Kohonen, “The self-organizing map,” *Proc. IEEE*, vol. 78, no. 9, pp. 1464–1480, 1990.
- [185] M. Kusano *et al.*, “Tensile properties prediction by multiple linear regression analysis for selective laser melted and post heat-treated Ti-6Al-4V with microstructural quantification,” *Mater. Sci. Eng. A*, vol. 787, p. 139549, 2020.
- [186] I. Arganda-Carreras *et al.*, “Trainable Weka Segmentation: a machine learning tool for microscopy pixel classification,” *Bioinformatics*, vol. 33, no. 15, pp. 2424–2426, 2017.
- [187] L. E. Lindgren, A. Lundbäck, M. Fisk, R. Pederson, and J. Andersson, “Simulation of additive manufacturing using coupled constitutive and microstructure models,” *Addit. Manuf.*, vol. 12, pp. 144–158, 2016.
- [188] A. Arsenlis *et al.*, “Enabling strain hardening simulations with dislocation dynamics,” *Model. Simul. Mater. Sci. Eng.*, vol. 15, no. 6, pp. 553–595, 2007.
- [189] P. Coffman, W. Jiang, and N. Romero, “LAMMPS strong scaling performance optimization on Blue Gene/Q,” Argonne National Laboratory, ANL/ALCF-14/3, 2014.
- [190] P. Noell *et al.*, “Mechanistic origins of stochastic rupture in metals,” Sandia National Laboratories, SAND2019-13016, 2019.
- [191] R. A. Lebensohn, “N-site modeling of a 3D viscoplastic polycrystal using Fast Fourier Transform,” *Acta Mater.*, vol. 49, no. 14, pp. 2723–2737, 2001.
- [192] A. Rovinelli, H. Proudhon, R. A. Lebensohn, and M. D. Sangid, “Assessing the reliability of fast Fourier transform-based crystal plasticity simulations of a polycrystalline material near a crack tip,” *Int. J. Solids Struct.*, vol. 184, pp. 153–166, 2020.
- [193] M. A. Groeber and M. A. Jackson, “DREAM.3D: A Digital Representation Environment for the Analysis of Microstructure in 3D,” *Integr. Mater. Manuf. Innov.*, vol. 3, no. 1, pp.

- 56–72, 2014.
- [194] R. Quey, P. R. Dawson, and F. Barbe, “Large-scale 3D random polycrystals for the finite element method: Generation, meshing and remeshing,” *Comput. Methods Appl. Mech. Eng.*, vol. 200, no. 17–20, pp. 1729–1745, 2011.
 - [195] S. Aubry, M. Rhee, G. Hommes, V. V. Bulatov, and A. Arsenlis, “Dislocation dynamics in hexagonal close-packed crystals,” *J. Mech. Phys. Solids*, vol. 94, pp. 105–126, 2016.
 - [196] Air Force Research Laboratory, “CHALLENGE 4: Microscale Structure -to- Properties- Problem Statement,” *AM Modeling Challenge Series*, 2019. [Online]. Available: https://materials-data-facility.github.io/MID3AS-AM-Challenge/Challenge4ProblemStatement_2019Release.pdf.
 - [197] M. Groeber *et al.*, “A Preview of the U.S. Air Force Research Laboratory Additive Manufacturing Modeling Challenge Series,” *Jom*, vol. 70, no. 4, pp. 441–444, 2018.
 - [198] K. Corey, “Air Force Research Laboratory Additive Manufacturing Modeling Challenge,” *The Simulia Blog*, 2020. [Online]. Available: <https://blogs.3ds.com/simulia/air-force-research-laboratory-additive-manufacturing-modeling-challenge/>. [Accessed: 16-Jul-2020].
 - [199] NIST, “Additive Manufacturing Benchmark Test Series (AM-Bench),” *NIST*, 2020. [Online]. Available: <https://www.nist.gov/ambench>. [Accessed: 16-Jul-2020].
 - [200] S. Davies, “TWI and Simulia partner to win AM Bench Test Series’ residual elastic strains category,” *TCT magazine*, 2018. [Online]. Available: <https://www.tctmagazine.com/additive-manufacturing-3d-printing-news/twi-simulia-am-bench-test-series-residual-elastic-strain/>. [Accessed: 16-Jul-2020].
 - [201] NIST, “AM-Bench 2018 Benchmark Challenge Submissions and Awards,” *AM-Bench NIST*, 2018. [Online]. Available: <https://www.nist.gov/ambench/awards>. [Accessed: 16-Jul-2020].
 - [202] Y. Yang, M. Allen, T. London, and V. Oancea, “Residual Strain Predictions for a Powder Bed Fusion Inconel 625 Single Cantilever Part,” *Integr. Mater. Manuf. Innov.*, 2019.
 - [203] AO, “AMP2,” *Applied Optimization*, 2020. [Online]. Available: <http://appliedo.com/amp2/>. [Accessed: 16-Jul-2020].
 - [204] J. Robichaud, T. Vincent, B. Schultheis, and A. Chaudhary, “Integrated Computational Materials Engineering to Predict Melt-Pool Dimensions and 3D Grain Structures for Selective Laser Melting of Inconel 625,” *Integr. Mater. Manuf. Innov.*, 2019.



Applied Materials Division

Argonne National Laboratory
9700 South Cass Avenue, Bldg. 212
Argonne, IL 60439

www.anl.gov



Argonne National Laboratory is a U.S. Department of Energy
laboratory managed by UChicago Argonne, LLC